DEVELOPMENT OF A HIGH PERFORMANCE AND ROBUST CONTROLLER FOR HARD DISK DRIVE SERVO SYSTEM

AMAR NATH

A THESIS SUBMITTED IN PARTIAL FULFILLMENT

OF THE REQUIREMENT FOR THE DEGREE OF

MASTER OF ENGINEERING IN DATA STORAGE TECHNOLOGY

COLLEGE OF DATA STORAGE INNOVATION

KING MONGUT'S INSTITUTE OF TECHNOLOGY LADKRABANG

2010

KMIT -2010-DS-M-001-04

ชื่อหัวข้อวิทยานิพนธ์:	การพัฒนาตัวควบคุมสมรรถนะสูงและคงทนสำหรับระบบเซอร์โวฮาร์ดิสก์ไดร์ฟ
หน่วยกิตของวิทยานิพนธ์:	12 หน่วยกิต
นักศึกษา:	นายอัมมาร์ แนธ์
อาจารย์ที่ปรึกษาวิทยานิพนธ์:	ดร.สมยศ เกียรติวนิชวิไล
หลักสูตร:	วิศวกรรมศาสตรมหาบัณฑิต
สาขาวิชา:	ระบบควบคุมสำหรับฮาร์ดิสก์ไดร์ฟ
คณะ:	วิทยาลัยร่วมด้านเทคโนโลยีการบันทึกข้อมูลและการประยุกต์ใช้งาน

บทคัดย่อ

วิทยานิพนธ์นี้นำเสนอเทคนิคใหม่ในการออกแบบตัวควบคุมที่มีประสิทธิผลสำหรับทั้ง Voice Coil Motor Actuator (VCM) และ Dual Stage Actuator (DSA) ในระบบเซอร์โวฮาร์ดิสก์ไดร์ฟ (Hard Disk Drive Servo System) เพื่อให้ฮาร์ดดิสก์สามารถมี aerial density สูงนั้นจะต้องมีการปรับปรุงสมรรถนะและความคงทนของระบบเซอร์โวฮาร์ดดิสก์ ตัวควบคุมแบบคงทนโดยวิธีเอช-อินฟินิตี้ (H_∞) เป็นเทคนิคหนึ่งที่นิยมใช้สำหรับแก้ปัญหาดังกล่าวอย่างไรก็ตามลำดับของตัวควบคุมที่ออกแบบด้วยเทคนิคนี้มักจะสูงกว่าของระบบที่ถูกควบคุมทำให้ยากต่อการนำไปใช้งานในทางปฏิบัติ เพื่อแก้ปัญหานี้วิทยานิพนธ์นี้จึงเสนอเทคนิคใหม่สำหรับการออกแบบตัวควบคุมแบบคงทนสำหรับระบบเซอร์โวฮาร์ดิสก์ไดร์ฟ ในวิธีที่นำเสนอ ค่านอร์มอนันต์ (infinity norm) ของฟังก์ชันถ่ายโอนจากตัวรบกวน (disturbances)ไปยังสถานะ(states)จะถูกนำมาใช้เป็นฟังก์ชันต้นทุน(Cost Function)ในปัญหาการหาค่าเหมาะสมที่สุด ขั้นตอนวิธีเชิงพันธุกรรม(Genetic Algorithms : GA) จะถูกนำไปแก้ปัญหาและใช้หาค่าพารามิเตอร์ของตัวควบคุมที่เหมาะสมที่สุด เทคนิคที่นำเสนอนี้ไม่เพียงแต่สามารถแก้ปัญหาตัวควบคุมที่มีโครงสร้างซับซ้อนและลำดับสูงเท่านั้นแต่ยังคงรักษาความคงทนสมรรถนะ (robust performance) ของการควบคุมแบบเอช-อินฟินิตี้(H_∞)แบบเดิมด้วย นอกจากนี้ในวิทยานิพนธ์นี้ยังใช้ขั้นตอนวิธีเชิงพันธุกรรมในการออกแบบตัวควบคุมที่มีโครงสร้างแบบสององศาอิสระ(2 DOF controller) เพื่อเพิ่มสมรรถนะในโดเมนเวลา ผลการทดลองและการจำลองในคอมพิวเตอร์ในระบบควบคุมเซอร์โวฮาร์ดิสก์ไดร์ฟพิสูจน์ให้เห็นถึงความมีประสิทธิผลของเทคนิคที่นำเสนอ

คำสำคัญ: ระบบเซอร์โวฮาร์ดิสก์ไดร์ฟ, VCM, Dual Stage Actuator, การควบคุมแบบจัดสัณฐานวงรอบแบบคงทน

Thesis:	Development of a High Performance and Robust Controller for HDD Servo System
Student:	Mr. Amar Nath
Student ID:	51068920
Degree:	Master of Engineering (M.E)
Program:	Data Storage Technology
Year:	2010
Thesis Advisor:	Dr. Somyot Kaitwanidvilai

ABSTACT

This thesis proposes a new technique to design an effective controller for both the Voice Coil Motor actuator (VCM) and Dual Stage Actuator (DSA) in a HDD servo system. In order to achieve high aerial density, tracking performance and robustness of the HDD servo system need to be improved. H_∞ robust controller is one of the most popular techniques for solving the mentioned problem; however, the order of this controller is usually higher than that of the plant, making it difficult to implement in practice. To overcome this problem, this thesis proposes a new technique for designing a robust controller for HDD servo system. Infinity norm of transfer function from disturbances to states is used as the cost function in our optimization problem. Genetic Algorithms is adopted to solve this problem and is used to find the optimal controller parameters. The proposed technique does not only solve the problem of complicated and high order controller but also still retains the robust performance of conventional H_∞ control technique. In addition, structured pre-filter in the 2 DOF controller structure is also designed by GA to enhance the performance in time-domain. Experimental and simulation results in a HDD control system verify the effectiveness of the proposed technique.

Keywords: HDD servo system, VCM actuator, Dual Stage Actuators, Robust Loop Shaping Control

Acknowledgements

This thesis is dedicated to my wife and my kids for their understanding, sacrifice motivating, encouraging and helping me during my research work. I would to express my deepest gratitude to Dr Somyot Kaitwanidvilai for his continuous advice, encouragement and dedication to this thesis. Dr. Somyot instructed and gave me a lot of significant comments during my thesis research. I would like to show my appreciation to all of the thesis committees for their valuable time and advices to improve the research method.

I would like to wish my gratitude to my boss Dick Lesage, to my technical support, WD HR Manager Pricha for their helping during my research publication. I would also like to thank WD IP department, Servo department for their helps and supports during research publication.

Contents

List of tables

List of figures

Chapter 1

Introduction

1.1 Statement and significance of the problems

Hard disk drives (HDDs) provide an important data-storage medium for computers and other data-processing systems. In most commercial HDDs, media is coated with a thin magnetic layer or recording medium is written with data that are arranged in concentric circles called tracks. Data are read or written with a read/write (R/W) head, which consists of a Magneto Resistive (MR) element controlled by the voice-coil motor (VCM) actuator. Figure 1.1 shows a simple illustration of a typical hard disk with VCM actuator.

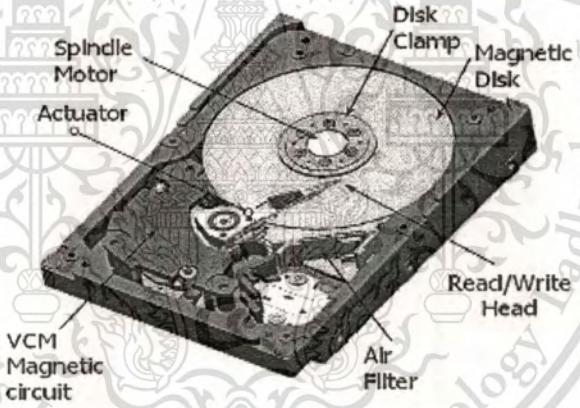

Fig 1.1 HDD servo system [3]

A HDD servo system needs to accomplish two main tasks, first is to move the head to the desired track as quickly as possible and then position the head on the center of the track as precisely as possible so that data can be read/written quickly and reliably. The first task is commonly referred to as track seeking, while the second task is commonly referred to as track following [1]. The performance of track-following servo system is normally measured by an index, Track Mis-Registration (TMR), which is the variance of the deviation between the center of the read/write head and the center of the track. It is generally accepted in the magnetic recording industry that the 3σ value of the TMR should be less than 10% of the track pitch [1]. The implementation of track seeking

and track-following servo system relies on servo sectors, which are embedded in the data sectors and arranged radically as shown in the Figure 1.2 [2]. Each servo sector typically includes Phase Lock Loop (PLL), a servo sync mark (SSM), a track identification (TKID), and a sector ID having binary encoded sector ID numbers for identifying the sector and a group of servo burst [2].

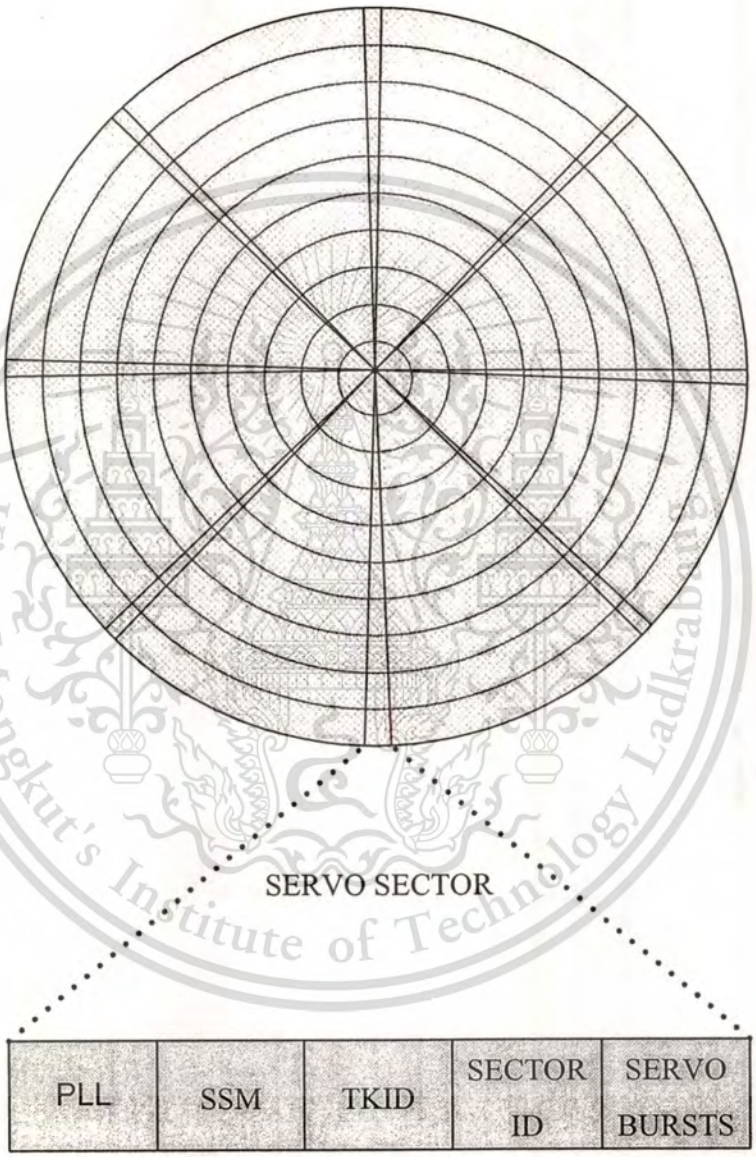

Fig 1.2 HDD servo sector format [2]

Typically, the servo control system moves the read head towards the desired track during seek mode using TKID as control input. Once the R/W head is on the track, the servo control system uses

the servo bursts to keep the R/W head over the track during track following mode. During track following mode, the head repeatedly reads the sector ID filed of each successive servo sector to obtain the binary encoded sector ID number that identifies each sector of the track. In this way, the servo control system continuously knows where the R/W head is relative to the disk.

Position error signals (PES) are essential feedback signal for servo control system during track following operations. The PES signal may be derived from read servo burst as the head flies over the servo burst of the servo sector of the disk. There are various PES demodulation methods to calculate the PES value from the burst profile.

The prevalent trend in hard disk design is smaller hard disks with increasingly larger capacities. The recording density is increasing at an impressive annual rate of more than 100% while the access time is decreasing; very soon the storage density is going to cross 1 terra bit per square inch. The expected necessary track density for 1 terra-bit per square inch recording will be 500,000 tracks-per-inch (TPI), which requires a TMR budget of less than 5nm (3-sigma value) [1]. The existing conventional HDD servo technology cannot support this new requirement; a new class of VCM actuator (Dual stage actuators) along with high performance servo controller is required to handle both the performance and robustness.

As the TPI increases, the track width becomes narrow which leads to lower error tolerance in the positioning of the head. The controller for track following has to achieve tighter regulation in the control of the servo mechanism. A rigorous analysis of sources of TMR and the development of advanced techniques to eliminate these sources are required. Currently, HDD uses many control techniques such as lead lag compensators, PI compensators, robust control and notch filters. Some classical methods for controlling HDD servo mechanism can no longer meet the demand of higher performance. Several control approaches have been adopted to solve the above mentioned problem, e.g. identification and high bandwidth control [4], mixed H_2/H_∞ Control for improving TMR [5], dynamic nonlinear control for fast seek-settling [6], and gradient based parameter optimization method [7]. Since the performance of servo controllers are governed by the mechanical repeatable run out (RRO) and non repeatable run-out (NRRO) as well; a lot of research has been done to improve RRO/NRRO and thus improve the servo performance. e.g. Western Digital Inc US patent documents US7616399 Nov 2009 [2]. This invention preserves the PES continuity during track following mode.

Western Digital Inc US patent documents US6545835 B1 Apr 2003 [8] describes a method of RRO learning before and after shipping to cancel RRO in a disk drive.

The most important aspect in HDD servo control system is to ensure both the stability and the performance of the system under the perturbed conditions. One of the most popular techniques is H_∞ optimal loop shaping control. In this technique, the uncertainty and performance are incorporated into the controller design [9-10]. Unfortunately, the order of the resulting controller from this technique is usually high, making it difficult to implement the controller in practice. In this thesis, we illustrate the design of a HDD controller which can guarantee stability under the perturbed conditions and which also has a simple structure. This thesis uses a more recent evolutionary technique, Genetic Algorithms (GA), to solve the specified structure H_∞ loop shaping optimization problem. The infinity norm of transfer function from disturbances to states is formulated as a cost function in our optimization problem. This problem is solved via searching and evolutionary computation by GA. The resulting optimal controller makes the system stable and also guarantees the robust performance. In addition, GA is adopted to find a structured pre-filter for increasing the tracking performance of the system. By the approach mentioned above, a high performance HDD servo system can be designed.

1.2 Objectives

This thesis focuses on the systematic design of HDD servo system. The main objectives of study are:

1. To study the model and dynamic systems of a single VCM actuator and a dual stage actuator,
2. To design a notch filter to compensate resonance modes in HDD servo system,
3. To implement a new technique of controller design, GA based Fixed Structure Robust Loop Shaping Control, on the HDD servo system.

1.3 Scope of the thesis

1. Design a high performance HDD servo system using GA based fixed structure robust loop shaping control for a single stage actuator,
2. Implement the controller in item 1 for a real HDD servo system,
3. Design a high performance controller for a dual stage actuator (simulation only).

1.4 Limitations of the thesis and budget

1. Time allocated for this thesis is only one year.
2. Budget allocated for this thesis is about 178,000 THB.

Chapter 2

Literature Reviews

The development in HDD control system has received much attention by many research works. Many researchers tried to improve the performance of servo control system using several new techniques. Several techniques about servo control system design, system identification and modeling, plant uncertainty condition, etc. have been proposed by several researchers. In addition, several researchers contributed their research works in repeatable and non repeatable detection and correction. In this chapter, some of them which are closely related to this thesis are described. This chapter is organized as follows. Section 2.1 describes the background works and basic theories of HDD servo system. Main issues on control system design have been described in Section 2.2. Single and dual stage actuators are illustrated in Section 2.3. Primary VCM actuator model, its resonance modes and parametric uncertainties are also described in this section. The micro-actuator model with its resonance modes and parametric uncertainty is described in Section 2.4. Section 2.5 shows the integration mechanism.

2.1 Background of the HDD servo system

Many immense developments in HDD servo system have been proposed by many researchers, and they are used extensively in HDD servo system. Western Digital Inc Patent US 7027256-B1 Apr 2006 [11] disclosed a method to reduce RRO. The magnetic disk has a plurality of embedded servo sectors and data sectors for storing user data. At the end of servo sectors, there is the RRO cancellation information along with error correction code (ECC) data. The actuator positions the transducer head in response to control signal generated by the sampled servo controller based on servo information including RRO cancellation and RRO ECC information at servo data rate. The RRO ECC data is only used for detecting and correcting errors in RRO. The flowchart of the RRO cancellation mechanism is given in Figure 2.1. This method is more reliable in reduction of RRO in the location of embedded servo sectors relative to concentric track center.

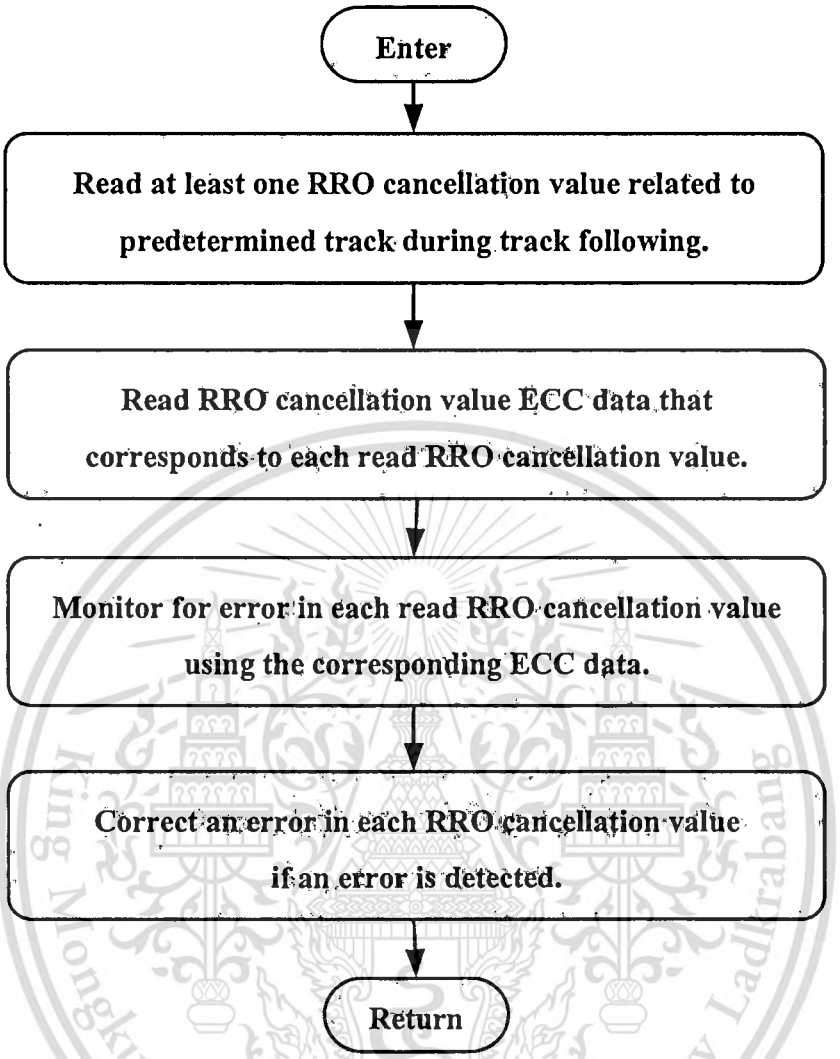

Fig 2.1 Flow chart for RRO cancellation [11]

Rotunno et. al. used an optimal control theory, H_∞ norm based control design, to design a controller for DSA (Dual Stage Actuator) [12]. They compared the performance between different strategies and power consumption. The techniques used in their paper are based on optimal control design to come up with a systematic approach to design a servo controller. The systematic design approach requires the specification of the shape of well defined weighting function. In this paper, a bandwidth (BW) of 0.45 kHz with gain margin (GM) of 8.8 dB and phase margin (PM) of 39 degree on a single stage actuator can be achieved. In the DSA, BW 1.1 kHz with GM of 8.1 dB and PM of 38 deg with a VCM and Magnum 5e dual-stage suspension can be achieved.

Huang et. al. presented the system modeling, the design and the analysis of multi-rate robust track following controller [13]. In this paper, they followed two approaches. In the first approach, the controller was designed using SISO method such as SD and PQ method. In the second approach, MIMO controller design was illustrated and they adopted the mixed H_2/H_∞ mixed H_2/μ and robust H_2 synthesizes. Performance comparisons of all controllers were given in their paper and were shown in the Table 2.1 below.

Table 2.1 Performance comparison between control design [14]

PERFORMANCE COMPARISON BETWEEN CONTROL DESIGNS

Design Approach	Unstable (/400)	PES (nm) Nominal	W-C	Degradation	u_m (mV) Nominal	W-C	Degradation	Controller Order
PQ method	0	7.75	10.00	29 %	205	234	14 %	6
SD method	0	7.11	8.35	17 %	277	316	14 %	6
Mixed H_2/H_∞	0	6.57	7.82	19 %	201	216	8 %	8
Mixed H_2/μ	0	5.31	5.88	11 %	261	298	14 %	8
Robust H_2 [1 1 1]	0	5.93	6.47	9 %	275	310	13 %	9
Robust H_2 [1 0 1]	0	5.96	7.10	18 %	308	388	26 %	10
Robust H_2 [1 1 0]	0	6.09	7.97	31 %	239	309	29 %	10
Robust H_2 [1 0 0]	0	7.66	9.45	23 %	278	399	44 %	10

As seen in this table, the results show that the robust MIMO design approaches generally achieve better nominal and worst case performance than the sequential SISO design approach.

Conway et. al. presented a semi-automated method for identifying parameters and parametric uncertainty for a set of dual stage hard disk drives [14]. They presented two methods for model reduction; first method combines the experimental data to directly extract the fewer parameters while second method uses optimized modal transaction methodology. Convex optimization and singular value decomposition are employed to obtain a minimally conservative, lower order approximation of uncertain parameters. The former method results in fewer initial uncertain parameters; the latter provides a better match with the full-order model. Finally, the result is a state space controller model of manageable size to be used in robust H_2 synthesis.

Law, et. al. investigated a new multi-objective Genetic Algorithm (GA) for tuning the servo controller parameters for HDD in order to satisfy all the desired performance [15]. His multi-objective GA works on the constrained optimization objective. The proposed controller-tuning scheme places the constraint objective at higher priority than the optimization objective. This

technique is extremely useful for the conditions where servo system needs to work under some constraints such as low power requirements, vibrating conditions etc.

Taghirad, et. al. developed an improved compensator, Adaptive Robust controller (IDARC), which is suitable for both track seeking and track following controls [16]. In addition, this technique can reduce the mode switching algorithm of conventional HDD. Their robust controller is powered by a dynamic adaptive term. In this paper, it is observed that even in the presence of large disturbances, IDARC performed better performance than the adaptive robust controller.

Venkataramanan, et. al. proposed a discrete time composite nonlinear feedback control for HDD servo system [17]. Their proposed scheme is composed by combining a linear feedback law and a nonlinear feedback law. The linear feedback law is designed to yield a fast response, while the nonlinear feed back law is used to increase the damping ratio of the closed-loop system as the system output approaches the command input. In the face of actuator saturation, this control law not only increases the speed of closed-loop response, but also improves the settling performance over 30%. Their proposed technique was able to work on both track seeking and track following mode and it does not require any mode switching control.

Chen et. al. presented a tutorial on iterative learning control (ILC) and the repetitive control (RC) techniques in HDD industry for compensation of repeatable run-outs (RRO) [18]. For ILC, a simple filtering-free implementation for written-in RRO compensation is presented. They focused on how to reject the repeatable run-outs in HDD servo. A tutorial on iterative learning control (ILC) with a simple application in HDDs without any filtering operation is presented.

2.2 Issues on control system design

Figure 2.2 shows a typical disk drive servo channel indicating the various sources of disturbances and errors. The major error sources and disturbances which produce bad TMR are given below.

1. TMR caused by the bearing hysteresis and poor velocity estimation during track seeking and track settling modes.
2. Written in servo pattern non-linearity due to head asymmetry, media imperfection etc.
3. Non-repeatable spindle run-out in the drive caused by bearing.
4. Mechanical resonance in the suspension and actuators are the another causes of poor TMR.

5. Electronic noise in the channel part got recorded through servo DE-MOD as well.

A good servo system should not only provide better seek and better track following but it needs to provide a robust performance and disturbance rejection caused by the errors mentioned above. Following are the robustness issues which one should consider while designing the HDD servo system.

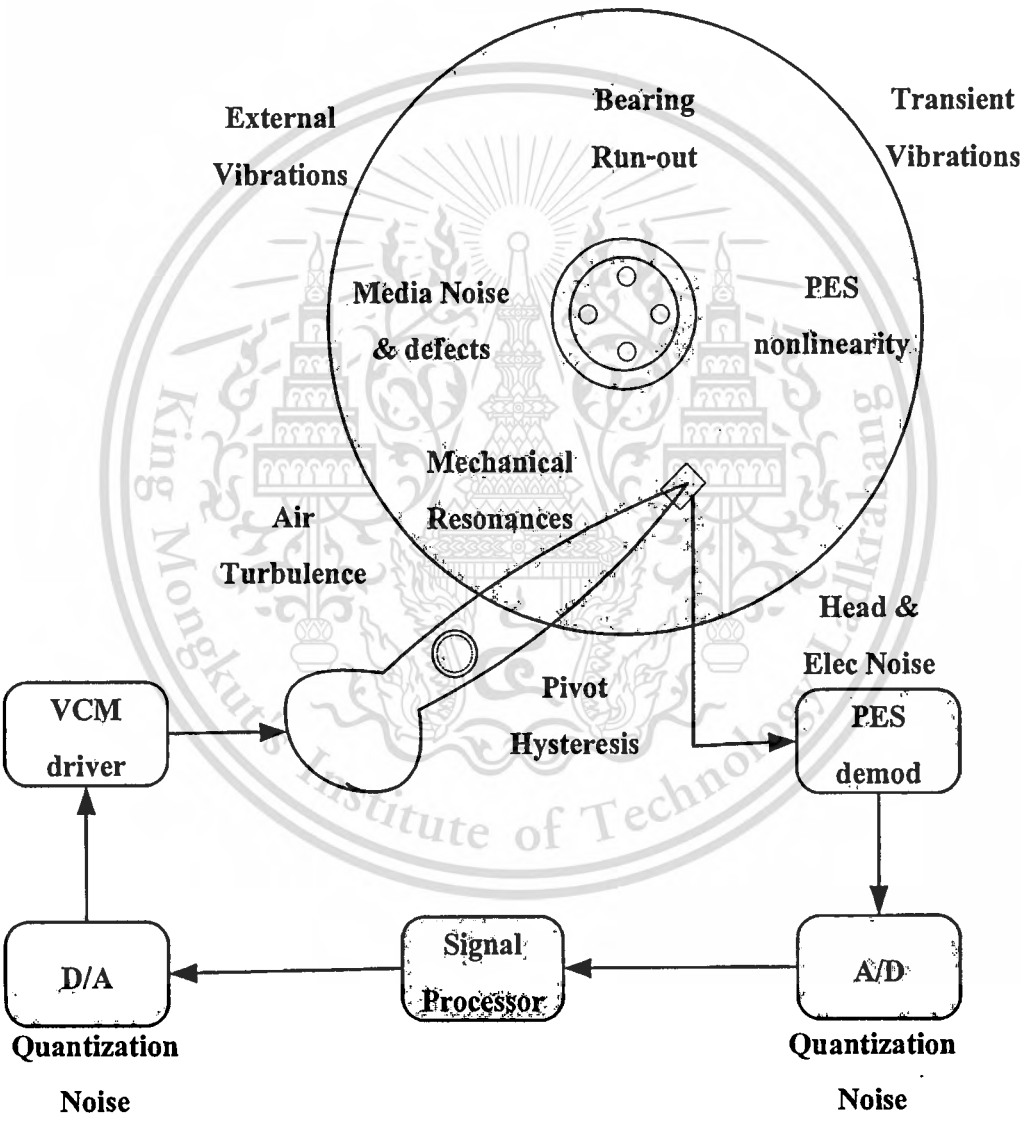

Fig 2.2 Noise sources in HDD [19]

2.2.1 Disturbance Rejection

There are three types of disturbances, which play an important role to make TMR bad those are: input disturbance, output disturbance and measured noise. These disturbances can be modeled as Figure 2.3.

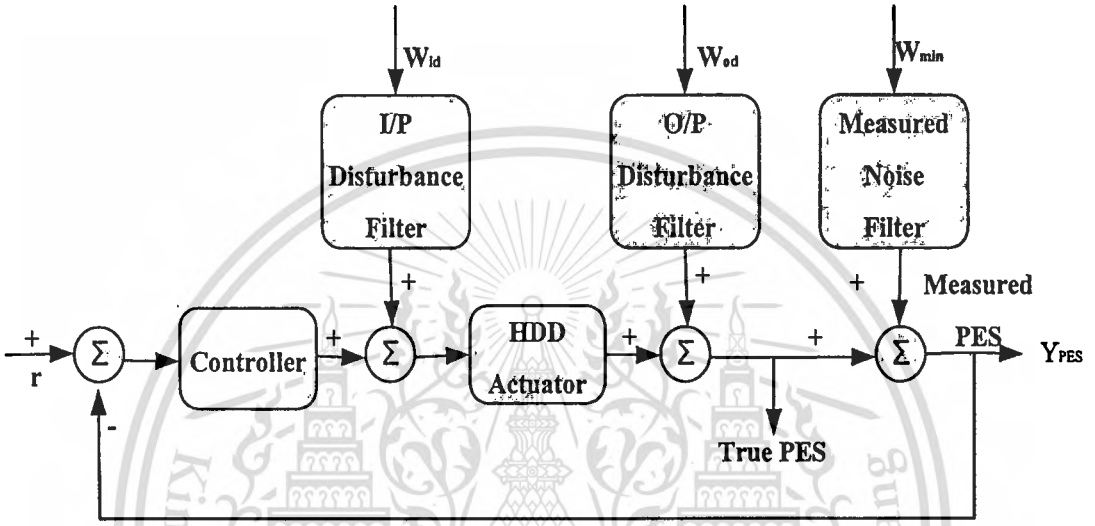

Fig 2.3 Disturbance modeling in HDD servo system [19]

The input disturbance is typically a color noise with superimposed electronic bias, which sensitive energy arises from natural frequencies of various mechanical perturbations such as resonances, vibration and friction. The output disturbance is also a color noise and mainly caused by spindle rotation and its effects such as run-out, wind-age and media noises. The measurement noise is a white noise due to the position measurement techniques and/or sensors. The objective will be to reject the effect of the disturbances and measurement noise. In this way, we can achieve minimum position error variance, σ_{pes}, which can be approximated by (2.1) [20]

$$\sigma_{pes} = \sqrt{\frac{1}{N-1}\cdot\sum_{i=1}^{N} Y_{pes}^{2}(i)} \qquad (2.1)$$

Where N is the number of samples. The problem to minimize σ_{pes} can be solved using appropriate H_2 optimal control method.

2.2.2 Run-out compensation

The position feedback signals in HDD servo mechanisms are derived through pre-recorded servo sectors at the time of manufacturing using either a dedicated servo writer or using self servo writing technique. Ideally, the tracks should be perfect concentric circles. However, in the process of servo writing, the head that written tracks is not perfectly circle due to presence of vibration and NRRO effects. Figure 2.4 is a schematic diagram illustrates ideal servo tracks and written servo tracks exhibiting servo RRO.

This apparent track motion causes the R/W head to move in an attempt to minimize the position error, which results in positioning of the R/W head away from the real data track. Such an imperfection is termed a run out. This run-out, depending upon its nature can be classified as repeatable and non repeatable.

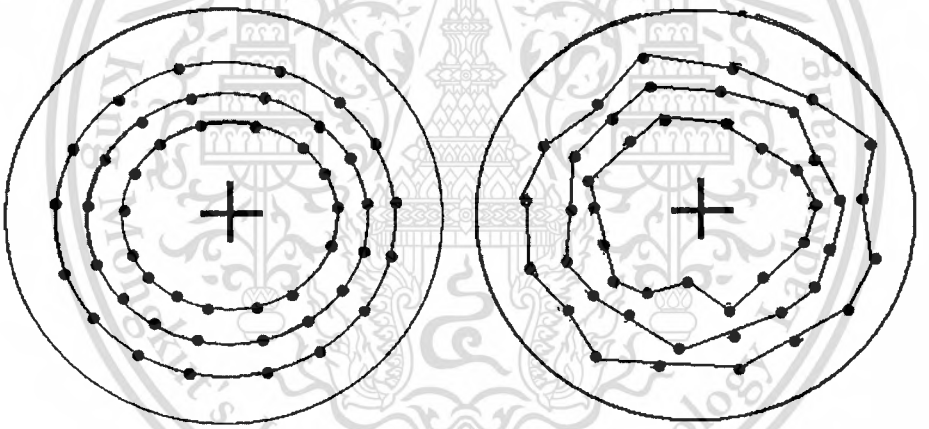

Fig 2.4 Ideal servo tracks and actual servo tracks [8].

2.2.2.1 Repeatable run-out

When the sampling frequency is equal to the spindle rotation frequency, or one of its multiple, the run-out motion produced by apparent tracks will be repeated. This repeated run-out is locked to spindle rotation in both frequency and phase. This is what we call repeatable run-out RRO. The major source of RRO is eccentricity of the track. Other sources include the offset of the track center with respect to spindle centre. RRO is a repetitive event in that both its amplitude and phase are locked to the rotation of the spindle. Therefore, this prior knowledge of RRO can be used as a

feed forward signal to compensate the tracking error. To be a little more specific, assuming that the RRO, *d(t)*, is a time-varying unknown disturbance consisting of a sum of *n* sinusoidal of known frequencies.

$$d(t) = \sum_{i=1}^{N} \left[a_i(t).\cos(w_i t) + b_i(t).\sin(w_i t) \right] \tag{2.2}$$

The adaptive feed forward compensation approach is to design a control

$$\hat{d}(t) = \sum_{i=1}^{N} \left[\hat{a}_i(t).\cos(w_i t) + \hat{b}_i(t).\sin(w_i t) + g_i.k_i.y(t) \right] \tag{2.3}$$

Where g_i is the adaptation gain and k_i is the digital loop gain. Next, an appropriate adaptive algorithm is used to adjust the estimates $\hat{a}_i(t)$ and $\hat{b}_i(t)$ so that these estimates are made equal to the nominal values.

$$\hat{a}_i(t) = a_i(t) \text{ and } \hat{b}_i(t) = b_i(t) \tag{2.4}$$

The RRO disturbance approximated as in (2.2) can then be canceled by the reproduced signal.

2.2.2.2 Non repeatable run-out

NRRO is a product of disk drive vibration and electrical noise in the channel. NRRO can be caused by spindle–bearing defects, windage, disk flutter, electronics noise, etc. in the channel. Since RROs are the harmonics of the motor rotational frequency in the frequency domain, an NRRO is the subtraction of the harmonics from the total indicated run-out (TIR), which can be defined as the distance difference between the R/W head and the previously written track in an HDD, and hence an NRRO in the time domain can be easily constructed by the inverse Fourier transform of an NRRO in the frequency domain [19].

$$RRO(j) = \frac{1}{N} \sum_{i=1}^{N} TIR(i, j) \qquad j = 1,2,....,M \tag{2.5}$$

$$NRRO(i,j) = TIR(i,j) - RRO(j) \text{ where } j = 1,2,....M \tag{2.6}$$

Where N is the number of revolutions of the rotor; M is the number of samples per revolution; i represents the number of disk revolutions, and j represents the number of phases from a fixed point of the slit. An NRRO can be taken care of by the servo controller through improved loop bandwidth. However, the increase in servo bandwidth to reject an NRRO is determined by servo sampling rate, spectrum of the measurement noise, and the existence of plant resonance modes. NRRO can be minimized via improved servo writing, use of better bearings, and the improved design of electronics.

2.2.3 Resonance Compensation

The actuator and HDD structures are not perfectly rigid and have hundreds of flexible modes. This flexibility gives rise on the vibrations, which result in a longer time to settle at the target track and account for a significant component of the TMR. It has been proved that resonance modes that exist within a decade away from the servo-crossover frequency degrade the system performance. The resonance or vibration modes are the major sources of NRROs. Each resonance mode can be modeled as a second-order transfer function. The VCM actuator transfer function displaying multiple resonance modes is given in Section 2.3 and Section 2.4. Although there are hundreds of such resonances in an actual disk drive, but only three or four modes play a significant role in TMR, as other modes have very little amplitude and far away from the interested frequency. One can use of three to four notch filters to suppress the plant model resonance modes. These filters are preferred instead of low-pass filters because the sharper the cutoff in the magnitude of the frequency response, the lower the phase introduced in the loop. The transfer function of an analog notch filter is commonly chosen as.

$$N_{r,i}(s) = \frac{s^2 + (2.\pi.f_0)^2}{s^2 + \frac{2.\pi.f_0}{Q}s + (2.\pi.f_0)^2} \tag{2.7}$$

Where f_0 is the center frequency Q and is the Quality-factor. To use with digital control, digital notch filers can be realized using microprocessors or high-speed Digital Signal Processors.

2.3 Primary VCM actuator model

The mechanical components of servo system in a HDD include VCM, E-block, suspension and slider are shown in Figure 2.5. As seen in this figure, R/W head is fabricated on the edge of slider. The slider is supported by the suspension and flies over the surface of disk on an air-bearing surface (ABS). The VCM controls the suspension with the slider about a pivot in the center of the E-block.

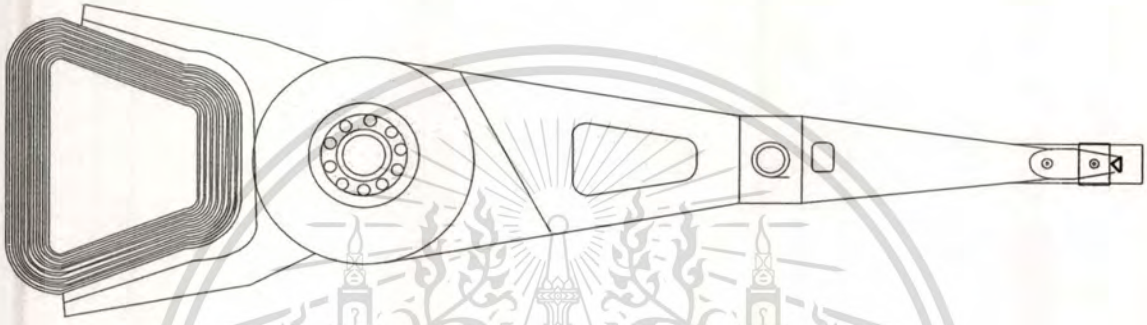

Fig 2.5 Single stage VCM actuator

Dynamic model of HDD servo system can be characterized as a double integrator cascaded with some high frequency resonance modes, which can reduce the system stability if neglected. There are some bias forces that cause steady-state errors in tracking performance. Moreover, there is also some non linearity in the system at low frequencies, which are primarily caused by the pivot-bearing friction. All these factors have to be taken into consideration when considering the design of a controller for the VCM actuator. For the purpose of developing a model, we have to compromise between accuracy and simplicity. The dynamic model of an ideal VCM actuator can be formulated as a second order state space model as follows [19].

$$\begin{pmatrix} \dot{y} \\ \dot{v} \end{pmatrix} = \begin{bmatrix} 0 & k_y \\ 0 & 0 \end{bmatrix} \begin{pmatrix} y \\ v \end{pmatrix} + \begin{pmatrix} 0 \\ k_v \end{pmatrix} u \tag{2.8}$$

Where u is the actuator input (in volts); y and v are the position (in tracks) and the velocity of the R/W head, respectively; k_y is the position measurement gain; $k_y = \frac{k_t}{m}$, k_t is the current/force conversion coefficient, and m is the mass of the VCM actuator. Consequently, the transfer function of an ideal VCM actuator model can be written as a double integrator. However, if the high-frequency

resonance modes are considered, a more realistic model for the VCM actuator will be [19]:

$$G_v(s) = \frac{k_v k_y}{s^2} \prod_{i=1}^{N} G_{r,i}(s) \tag{2.9}$$

Where N is the number of resonance modes; $G_{r,i}(s)$ is the i^{th} resonance mode term which can be modeled as:

$$G_{r,i}(s) = \frac{a_i . s^2 + b_i s + \omega_i^2}{s^2 + 2\xi_i \omega_i s + \omega_i^2} \tag{2.10}$$

Where a_i, b_i, ξ_i and ω_i are the coefficients of ith resonance mode dynamic. For example, in this thesis, a HDD servo system with the model shown in Table 2.2 is studied. Table 2.2 describes the parameters and the uncertainties considered for this VCM model [19, 22].

Table 2.2 VCM parameter with tolerances

Parameter	Value	Tolerance
m	.200Kg	-
k_t	20	-
k_v	6.4013e5	-
ω_1	$2\pi 1905$	3%
ω_2	$2\pi 2511$	5%
ω_3	$2\pi 5011$	5%
ω_4	$2\pi 8317$	5%
ξ_1	.015	10%
ξ_2, ξ_3, ξ_4	0.025	10%
a_1	0.912	-
a_2	0.7286	-
b_1	457.4	-
b_2	962.2	-
a_3, b_3, a_4, b_4	0	...

From Table 2.2, we can see that this VCM actuator have four resonance modes at resonance frequencies 1905, 2511 5011 and 8317 Hz. In order to reduce the effect of high frequency resonance mode, notch filter is added. The notch filter can be modeled using (2.9) and (2.10). For example, three notch filters described in Table 2.3 has been used to compensate the plant resonances. From the table, we can see that in order to compensate 4 resonance modes we are using 3 notch filters.

$$N_r(s) = \prod_{i=1}^{N} N_{n,i}(s) \tag{2.11}$$

Where

$$N_{r,i}(s) = \frac{s^2 + 2\xi_{ni}\omega_{ni}s + \omega_{ni}^2}{s^2 + 2\xi_{ni+1}\omega_{ni}s + \omega_{ni}^2} \tag{2.12}$$

Table 2.3 VCM notch parameters

Notch	ξ_{ni}	ξ_{ni+1}	ω_{ni}
1	0.01	0.10	$2\pi 1900$
2	0.01	0.10	$2\pi 2500$
3	0.01	0.20	$2\pi 5000$

By (2.9), (2.10) and parameters in Table 2.2 the VCM actuator plant can be modeled. The notch filter can be designed (2.11), (2.12) and Table 2.3. Bode diagrams for the plant with and without notch filter is shown in Figure 2.6

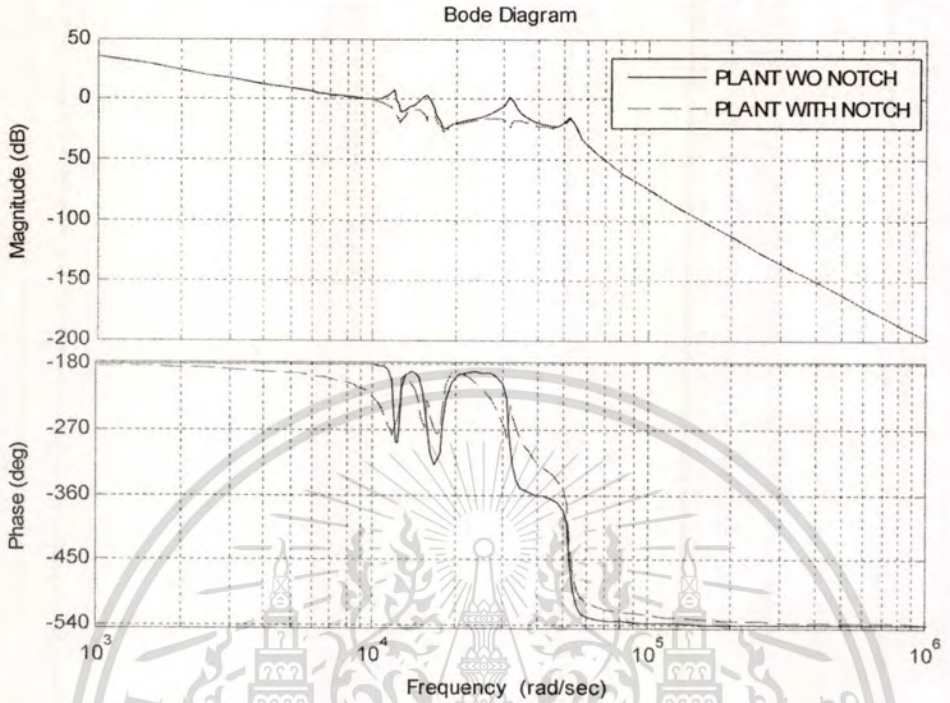

Fig 2.6 Bode plot for VCM actuator model

2.4 VCM micro-actuator model

As data densities in HDD increase and track widths decreases, this leads low error tolerance in positioning of the read/write head. The VCM actuator assembly is large and massive as a unit, the speed at which the head can be controlled is limited. Furthermore, the actuator assembly tends to have a low natural frequency, which can cause the vibration in the disk drive and thus causes for off-track errors. As the track density is going to approach one Terabit per square inch soon, the vibration induced by airflow in a disk drive alone is not enough to force the head off-track as the track pitch is very narrow. Nonlinear friction of the pivot bearing is the other factor of the limitation of the achievable servo precision. A solution to these problems is to complement the VCM with a smaller, second actuator to form a dual-stage servo system. The VCM continues to provide rough positioning, while the second actuator does fine positioning and rejects vibration and other disturbances. The smaller second actuator is typically designed to have a much higher natural frequency and less susceptibility to vibration than the VCM. However, the actuator used in a dual-stage system should be inexpensive to build, requires little power to operate, and preserves the suspension stiffness properties

to maintain an appropriate slider flying height. An example of dual stage actuator is given in Figure 2.7.

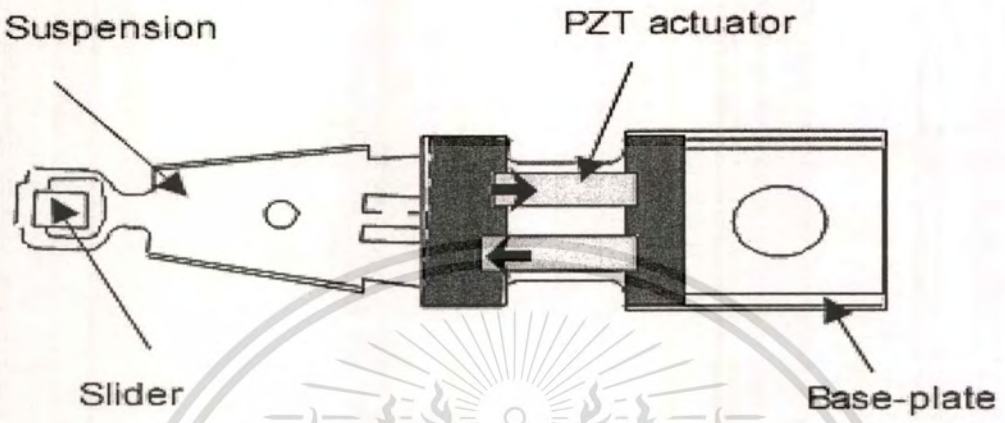

Fig 2.7 Dual stage VCM actuator [21]

The higher bandwidth of the micro-actuator allows the R/W heads to be positioned accurately. The two most fundamental choices in a dual-stage system are the actuator configuration and the control algorithm. They have been proposed for different kinds of micro-actuators such as electromagnetic, electrostatic, piezoelectric, shape memory and rubber micro-actuators etc., each with their own advantages and disadvantages. In this thesis, we focus on the design of HDD servo system with a dual-stage actuator with a piezoelectric actuator in its second stage (see Figure. 2.7).The micro-actuator model is described as [19].

$$G_m(s) = 0.5.\prod_{i=1}^{N} G_{m,r,i}(s) \tag{2.13}$$

Where N is the total number of resonance modes $G_{m,r,i}(s)$ is the ith resonance mode term which can be modeled as:

$$G_{m,r,i}(s) = \frac{a_i.s^2 + b_i s + \omega_i^2}{s^2 + 2\xi_i \omega_i s + \omega_i^2} \tag{2.14}$$

Where a_i, b_i, ξ_i and ω_i are coefficients of i^{th} resonance mode dynamic. HDD servo system with the model shown in Table 2.4 is studied. Table 2.4 describes the parameters and the uncertainty considered for this VCM micro-actuator model [19].

Table 2.4 Micro-actuator parameter with tolerance

Parameter	Value	Tolerance
ω_1	$2.\pi.5488$	-
ω_2	$2.\pi.6376$	-
ω_3	$2.\pi.6832$	-
ω_4	$2.\pi.7408$	5%
ω_5	$2.\pi.7758$	5%
ξ_3	0.0125	5%
$\xi_1, \xi_2, \xi_4, \xi_5$	0.005	5%
a_1	0.7938	10%
a_2	0.955	10%
a_3	0.8912	-
a_4	0.9772	-
b_1	767.9	
b_2	978.6	-
b_3	1013	-
b_4	460.1	
a_5, b_5	0	...

Based on (2.13)-(2.14) and parameters in Table 2.4, the micro-actuator plant can be modeled as 8^{th} order plant. Consequently, in order to minimize the effect of resonance modes in micro-actuator, the following filter in feed forward path is designed. Figure 2.8 shows the bode diagram of the micro-actuator plant.

$$Filter = \left\{ \frac{\begin{array}{l} 1.164\text{x}10^{5}s^{5} + 1.177\text{x}10^{9}s^{4} + 3.99\text{x}10^{14}s^{3} \\ +3.681\text{x}10^{18}s^{2} + 3.112\text{x}10^{23}s + 2.617\text{x}10^{27} \end{array}}{\begin{array}{l} .0002449s^{7} + 47.92s^{6} + 3.99\text{x}10^{6}s^{5} + \\ 1.953\text{x}10^{11}s^{3} + 5.71\text{x}10^{15}s^{3} + 1.058\text{x}10^{20}s^{2} \\ + 8.387\text{x}10^{23}s + 1.309\text{x}10^{27} \end{array}} \right\} \quad (2.15)$$

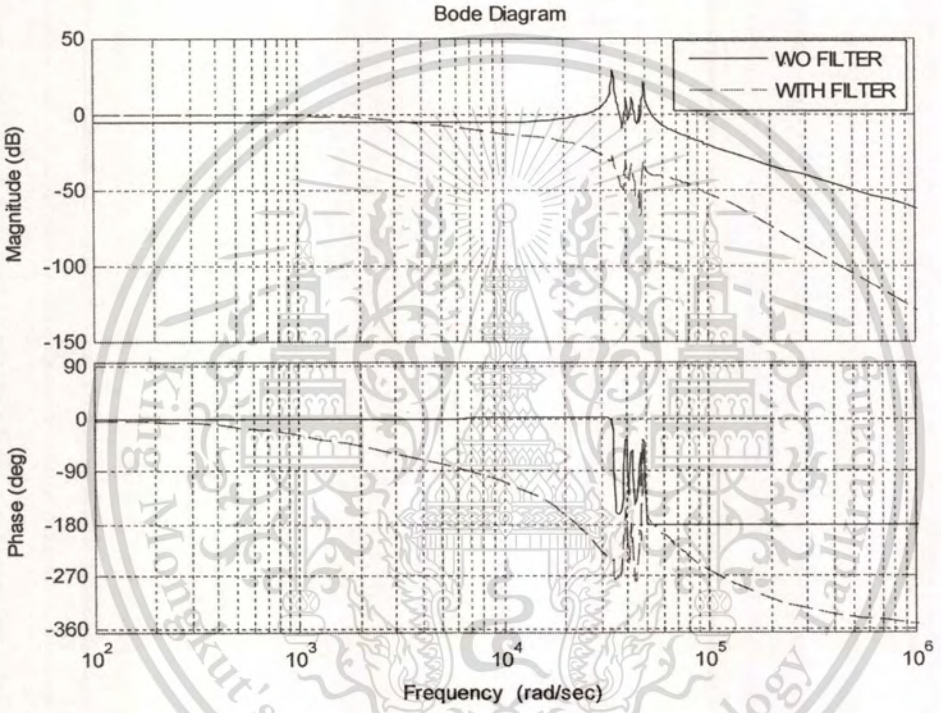

Fig 2.8 Bode diagram of micro-actuator

2.5 Basic controller design

According to the bode stability criteria, the typical shape of bode magnitude plot of a compensated plant open loop transfer function should have the following characteristics [23-24].

1. The bode magnitude plot of the compensated plant should have a high gain above 0 dB and decreases with increasing frequency at a rate of -20*N dB/decade, where N is an integer and N> 2.
2. The bode magnitude plot of the compensated plant crosses the 0 dB with a slope of approximately -20 dB/decade to ensure the stability.

3. The bode magnitude plot of the compensated plant should have low gain under 0 dB and decreases with increasing frequency at a rate of-20*N dB/decade (N>2).

Any typical approach to design the controller for HDD head positioning servo mechanism attempts to meet the above mentioned requirements, and to achieve high servo bandwidth. In order to design a servo controller, a rigid body, which has the model as the double integrator model k/(s)^2 with -40 dB/decade slope along with two to three resonance modes, are used to represent the nominal model of the servo plant. This simplification is reasonable, as the objective is to achieve the desired open loop servo bandwidth as much as possible. However, the bandwidth should be very low compared to the higher frequency of actuator resonances, power amplifier bandwidth, and the sampling frequency so that the ignored dynamics contribute negligible gain (approximately 0 dB) and phase (close to 0°) for frequencies below the servo bandwidth.

In order to change the slope of -40 dB/decade of the uncompensated nominal plant to a -60 dB/decade slope for the compensated plant in the frequencies between ω_1 and ω_2, we need a lag compensator.

$$C_g(s) = \frac{\frac{1}{\omega_2}.s+1}{\frac{1}{\omega_1}.s+1} \tag{2.16}$$

Where $\omega_2 > n_1 * \omega_1$. Accordingly, to change the slope from -40 dB/decade slope to a -20 dB/decade slope in the frequency range between ω_3 and ω_4, a lead compensator can be selected as:

$$C_d(s) = \frac{\frac{1}{\omega_3}.s+1}{\frac{1}{\omega_4}.s+1} \tag{2.17}$$

Where $\omega_4 > n_2 * \omega_3$. The values of n_1 and n_2 help to decide the lead action and the lag action of the lead-lag compensator. The open loop 0-dB crossover frequency f_v should be somewhere in the middle of ω_3 and ω_4. Because of 2 poles and 2 zeros in the combination of these two compensators, it results in 0 dB/decade slope in the high frequency. The required high frequency roll off -40 dB/decade at

frequencies higher than ω_4 is achieved by the actuator model itself. The combined lead-lag compensator $G_C(s)$ can be written as:

$$G_c(s) = K_C \frac{\left(\frac{1}{\omega_2}.s+1\right).\left(\frac{1}{\omega_3}.s+1\right)}{\left(\frac{1}{\omega_1}.s+1\right).\left(\frac{1}{\omega_4}.s+1\right)} \tag{2.18}$$

$$K_c = \left[\frac{\left(\frac{1}{\omega_2}.s+1\right).\left(\frac{1}{\omega_3}.s+1\right).s^2}{\left(\frac{1}{\omega_1}.s+1\right).\left(\frac{1}{\omega_4}.s+1\right).K}\right]_{s=j2\pi f_v} \tag{2.19}$$

This compensator makes the open loop transfer function $G_C(s).G_P(s)$ crossing the 0 dB line at frequency (f_V) with a slope of -20 dB/decade. The design can be further simplified by assigning pre-defined relations between frequencies of different poles and zeros of the compensator, and the desired cross-over frequency (f_V). The various transfer functions for the system can be illustrated below.

Open Loop transfer function: $L(s) = G_c(s).G_P(s)$

Controller Transfer function: $G_c(s)$

Sensitivity transfer function: $S(s) = \frac{1}{1+G_c(s).G_P(s)}$

Complementary sensitivity transfer function: $T(s) = \frac{G_c(s).G_P(s)}{1+G_c(s).G_P(s)}$

Shock transfer function: $S_h(s) = \frac{G_P(s)}{1+G_c(s).G_P(s)}$

2.6 Integration of VCM and micro-actuator systems:

In the dual-stage actuator, the primary actuator, i.e., the VCM actuator has larger inertia and lower bandwidth but provides a larger range of movement. The secondary actuator (micro-actuator), on the other hand, is lighter, has greater bandwidth but supports a very small range of displacement. Because of these trade-offs, the design of combination of two actuators must be carefully considered

in order to achieve maximum bandwidth. Followings are the guidelines while designing a controller for DSA.

1. The VCM actuator responds to low frequency components of error while the micro-actuator responds to the high frequency error signals.
2. Hand-off frequency: Hand-off is a frequency where the magnitudes of the compensated VCM branch and the compensated micro-actuator branch are equal. The phase difference between the outputs of the secondary stage and that of the VCM should be $\leq 120^{\circ}$ at the hand-off frequency to avoid destructive interference. Since the resultant displacement of the slider is sum of displacements contributed by two actuators, they cancel each other when they are out of phase.
3. The gain of the VCM actuator should exceed the micro-actuator's gain by 20 dB for frequencies below 60 Hz to avoid the saturation of the secondary stage actuator.

Various methods of designing controller for the DSA have been reported in many published papers. Common configurations used by those papers are:

1. parallel loop
2. decoupled master-slave loop

2.6.1 Parallel structure

The parallel structure of DSA control is shown in Figure 2.9. The open loop transfer function *Op(s)*, close-loop transfer function *Tp(s)*, sensitivity transfer function *Sp(s)* are given as [23]

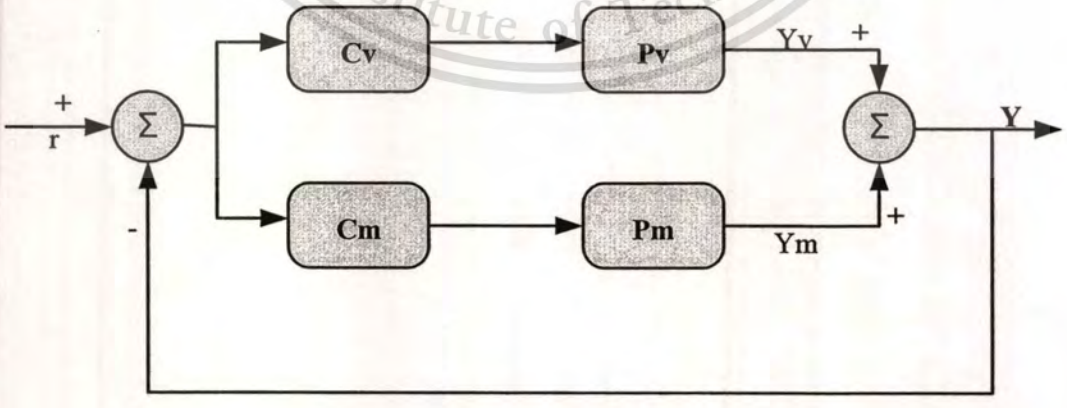

Fig 2.9 Parallel structure configuration [23]

$$O_P = C_V P_V + C_M P_M$$

$$T_P = \frac{C_V P_V + C_M P_M}{1 + C_V P_V + C_M P_M}$$

$$S_P = \frac{1}{1 + C_V P_V + C_M P_M}$$

Abdullah Al Mamun presented a controller design for parallel DSA structure [23] using PID controllers. As elaborated in his design, his approach gives a stable system although some aspects of hand-off frequency are not so desirable. From his design, he was able to achieve crossover frequency of the micro-actuator loop frequency (f_m) = 2.02 kHz, and the same for the VCM path frequency (f_v) = 1 kHz. The gain and phase delay of the micro-actuator loop at 2 kHz are 1 dB and 76°, respectively. The gain and phase of the VCM loop are 0.4133 dB and -139°, respectively at 2000 Hz. These two loops work in parallel and generate a loop gain of 1.2419 dB and phase delay of about 93° at frequency f_m. At the 0-dB crossover frequency, which is approximately 2020 Hz, the phase is about 80° above -180°.

2.6.2 Decouple master slave structure

For this configuration, the open loop transfer function L_{dms}, the closed-loop transfer function T_{dms} and the sensitivity transfer function S_{dms} are defined as: [23]

$$L_{dms} = (1+C_M P_M) C_V P_V + C_M P_M$$

$$T_{dms} = \frac{C_V P_V + C_M P_M + C_V P_V C_M P_M}{(1 + C_V P_V)(1 + C_M P_M)}$$

$$S_{dms} = \frac{1}{1+C_V P_V} \cdot \frac{1}{1+C_M P_M}$$

The decoupled master slave (DMS) configuration is shown in Figure 2.10.

Abdullah Al Mamun got following result for this structure from the same plant as in the parallel structure section. He chose the lag-lead compensator, such that the zero dB gain crossover occurs at

500 Hz for the VCM (Kv Pv) loop and at 2 kHz for the PZT loop. A 76° phase lag at 2 kHz for the PZT path, whereas the gain and phase of the VCM path at 2 kHz are 0.65 dB and 177°, respectively.

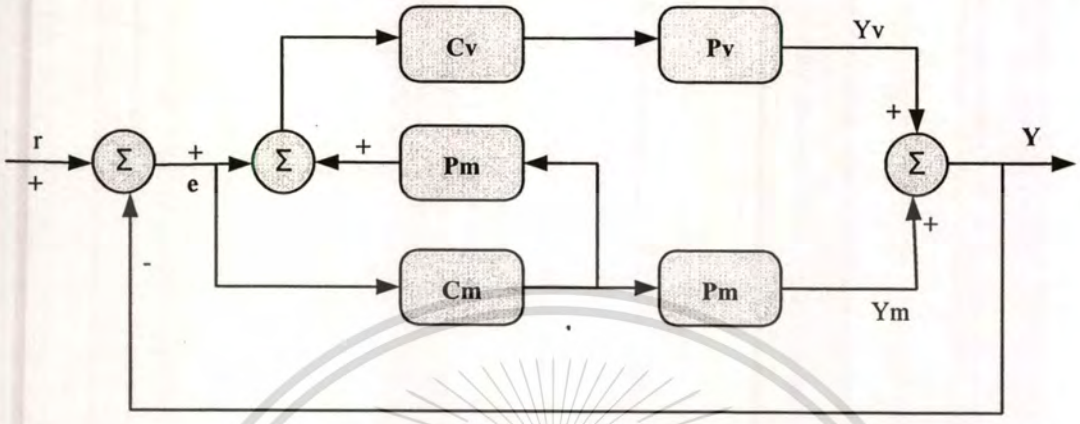

Fig 2.10 DMS Configuration [23]

With the addition of the PZT loop in the compensation of the VCM, the gain becomes 9.42 dB and the phase delay becomes 170° at 500 Hz. Overall, the combined dual-loop has a gain of about 1.08 dB and a phase delay of 68° at 2 kHz. The phase margin is about 69° considering the gain drop. The overall bandwidth is slightly higher than the bandwidth of the micro-actuator path.

2.6.3 PQ method

In the previous section, the Parallel structure and Decouple Master slave structure methods to design controller for Micro Electro Mechanical System (MEMS) DSA have been described. But the methods in those sections were not able to take care of the phase difference at the hands off frequency between two parallel paths. In order to take care of the above problem, the PQ method includes the proper hand off frequency into the design process itself. The block diagram for PQ method is given in Figure 2.11. This is a two step design approach; in the first step, we design a loop shaping control for a Dual input single output (DISO) converted into single input single output SISO. And finally we design a controller CSISO for SISO system.

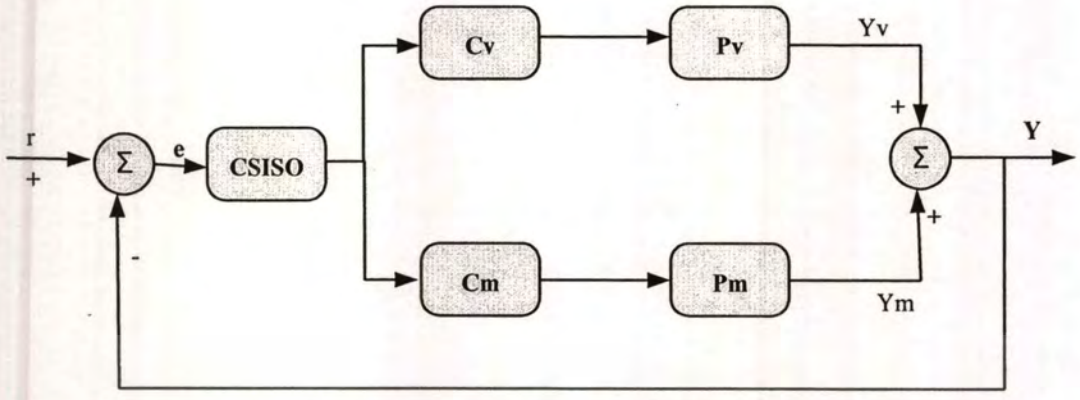

Fig 2.11 PQ method configuration [23]

In the first step of PQ design method, the controllers Cv and Cm are chosen simultaneously to address the issues of stable zeros, relative contribution of the two actuators to the combined output, and the interference between the two contributions. Lets define the ratio R(s) between the transfer functions of the VCM path and the transfer function of the micro-actuator path as following,

$$R(s) = \frac{Pv.Cv}{Pm.Cm} \tag{2.20}$$

Where Pv is the VCM plant Transfer function; Cv is the VCM controller transfer function; Pm is the Micro-actuator plant transfer function; Cm is the Micro-actuator controller transfer function.

This ratio determines the relative share of contribution between the two actuators. This division of task defines the desired shape of the ratio *R(s)* which should have large magnitude (>> 1) at low frequency and small magnitude (<< 1) at high frequency.

The transfer functions Cv(s) and Cm(s) are selected such that open loop transfer functions for the VCM (Cv(s)Pv (s)), micro-actuator (Cm(s).Pm(s)), and an acceptable frequency response for R(s) are obtained. After selecting these two compensators, the two parallel branches are combined to form a single-input single-output model P_{SISO} :

$$P_{SISO} = C_V(s).P_V(s) + C_M(s).P_M(s) \tag{2.21}$$

We can design CSISO by any kinds of simple lead-lag controller to fulfill our desired loop shape. The PQ method provides a simple, but effective way to allocate the control effort between two actuators of a dual-stage actuation system. One can use various optimal control methods instead of the simple lead-lag compensator as shown above to design the controller for the compensated model PSISO.

2.7 Conclusion

In this chapter, several literature reviews on the most recent methods for designing servo controller and the way to enhance the bandwidth (BW) of the entire system are discussed. The issues on the HDD servo system and the way to handle them have been illustrated. We also discussed the VCM and micro-actuators model along its resonance modes. These models and modes are used in the next chapters for simulation studies. In addition, a simple lead-lag controller design and the integration method in designing the servo controller has been discussed.

Chapter 3

Research Methodology

In this thesis, the designed controller is based on the concept of H_∞ robust loop shaping control, which is a sensible method to design a robust controller. This chapter describes the research methodology and is organized as follows. Section 3.1 describes the concept of conventional H_∞ loop shaping control. Section 3.2 describes the proposed technique, which is based on the conventional robust loop shaping technique; GA which is an optimization technique in order to find the controller parameters is also described. In order to improve the tracking performance, a structure of 2DOF controller in section 3.3 is discussed. Section 3.4 illustrates the list of equipment used in this research work. Finally, we conclude this chapter with data analysis method in Section 3.5

3.1 Conventional H_∞ loop shaping

This approach requires two weighting functions, W_1 (pre-compensator) and W_2 (post-compensator), for shaping the nominal plant G_0 so that the desired open loop shape is achieved. In this approach, the shaped plant is formulated as normalized co-prime factor, which separates the shaped plant G_s into normalized co-prime factors N_s and M_s [10]. Note that,

$$G_s = W_1.G_0.W_2 = N_s.M_s^{-1} \tag{3.1}$$

Step 1: Shape the singular values of the nominal plant G_0 by using a pre-compensator W_1 and/or a post-compensator W_2 to get the desired loop shape. In SISO system, the weighting functions W_1 can be chosen as:

$$W_1 = K_W \frac{s+a}{s+b} \tag{3.2}$$

Where a, b, K_W are positive and real numbers.

The weight W_2 can be chosen as:

$$W_2 = \frac{s+c}{s+d} \tag{3.3}$$

Where c and d are positive and real numbers. The perturbed plant of shaped plant (Figure 3.1) can be written as

$$G_\Delta = (N_s + \Delta_{N_s})(M_s + \Delta_{M_s})^{-1} \tag{3.4}$$

Where Δ_{N_s} and Δ_{M_s} are uncertainty transfer functions and $\left\|\Delta_{N_s}, \Delta_{M_s}\right\| \leq \varepsilon$; ε is uncertainty boundary called stability margin. The objective of robust stabilization is to stabilize not only the nominal model but a family of perturbed plants defined by.

$$G_\Delta = \{(N_s + \Delta_{N_s})(M_s + \Delta_{M_s})^{-1} : \left\|\Delta_{N_s}\ \Delta_{M_s}\right\|_\infty < \varepsilon\} \tag{3.5}$$

There are some guidelines for selecting the weights available in [10].

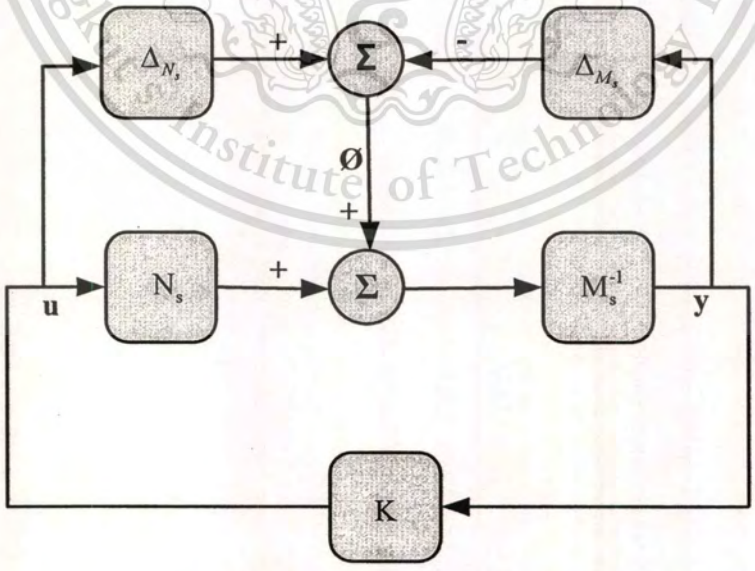

Fig 3.1 Prime cofactor uncertainty

Step 2: Calculate ε_{opt} by solving the following inequality.

$$\gamma_{\text{opt}} = \varepsilon_{opt}^{-1} = \inf_{stab\ K} \left\| \begin{bmatrix} I \\ K \end{bmatrix} (I + GK)^{-1} M_s^{-1} \right\| \tag{3.6}$$

Given a shaped plant *Gs* and *A, B, C, D* represent the shaped plant in the state-space form. To determine ε_{opt}, there is a unique method as follows

$$\gamma_{\min} = \varepsilon_{\max}^{-1} = (1 + \lambda_{\max}(\mathrm{X}.\mathrm{Z}))^{1/2} \tag{3.7}$$

Where *X* and *Z* are the solutions of two Riccati in (3.8) and (3.9) respectively; λ_{max} is the maximum eigen value.

$$(\mathrm{A} - \mathrm{B}.\mathrm{S}^{-1}\mathrm{D}^{\mathrm{T}}\mathrm{C}).\mathrm{Z} + \mathrm{Z}.(\mathrm{A} - \mathrm{B}.\mathrm{S}^{-1}\mathrm{D}^{\mathrm{T}}\mathrm{C})^{\mathrm{T}} - \mathrm{Z}\mathrm{C}^{\mathrm{T}}.\mathrm{R}^{-1}\mathrm{C}.\mathrm{Z} + \mathrm{B}.\mathrm{S}^{-1}\mathrm{B}^{\mathrm{T}} = 0 \tag{3.8}$$

$$(\mathrm{A} - \mathrm{B}.\mathrm{S}^{-1}\mathrm{D}^{\mathrm{T}}\mathrm{C}).\mathrm{X} + \mathrm{X}.(\mathrm{A} - \mathrm{B}.\mathrm{S}^{-1}\mathrm{D}^{\mathrm{T}}\mathrm{C})^{\mathrm{T}} - \mathrm{X}\mathrm{B}\mathrm{S}^{-1}\mathrm{B}^{\mathrm{T}}\mathrm{X} + \mathrm{C}^{\mathrm{T}}.\mathrm{R}^{-1}\mathrm{C} = 0 \tag{3.9}$$

Where

$$\mathrm{S} = \mathrm{I} + \mathrm{D}^{\mathrm{T}}.\mathrm{D}$$
$$\mathrm{R} = \mathrm{I} + \mathrm{D}.\mathrm{D}^{\mathrm{T}}$$

To ensure the robust stability of the nominal plant, the weighting function is selected so that $\varepsilon_{opt} \geq 0.25$ [10]. If ε_{opt} is not satisfied, then go to Step 1 to adjust the weighting functions.

Step 3: Select $\varepsilon < \varepsilon_{opt}$ and then synthesize a controller K_∞ that satisfies (3.10)

$$\left\| \begin{bmatrix} I \\ K_\infty \end{bmatrix} (I + G_s K_\infty)^{-1} M_s^{-1} \right\| \leq \varepsilon^{-1} \tag{3.10}$$

Controller K_∞ is obtained by solving the sub-optimal control problem in (3.10). The details of this solving are as follows [10]. G_s and *A, B, C, D* represent the shaped plant in the state-space form. *Gs* has a minimal state-space realization as given below

$$G_s = \left[\begin{array}{c|c} A & B \\ \hline C & D \end{array}\right]$$

Then a minimal state-space realization of a normalized left co-prime factorization is given by

$$[N, M] = \left[\begin{array}{c|cc} A + HC & B + HD & H \\ \hline R^{-1/2}.C & R^{-1/2}D & R^{-1/2} \end{array}\right]$$

$$H = -(BD^T + Z.C^T).R^{-1}$$

Step 4: Final controller (K) is determined by.

$$K = W_1 K\infty W_2 \tag{3.11}$$

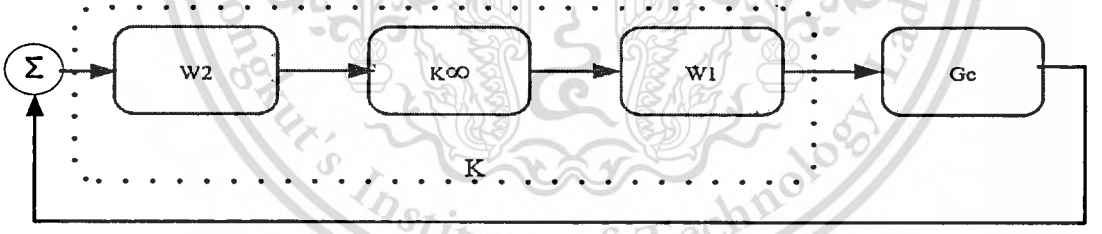

Fig 3.2 H_∞ Loop shaping controller

3.2 Genetic algorithm based fixed -structure H_∞ loop shaping optimization

In the proposed technique, GA is adopted in control synthesis. Genetic algorithms are well known as a biologically inspired class of algorithms applicable to any nonlinear optimization problems. This algorithm applies the concept of chromosomes and the genetic operations of crossover, mutation and reproduction. A chromosome is an individual sample in a population. Each individual is assigned a fitness based on evaluation and objective function. At each step called

generation, fitness values of all individuals in a population are calculated. Individual with maximum fitness value is retained as a solution in the current generation and passed to the next generation. To form a new population of the next generation, crossover, mutation, and reproduction are used. Crossover randomly selects a site along the length of two chromosomes and then splits the two chromosomes at the crossover site. New chromosomes are then formed by matching the head of one chromosome with the tail of the other. Mutation forms a new chromosome by randomly changing a single bit in the chromosome. Reproduction forms a new chromosome by copying the old chromosome. The process of these operations is illustrated in the Figure 3.3 given below. Chromosome selection in genetic algorithms depends on the fitness value. High fitness means a higher chances of being selected. Mutation, reproduction, or crossover depends on the pre-specified operation's probability. Individual samples in the genetic population are coded in binary. For real numbers, decoding binary to floating-point numbers is used [9].

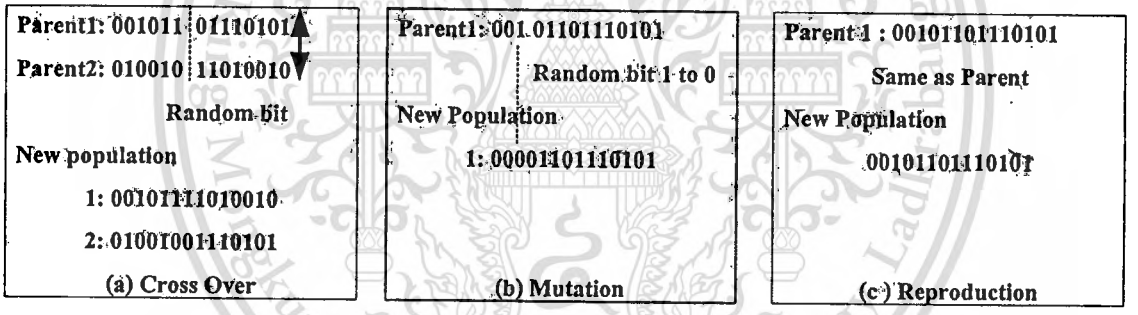

Fig 3.3 Genetic operations (a) Crossover, (b) Mutation, (c) Reproduction

In this thesis, the genetic searching algorithm is adopted to solve the Fixed-Structure H_∞ Loop Shaping Optimization problem. Although the proposed controller is structured, it still retains the entire robustness and performance guarantee as long as a satisfactory uncertainty boundary ε is achieved. Assume that the predefined structure controller $K(p)$ has specified parameter p, based on the concept of H∞ loop shaping, optimization goal is to find parameter p in the controller $K(p)$, that minimizes infinity norm from disturbances w to states z, $\|T_{ZW}\|_\infty$. From (3.11), assuming that W_1 and W_2 are invertible, then $K_\infty = W_1^{-1}K(p)W_2^{-1}$. Substituting this equation into (3.6), the ∞-norm of the transfer function matrix $\|T_{ZW}\|_\infty$ which is subjected to be minimized can be written as:

$$J_{\text{cost}} = \gamma = \|T_{ZW}\|_\infty = \left\| \begin{bmatrix} I \\ W_1^{-1} K(p) W_2^{-1} \end{bmatrix} (I + G_s W_1^{-1} K(p) W_2^{-1})^{-1} M_s^{-1} \right\|_\infty \tag{3.12}$$

The optimization problem can be written as

Minimize $\left\| \begin{bmatrix} I \\ W_1^{-1} K(p) W_2^{-1} \end{bmatrix} (I + G_s W_1^{-1} K(p) W_2^{-1})^{-1} M_s^{-1} \right\|_\infty$ subject to $p_{i,\min} < p_i < p_{i,\max}$

where $p_{i,\min i}, p_{i,\max}$ are lower and upper bounds of the parameter p_i in controller $K(p)$ respectively. The fitness function in the controller synthesis can be written as following

$$Fitness = \begin{cases} \left(\left\| \begin{bmatrix} I \\ W_1^{-1} K(p) W_2^{-1} \end{bmatrix} (I + G_s W_1^{-1} K(p) W_2^{-1})^{-1} M_s^{-1} \right\|_\infty \right)^{-1} \\ \qquad \text{If K(p) stabilizes the plant.} \\ 0.00001 \qquad \text{Otherwise} \end{cases} \tag{3.13}$$

The fitness is set to a small value (in this case is 0.00001) if *K(p)* does not stabilize the plant. Our proposed algorithm is summarized as follows. The flow chart of the proposed technique is given in Figure. 3.4

Step 1 Follow steps 1 and 2 in the conventional H_∞ Loop Shaping Optimization to select the weights. Specify the genetic parameters such as initial population size, crossover and mutation probability, maximum generation, etc.

Step 2 Select a controller structure *K(p)* and randomly initialize several sets of parameters *p* as population in the 1st generation.

Step 3 Evaluate the fitness value of each chromosome using (3.13). Select the chromosome with maximum fitness value as a solution in the current generation. Increment generation for a step.

Step 4 While the current generation is less than the maximum generation, create a new population using genetic operators and go to step 3. If the current generation is the maximum generation, then stop.

Step 5 Check performances in both frequency and time domains. If the performance is not satisfied such as too low $\mathcal{E}$ (too low fitness function), then go to step 2 to change the structure of controller.

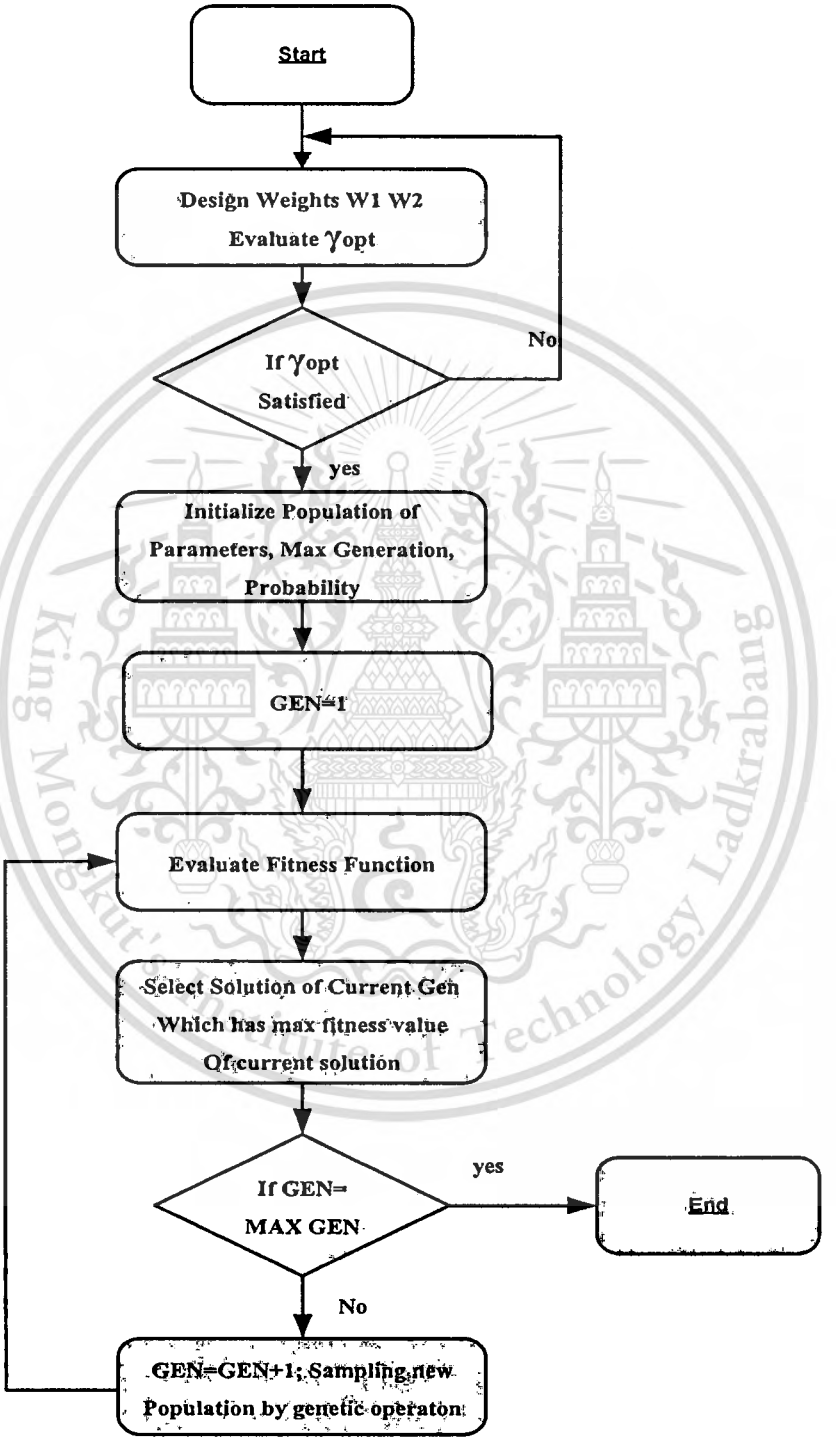

Fig 3.4 Flow chart of GA [9]

3.3 Method to improve tracking performance

It is noted from the literature review that PID control generates large overshoots compared to other advanced controllers [19]. It is very hard to achieve very good reference input tracking and disturbance rejection simultaneously with single feedback control, and the main reason for that is shortcoming of the PID control is mainly due to its structure *i.e.* it only feeds in the error signal, (r – ym) , instead of feeding in both reference signal r and output y_m independently. The solution is to use a two degrees-of-freedom controller where the reference signal r and output measurement y_m are independently treated by the controller, rather than operating on their difference (r - y_m) as in a one degree-of-freedom controller. There are several alternative implementations of a two degrees-of-freedom controller. We follow one of the common structures in our design as shown is Figure 3.5.

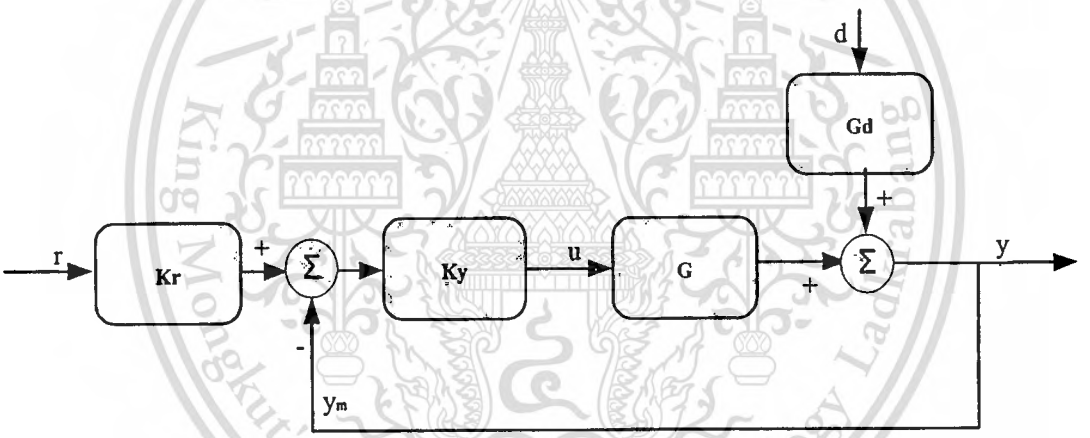

Fig. 3.5 Two Degree of freedom control configuration

Where K_y denotes the feedback part of the controller, and Kr is a reference pre-filter. The feedback controller Ky is used to reduce the effect of uncertainty (disturbances and model error) whereas the pre-filter Kr shapes the command r to improve tracking performance. In general, it is optimal to design the combined two degree-of-freedom controller K in one step [21]. However, in practice Ky is often designed first for disturbance rejection, and then Kr is designed to improve reference tracking. A convenient choice of the pre-filter is the lead-lag controller.

$$K_r(s) = \frac{\tau_{lead}.s + 1}{\tau_{lag}.s + 1} \tag{3.14}$$

Here we select $\tau_{LEAD} > \tau_{LAG}$ if we want to speed up the response, and $\tau_{LEAD} < \tau_{LAG}$ if we want to slow down the response [10]. If one does not require fast reference tracking, which is the case in several process control applications, a simple lag is often used $\tau_{LEAD} = 0$.

3.4 List of equipments and software

Following equipment and software are used to perform the experiment of this thesis.

1. WD Spiral Seeded HDD,
2. S4W Interface equipment,
3. Oscilloscope with Differential Probe,
4. Power Supply,
5. MATLAB with SIMULINK,
6. ARM Compiler.

3.5 Data analysis and Verification

For designing and simulation of the controller, MATLAB with SIMULINK software is used; however, for actual implementation we adopted the proposed controller on the WD VCM actuator model. After implementation of the controller on HDD, we use the history and S/W log files for data analysis. Thus, in this chapter, the conventional H_∞ technique has been discussed and after that the proposed technique using GA to optimize H_∞ Robust controller has been discussed. The way to improve the tracking performance by 2 DOF controllers has been explained in the next chapter.

Chapter 4

Controller design for single stage VCM actuator

This chapter describes a robust controller design using conventional H_∞ loop shaping technique followed by the fixed-structure H_∞ loop shaping control using our own proposed technique. Section 4.1 explains the basic requirement specifications and the classical robust H_∞ controller. Next, the design of a robust controller using GA is illustrated. In order to improve the tracking performance, we added an additional compensator in the structure of 2DOF controller, which is explained in Section 4.2. Robustness test on our proposed controller is explained in Section 4.3. Hardware implementation of our proposed controller is described in Section 4.4. At the end of this chapter, based on the simulation and experimental results, the proposed technique is superior to several other existing techniques.

4.1 H_∞ loop shaping controller design

According to bode stability criteria, in this thesis, typical shape of bode magnitude plot of the compensated plant open loop transfer function should follow the characteristics explained in section 2.5 along with following specifications [25].

1) Overshoot and undershoot of the step response should be kept less than 5% as the R/W head can start to read or write within 5% of the target.

2) The 5% settling time in the step response should be less than 2ms.

This section describes the robust controller design using classical H_∞ loop shaping technique followed by robust controller design using the proposed H_∞ loop shaping technique. The proposed controller parameters are optimized using GA. We have selected plant and notch filters based on the Tables 2.2 and 2.3. The weights have been designed based on the guidelines in Section 3.1; the weight W_1 and W_2 can be selected as [10]:

$$W_1 = 4.99 * \frac{s + 617.41}{s + 1.09} \tag{4.1}$$

$$W_2 = \frac{s + 81.23}{s + 130470} \tag{4.2}$$

By these weights, a slope of -20 dB/decade at the cross over point can be achieved, and it provides gain margin of 12dB and phase margin of 67.5^0. First, we applied the conventional H_∞ loop shaping (HLS) technique to design a robust controller as the guideline provided in Sections 3.1. The resulting controller by this approach is 18^{th} order robust controller as shown in following:

$$HLS\_con = \left\{ \frac{\begin{array}{l} 2.238x10^4 s^{17} + 3.453x10^9 s^{16} + 1.968x10^{14} s^{15} \\ + 1.903x10^{18} s^{14} + 5.649x10^{23} s^{13} + 3.56x10^{28} s^{12} \\ + 6.737x10^{32} s^{11} + 2.992x10^{37} s^{10} + 3.718x10^{41} s^9 \\ + 1.224x10^{46} s^8 + 1.008x10^{50} s^7 + 2.542x10^{54} s^6 \\ + 1.314x10^{58} s^5 + 2.569x10^{62} s^4 + 6.883x10^{65} s^3 \\ + 9.995x10^{69} s^2 + 4.703x10^{72} s + 3.194x10^{74} \end{array}}{\begin{array}{l} s^{18} + 1.74x10^5 s^{17} + 1.19x10^{10} s^{16} + 1.03x10^{15} s^{15} \\ + 4.27x10^{19} s^{14} + 2.162x10^{24} s^{13} + 6.332x10^{28} s^{12} \\ + 2.046x10^{33} s^{11} + 4.513x10^{37} s^{10} + 9.5x10^{41} s^9 \\ + 1.646x10^{46} s^8 + 2.261x10^{50} s^7 + 3.14x10^{54} s^6 \\ + 2.659x10^{58} s^5 + 2.966x10^{62} s^4 + 1.272x10^{66} s^3 \\ + 1.089x10^{70} s^2 + 7.071x10^{72} s + 5.031x10^{74} \end{array}} \right\} \tag{4.3}$$

HLS controller is able to satisfy all the uncertain modes with the γ = 1.7137. As shown in (4.3), the order of HLS controller is 18 and it is not easy to implement practically.

Next, a fixed-structure robust controller using the proposed algorithm is designed. We follow the guidelines in Section 3.2 to design the controller [2]. The structure of controller is selected as the second order lead-lag controller which can be expressed in (4.4).

$$Cont = \left\{ K_3 \frac{(s + k1)(s + k2)}{(s + k4)(s + k5)} \right\} \tag{4.4}$$

In the optimization, the ranges of search parameters and GA parameters are set as follows. By considering W_1 and W_2, range of controller parameters can be selected in order to maintain the

integrity of bode stability criteria [10-11]. $k_1 \in [10\ 100]$; $k_2 = [500\ 1500]$; $k_3 \in [1\ 10]$; $k_4 \in [0.01\ 10]$; $k_5 \in [10000\ 150000]$. Population size=100; crossover probability =0.6; mutation probability=0.1; maximum generation = 30. When running GA for 14 generations, an optimal controller can be found as [2]:

$$Cont(PPD) = \left\{ 4.7787 \frac{(s+51.87)(s+689.89)}{(s+0.4879)(s+134600)} \right\} \tag{4.5}$$

Figure 4.1 shows a plot of convergence of fitness function (stability margin) versus generations by genetic algorithm. As shown in Figure 4.1, the optimal robust PID controller provides a satisfied stability margin of 0.5156.

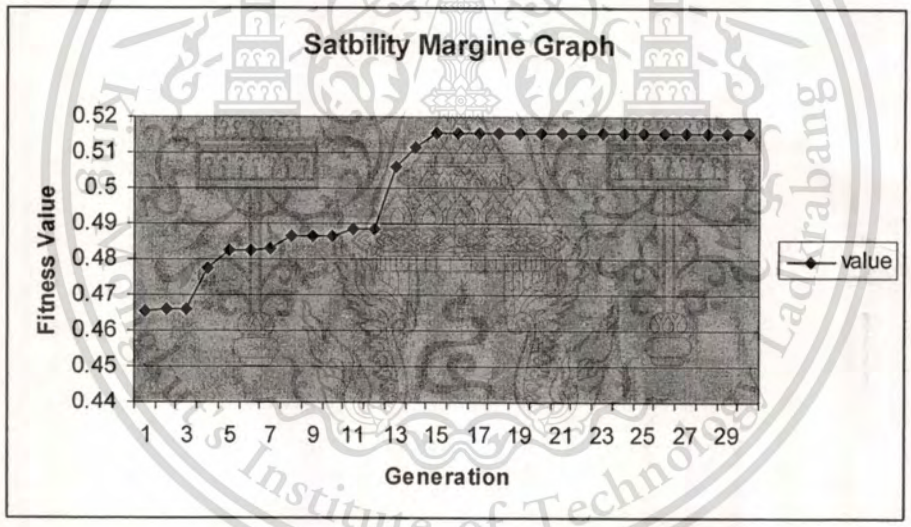

Fig 4.1 Convergence of fitness value

Figure 4.2 shows the comparison of the open loop bode plots by the proposed controller and HLS. In this figure, the HLS controller is able to provide gain margin of 13.4 dB with phase margin of 65.3^0, while our GA based controller without pre-filter is able to provide gain margin of 12.6dB and phase margin of 66.1^0

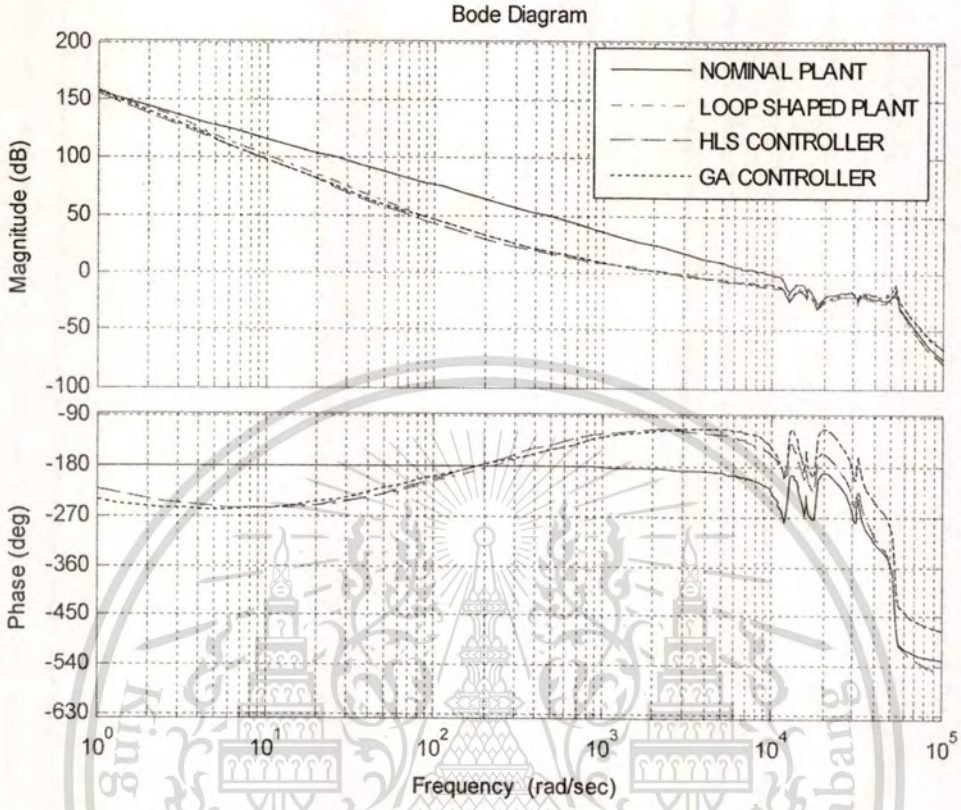

Fig 4.2 Bode diagram of the open loop transfer function for the shaped plant, Nominal Plant, Plant with HLS and proposed controller

Disturbance rejection curves normally referred as sensitivity transfer function can be derived by the equation given below:

$$S(s) = \frac{1}{1 + G_c(s).G_p(s)}$$

Where G_c is the controller transfer function, and G_p is the plant transfer function. With the feedback part, the controller is able to use the output to shape the input of the system. In this way, various disturbances do not affect the system as much and do not create such huge deviations from our desired output. Disturbance rejection curve of the system controlled by our proposed controller, HLS controller, and the shaped plant are given in Figure 4.3. From the figure, we can see that the

proposed controller is able to provide the same quality of disturbance rejection as HLS. The disturbance rejection at lower frequency is very good and there is no amplification of disturbance below and above zero crossing. If margins are too low, we could have a seek settle problem, performance degradation, higher TMR, higher error rates. However, if margins are too high, TMR may not reach its target. Another issue is with bandwidth (BW); If BW is too low due to higher margins, it may not pass the required specifications. This is the trade-off for lower margin and higher margin. Here, in this case, the sufficient margin for the designed system is considered. However, increasing BW always leads both system and resonance towards instability. Thus, too much BW increase is overreacting and has no extra benefits.

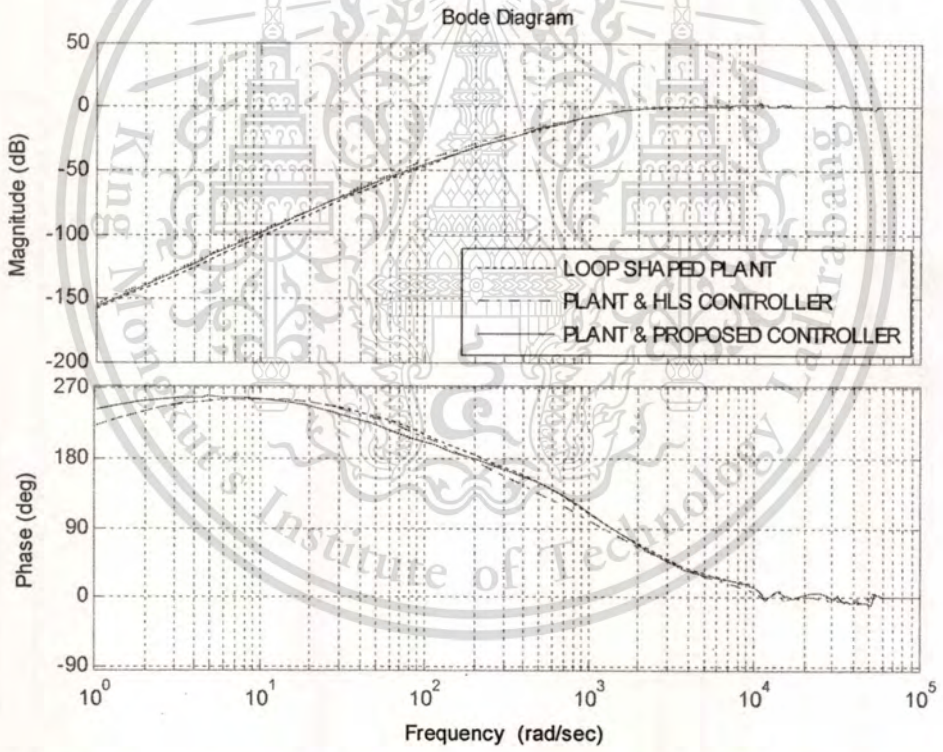

Fig 4.3 Error Rejection curve of the shaped plant, plant with HLS and proposed controller

4.2 Compensator for tracking performance

In addition, a fixed-structure pre-filter is designed to achieve the tracking performance specification. In this filter, we selected a 1st order lead-lag controller, *Kr(s)* as [10].

$$K_r(s) = \frac{\tau_{lead}.s + 1}{\tau_{lag}.s + 1} \tag{4.6}$$

Thus, our overall system with pre-filter is given in Figure 4.4. Detailed method for improving the tracking response with 2DOF controller structure is explained in Section 3.3.

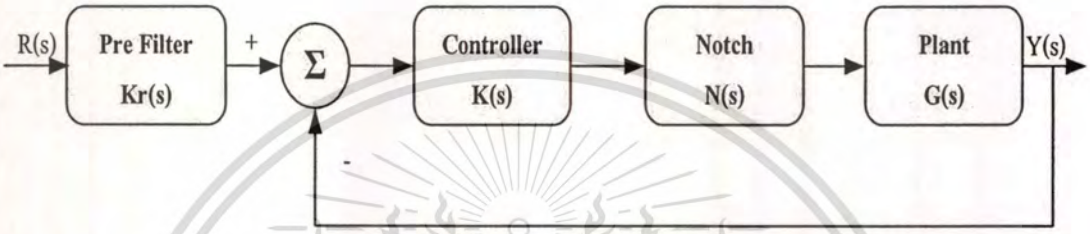

Fig 4.4 Over all system with pre filter

The pre-filter was also designed by GA. As the specifications, we set the constraints as follows: over shoot <=5%, and 5% settling time <= 1.5ms. For pre-filter, the critical parameters are time constant. τ_{lead} and τ_{lag} are the parameters needed to be designed. By running GA, we found that the value of Kr(s) is [2]

$$K_r(s) = \frac{.001671.s + 1}{.002122.s + 1} \tag{4.7}$$

This pre-filter can improve the gain margin a bit up to 14.6 dB while it can achieve phase margin 60.2^0. Responses from the unit step command by the HLS and the proposed robust control at the nominal plant are shown in Figure 4.3. Table 3 shows the performance obtained by all controllers. As seen in Figure 4.5 and Table 3, the maximum overshoot obtained by HLS controller and the conventional PID is much higher than that of the proposed PID. In our proposed controller the maximum over shoot is always less than 5% (the settling criteria) the settling time chosen hear as the time response reaches to 95% which is less than 1ms. 5% settling time of our proposed controller is much faster than that of the other controllers. Clearly, time domain specifications can be achieved by our proposed technique.

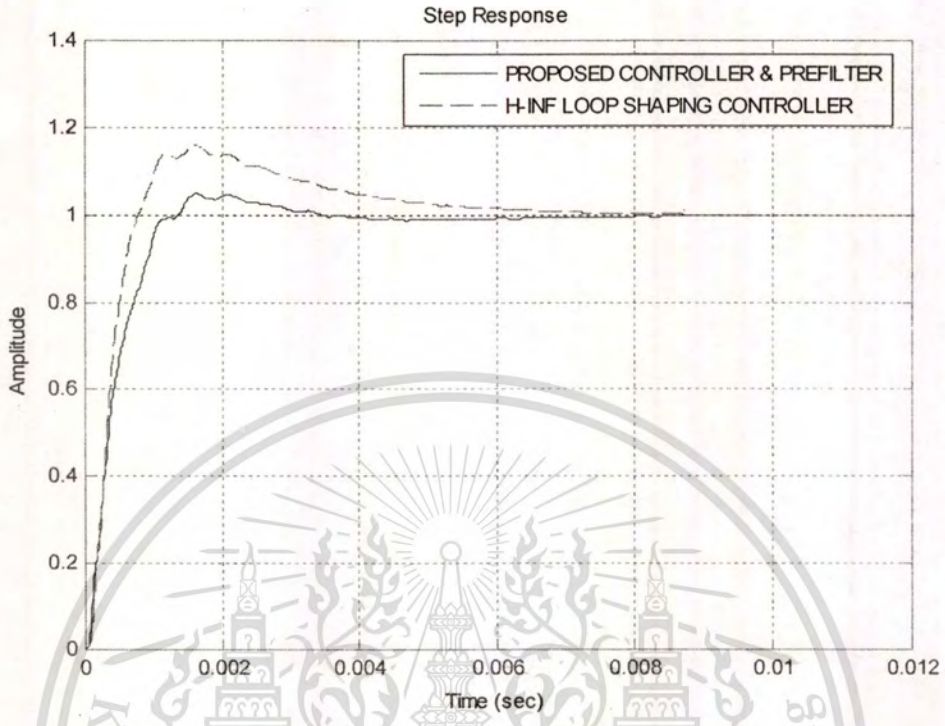

Fig 4.5 Step responses from HLS and PPID (the proposed PID) with pre-filter.

Performance comparison between the conventional PID [19], HLS and the proposed controller with pre-filter is given in Table 4.1 which indicates the superior performance of the proposed technique.

Table 4.1 Performance comparison table

Controller	PID	HLS	The proposed controller
Order	2	18	3(incl. pre-filter)
Over shoot	18.6%	15.8%	4.9%
Settling time	3.36ms	3.89ms	0.96ms
Rise time	0.47ms	0.48ms	0.80ms

4.3 Robustness test

Table 4.1 shows the performance comparison. To verify the robustness of the proposed controller, the step responses at perturbed conditions which are worse than the nominal condition, are given in Figure 4.6. In this perturbed condition, resonance mode frequencies ($\omega_1, \omega_2, \omega_3, \omega_4$) and damping coefficients ($\xi_1, \xi_2, \xi_3, \xi_4$) of the system have been changed to the values specified in Table 4.2. The green line indicates the response of lower bound perturbed condition, blue line for nominal plant condition while red line for extreme upper bound perturbed conditions.

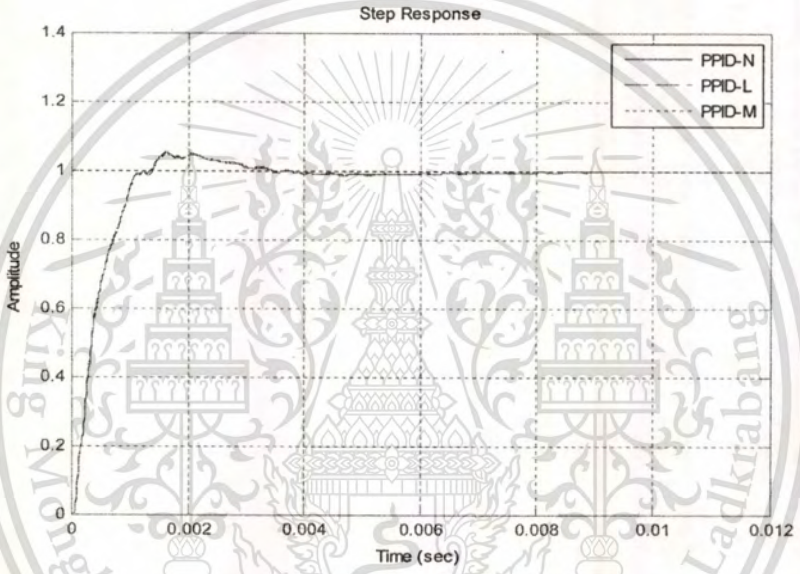

Fig 4.6 Step responses of the proposed controller at nominal and perturbed plants

Table 4.2 Parameters at perturbed condition

Parameter	*Nominal Value*	*Extreme Perturbed Lowest Values*	*Extreme Perturbed Highest Values*
ω_1	6880.1	6779.9	6983.3
ω_2	15777	15383	16172
ω_3	31845	30698	32272
ω_4	52257	50951	53564
ξ_1	0.015	0.0142	0.0158
ξ_2, ξ_3, ξ_4	0.025	0.0238	0.0263

The responses of the proposed controller at the perturbed conditions are almost the same as the response at the nominal plant with controller. Thus, as the results indicated, the controller designed by the proposed technique is robust against the parameter changing. To test the robustness of the proposed controller, the plant parameters are changed according to Table 4.3. The open loop bode, step response and stability robustness under close loop system has been analyzed.

Table 4.3 Parameters Uncertainty Table

Parameter	*Nominal Value*	*Uncertainty Tolerance*
ω_1	6880.1	+/- 3%
ω_2	15777	+/- 5%
ω_3	31845	+/- 5%
ω_4	52257	+/- 5%
ξ_1	0.015	+/- 10%
ξ_2, ξ_3, ξ_4	0.025	+/- 10%

Open loop bode plots for nominal and uncertain systems are given in Figure 4.7. According to the figure, we can see at the above and below resonance modes, the nominal and uncertain plots are almost the same. Even during uncertain zone, it still lies within few dB variations than the nominal plant.

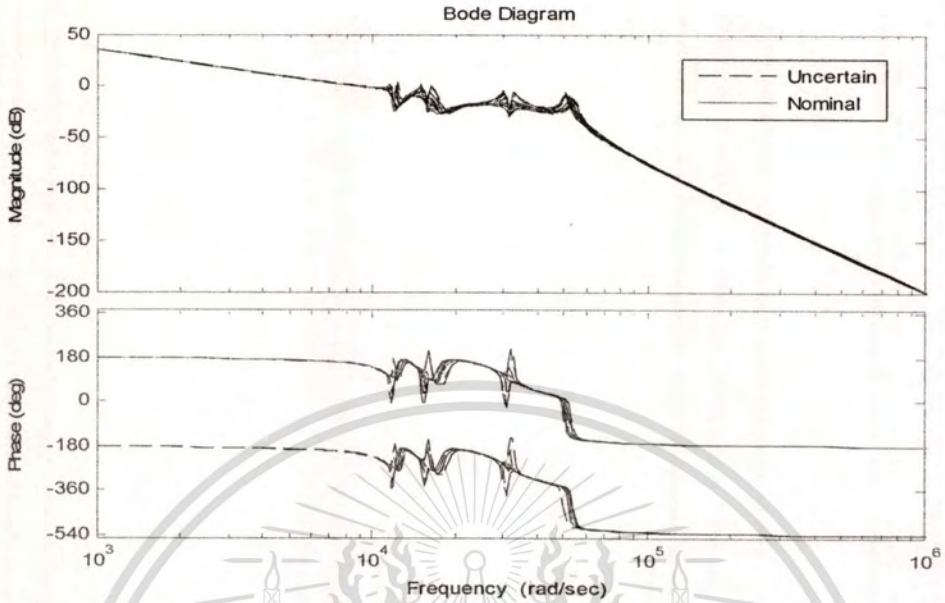

Fig 4.7 Open loop plot under nominal and uncertain condition

The step response of close loop system with pre-filter is given in the Figure 4.8 below.

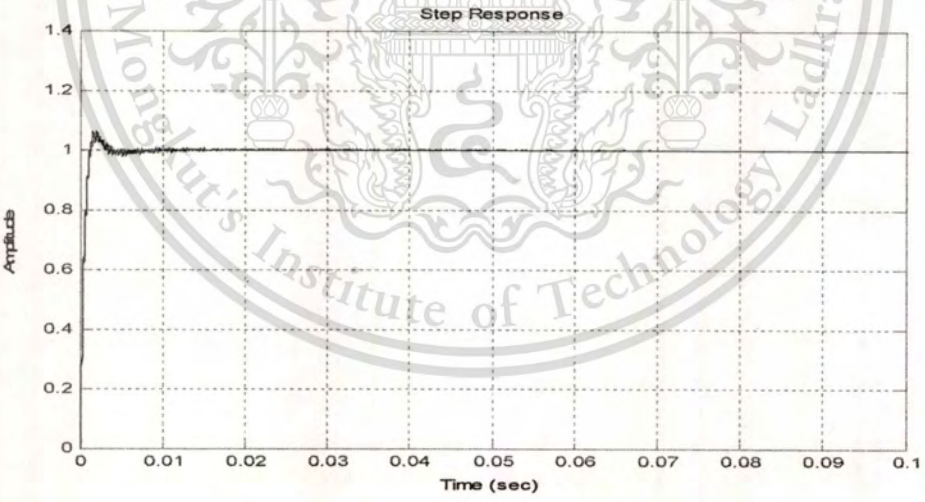

Fig 4.8 Open loop plot under nominal and uncertain condition

Our MATLAB generated stability report is as given below which indicates that our system is stable.

REPORT =

Uncertain System is robustly stable to modeled uncertainty.

-- It can tolerate up to 146% of the modeled uncertainty.

-- No modeled uncertainty exists to cause an instability

-- Sensitivity with respect to uncertain element ...

'f1' is 71%. Increasing 'f1' by 25% leads to a 18% decrease in the margin.

'f2' is 98%. Increasing 'f2' by 25% leads to a 25% decrease in the margin.

'f3' is 91%. Increasing 'f3' by 25% leads to a 23% decrease in the margin.

'f4' is 5%. Increasing 'f4' by 25% leads to a 1% decrease in the margin.

'z1' is 15%. Increasing 'z1' by 25% leads to a 4% decrease in the margin.

'z2' is 2%. Increasing 'z2' by 25% leads to a 1% decrease in the margin.

'z3' is 1%. Increasing 'z3' by 25% leads to a 0% decrease in the margin.

'z4' is 0%. Increasing 'z4' by 25% leads to a 0% decrease in the margin.

4.4 Hardware implementation

In order to verify the proposed technique, we implemented our technique to design a controller in real HDD servo system with single stage VCM actuator. Figure 4.9 shows our experimental setup.

Fig 4.9 Experimental setup.

As seen in this figure, only power supply, HDD, S4W Interface Board and Notebook are required for implementation. The controller was implemented on firmware (F/W). The graphical user interface (GUI) is used to download the F/W on HDD and to command the input e.g. perform seek etc. MATLAB scripts are used for analysis and to plot the data. The plant and notch filters in the experiment are different from the one we used in our simulation. Since the plant and notch filters are proprietary to the company, they are not stated in detail in this thesis. Based on the actual plant, our controller is different from (4.5). In our experiment, the designed controller along with Adaptive Feed Forward compensator (AFC) is used to control the real plant. The AFC is used to compensate frequency components at 600Hz and 1200 Hz RRO components which are the sub-harmonics or the motor RPM. Thus, the block diagram of our implemented controller is given in Figure 4.10.

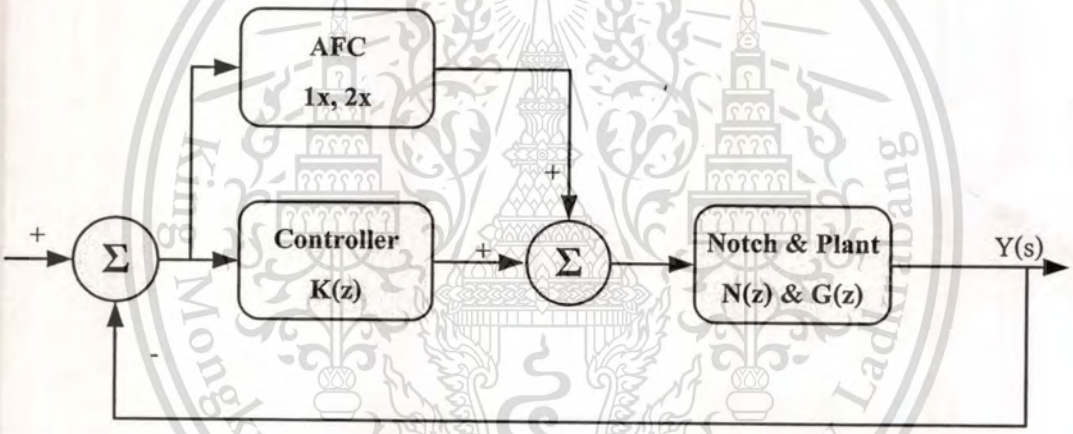

Fig 4.10 System block diagram with AFC.

The experimental results are shown in Figure 4.11 and Figure 4.12. We can see from Figure 4.11 that our proposed controller along with AFC is able to work well within 14.8% of the track width. From Figure 4.11 and 4.12, we can see that our proposed system can perform well within +/- 20nm [28]. The Histogram was plotted based on 4K (4096) samples. Based on these samples, we can see that over 84% of the total samples (3450 samples) were controlled well within +/- 10nm.

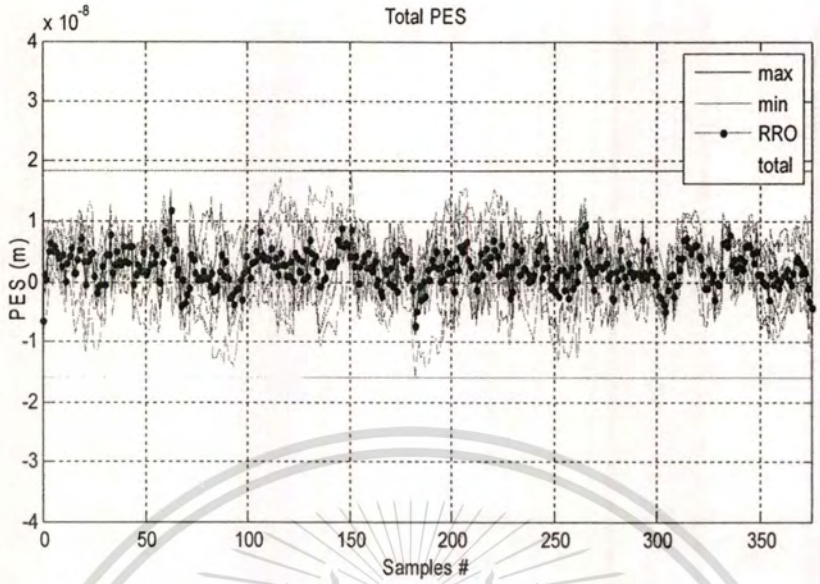

Fig 4.11: PES on track with the proposed controller

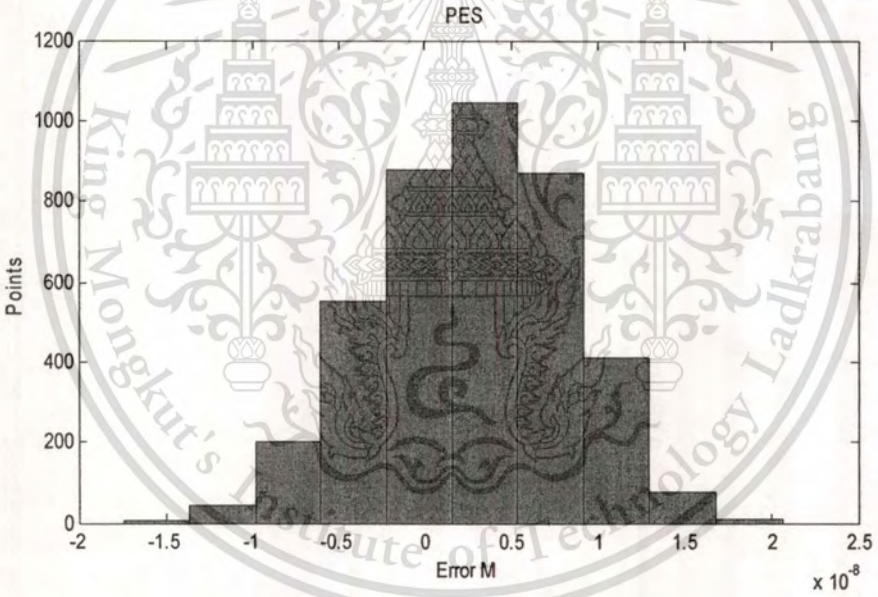

Fig 4.12 Histogram of the PES error.

Figure 4.13 shows the Fast Fourier Transform (FFT) plot on the total PES and Non Repeatable Run out (NRRO). Figure 4.14 shows the FFT on NRRO components while Figure 4.15 shows the FFT on repeatable run out RRO components. These plots indicate that no major energy component is available on any specific frequency. The available components can be taken care well by the compensator itself and we do not require any tuning for notch filters. Figure 4.13 to Figure 4.15

provides the analysis which shows that our system works well with the actual HDD. The Wedge repeatable run out (WRRO) compensator is not used in our system. RRO FFT can be further improved if we use WRRO compensator.

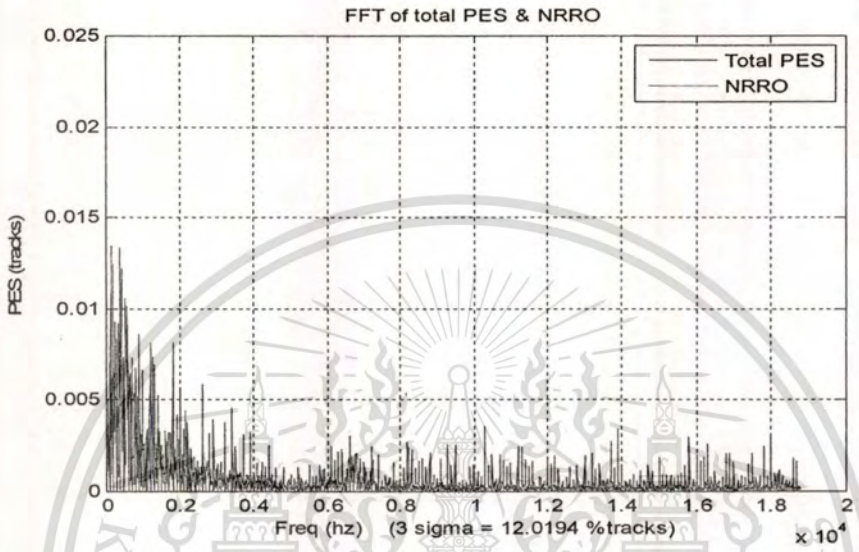

Fig 4.13 FFT on total PES and NRRO

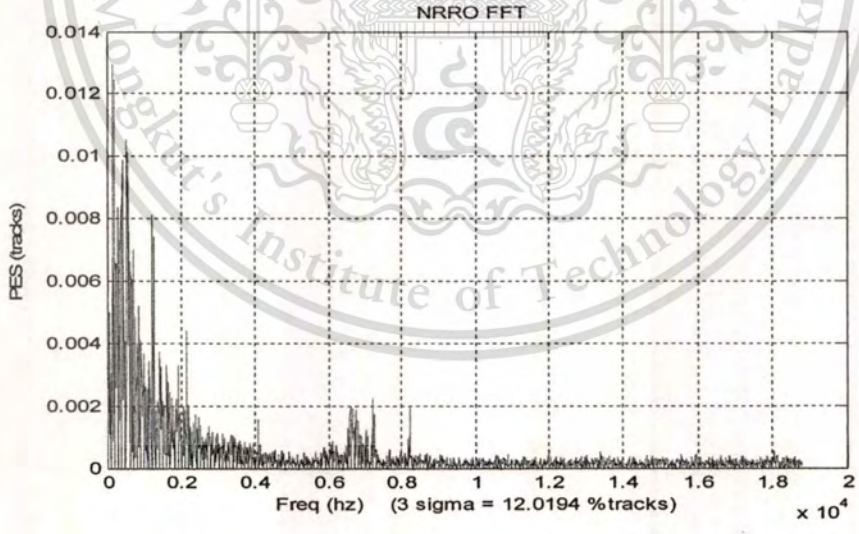

Fig 4.14 FFT on NRRO

The PES Spectrum informs about the PES components in frequency domain. If we accumulate the areas under spectrum and square it (spectrum^2), we get the variance, and thus we can calculate

the sigma values as well. From the NRRO and RRO plots, we can see where the PESs are heavy. We can take actions to reduce the contributing sources. We can adjust notches to improve variance error.

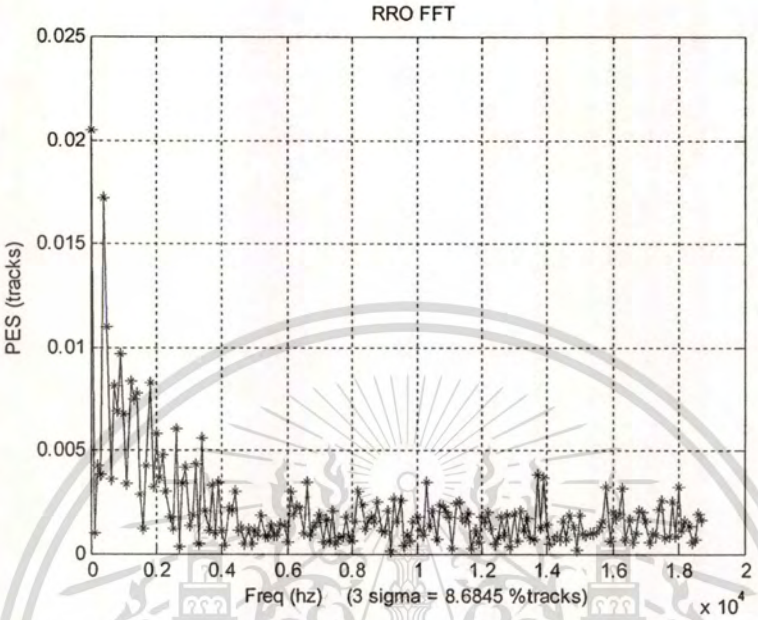

Fig 4.15 FFT on RRO

4.5 Conclusions

In this chapter, the design of high-performance and robust controller for HDD servo system using Genetic Algorithm has been proposed. A detailed approach to perform robustness test has been developed. During the robustness test, we found that our proposed controller is robust. Our experimental results illustrate that our proposed controller is working well with actual HDD. Results show that the response from our proposed technique has significantly lower overshoot compared to that of the conventional PID and HLS.

Chapter 5

Controller design for DSA in HDD servo system

It is well known that the recording density is increasing at an impressive annual rate of 40%. The access time is decreasing; very soon the storage density might cross 1 Terra bit per square inch. It is expected that for the necessary track density for 1 Terra-bit per square inch, the required TPI should be 500,000 and it also requires a track mis-registration (TMR) budget of less than 5nm (3-sigma value) [1]. Currently, HDD uses combination of control techniques such as lead lag compensators, PI compensators, robust control and notch filters. However, several classical methods for controlling HDD servo mechanism can no longer meet the demand of higher performance of HDD.

The VCM actuator used in conventional disk drives has hundreds of flexible resonances at high frequencies, which limit the increase of bandwidth and hence the positioning accuracy. In order to develop high band width (track-following) servo systems, dual-stage actuator has been proposed as a possible solution to this problem. In Dual-stage actuator, there is a micro-actuator mounted on a large conventional VCM actuator. Thus, the VCM actuator will be mainly used for seeking control and rough positioning, while the micro-actuator is used to provide fine positioning. This chapter is organized as follows. Section 5.1 provides the detailed descriptions of micro-actuator model. Section 5.2 describes the topology design. In this chapter, the design of direct control using multi input single output (MISO) technique is described. The drawbacks of the conventional Parallel and Decoupled Master slave controller, and how the MISO controller overcomes the mentioned drawbacks are shown in this section. Finally, Section 5.3 describes the simulation results and concludes the results.

5.1 Modeling for a dual stage actuator

The VCM actuator and micro-actuator are used to construct a Dual-Stage actuator which contains a fine positioner based on the piezoelectric based suspension mounted on the end of the primary VCM arm. The micro-actuator produces the relative motion of the read/write head along the radial direction [19]. The detailed descriptions of the VCM actuator and micro-actuator model are given in Section 2.3 and 2.4, respectively. The fixed-structure loop shaping control for VCM actuator using

GA is described in Chapter 3. In this section, the same VCM actuator along with micro-actuator has been designed; thus, the same work with some modifications from chapter 3 and 4 are used. For micro-actuator modeling, the detailed description of the micro-actuator plant is given in Section 2.4. From this section, micro-actuator model along with its resonance modes is of 10 orders. As seen in the bode plot, the phase starts from 0 degree at lower frequencies and it reaches to 180 degree at high frequencies. Thus, a propositional controller is sufficient to shape this plant. As seen in the simulation results, we found that a proportional controller of 5.5 is able to provide a phase margin of 52.8 degree and a gain margin of 5.16 dB which is sufficient for the case of HDD. The bode plot of the shaped plant is given in Figure 5.1

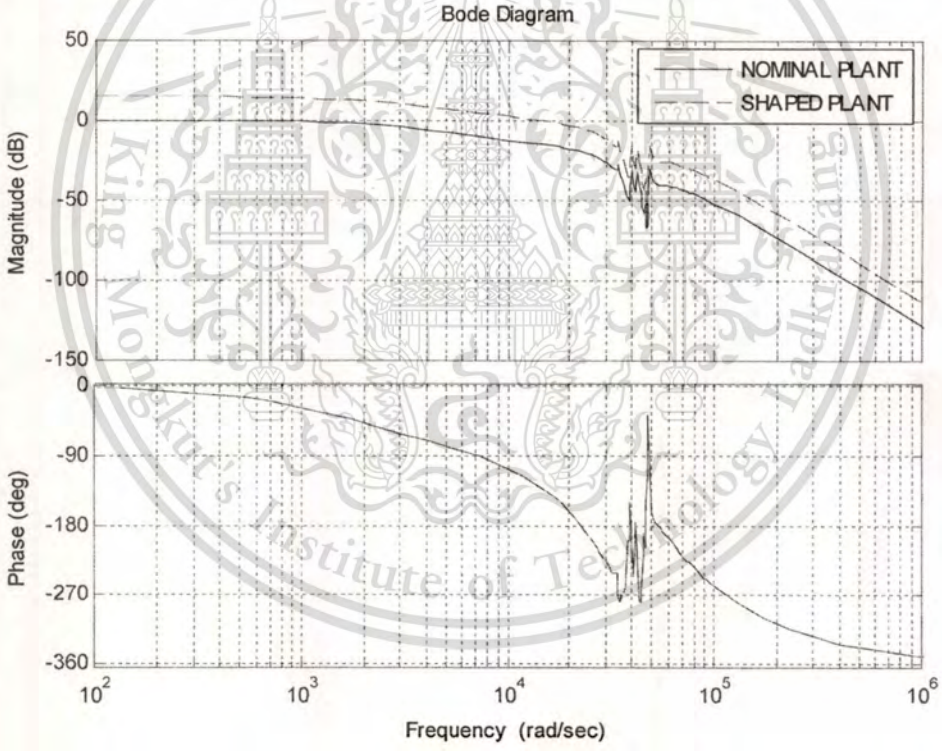

Fig 5.1: Bode plot with proportional controller for Micro-actuator

5.2 Controller Design Topology

The Parallel structure and Decouple Master slave structure method to design a controller for micro-electro mechanical system (MEMS) and Dual stage actuator (DSA) have been described in the

Chapter 2, Sections 2.6.1 and 2.6.2. These controllers are not able to take care of the phase difference at the hands-off frequency between the two parallel paths [25]. To overcome this problem, the direct MISO controller method which can automatically take care of the hand-off frequency in the design process is adopted. The designed controller using classical H_∞ loop shaping technique is described in Section 3.1. The block diagram of MISO controller is given in Figure 5.2. CMISO controller will provide two inputs, one for the VCM PLANT and the other for the micro-actuator plant. The outputs of both the plants are added to get the final output which is fed back via to the sensor of the system.

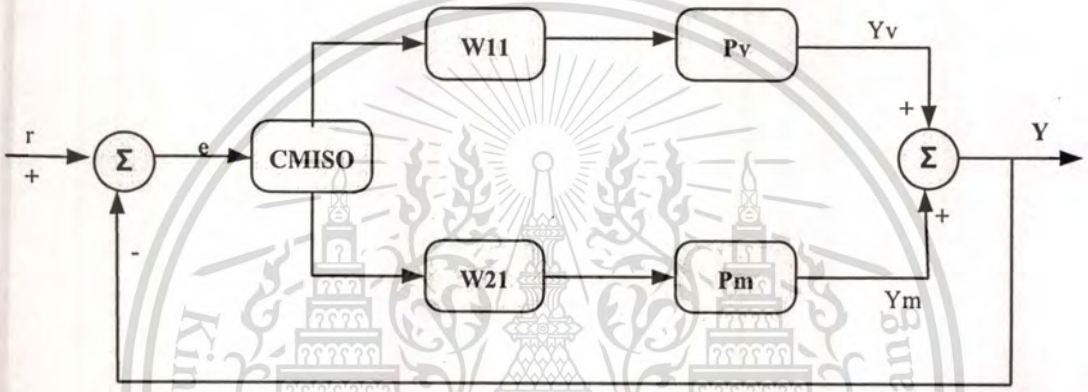

Fig 5.2: MISO Controller design block

where PV is the VCM plant transfer function; CV is the VCM controller transfer function; CMISO is the multi input single output controller. The model of the dual-stage actuator is:

$$y = \begin{bmatrix} G_m & G_v \end{bmatrix} \begin{bmatrix} u_m \\ u_v \end{bmatrix} \tag{5.1}$$

Where G_m and G_v are the plant dynamics with notch filters of micro-actuator and VCM, respectively. The MISO plant in (5.1) can be shaped with two weights, W11 and W21 as followings. With help of chapter 2, we can rewrite the shaped plant as:

$$W = \begin{bmatrix} W11 \\ W21 \end{bmatrix}$$

$$W11 = \left\{ 4.7787 \frac{(s+389.89)(s+51.87)}{(s+134600)(s+300)} \right\}$$
$$W21 = \{ 5.5 \} \quad (5.2)$$

By putting these transfer functions into (5.1), we can get the shaped plant for controller design. First, the robust controller based on the concept of classical H_∞ loop shaping method is designed. The controller order is 35th and it can control the DSA MEMS actuator very well. The infinity norm from disturbances to states obtained from this designed controller is γ = 1.7653, and the stability margin obtained is 0.5205. This indicates that the controller achieved here is robust. Since this controller is difficult to implement, the order of controller can be reduced from 35th order to 7th order (in association with the weighting function W11 and W21) using Hankle Norm model reduction technique. The new reduced order controller is given below. With this controller, the stability margin 0.3917 is obtained. Followings are the state space model of the designed reduce order controller.

$$A_{\text{reduced order}} = 1.0\times10^{4} \begin{bmatrix} -5.7217 & 4.7111 & -1.451 & 0.33 & -1.965 \\ -4.7114 & -0.0998 & 0.6527 & -0.0189 & 0.6968 \\ -1.4590 & -0.6527 & -0.4589 & 4.994 & -0.6527 \\ -0.3410 & 0.024 & -4.997 & -0.0055 & 0.7469 \\ -1.9650 & -0.6969 & -0.6498 & -0.7513 & -0.9336 \end{bmatrix}$$

$$B_{\text{Reduced Order}} = \begin{bmatrix} 245.1040 \\ 27.5919 \\ 42.9014 \\ 4.663 \\ 55.17 \end{bmatrix}$$

$$C_{\text{Reduced Order}} = [\, -245.1033 \quad 27.5855 \quad -42.9 \quad 4.3574 \quad -55.17 \,]$$

$$D_{\text{Reduced Order}} = 0 \quad (5.3)$$

Next, a fixed-structure robust controller using GA for MISO system is designed. The structure of the controller is fixed as the following state space model in (5.3). As seen in the model, the order of the controller is 2.

$$A_{GA\ CONTROLLER} = \begin{bmatrix} K_1 & K_2 \\ K_3 & K_4 \end{bmatrix}$$

$$B_{GA\ CONTROLLER} = \begin{bmatrix} K_5 \\ K_6 \end{bmatrix}$$

$$C_{GA\ CONTROLLER} = \begin{bmatrix} K_7 & K_8 \end{bmatrix}$$

$$D_{GA\ CONTROLLER} = 0 \qquad (5.4)$$

In the optimization, the ranges of the search parameters, and GA parameters are set as follows. $k_1 \in$ [-85000 0]; k_2 = [0 20000]; $k_3 \in$ [-30000 -10000]; $k_4 \in$ [-1000 -100]; $k_5 \in$ [0 500] ; $k_6 \in$ [0 100]; $k_7 \in$ [-500 0]; $k_8 \in$ [0 100];. Population size=100; crossover probability =0.6; mutation probability=0.1; maximum generation = 30. When running GA for 27 generations, an optimal controller can be found as. The selection for range for controller parameter is done with help of the study of reduced order controller parameters and some trial and error method.

$$A_{GA\ CONTROLLER} = \begin{bmatrix} -81615 & 1151 \\ -10167 & -364 \end{bmatrix}$$

$$B_{GA\ CONTROLLER} = \begin{bmatrix} 242.9924 \\ 25.9629 \end{bmatrix}$$

$$C_{GA\ CONTROLLER} = [-117.2772 \quad 25.7505]$$

$$D_{GA\ CONTROLLER} = 0 \qquad (5.5)$$

Figure 5.3 shows a plot of convergence of fitness function (stability margin versus generations) by genetic algorithm. As shown in the figure, the optimal robust controller with our proposed structure provides a satisfied stability margin at 0.4289. The order of the final controller is only 4 when is used in association with weights W11 and W21.

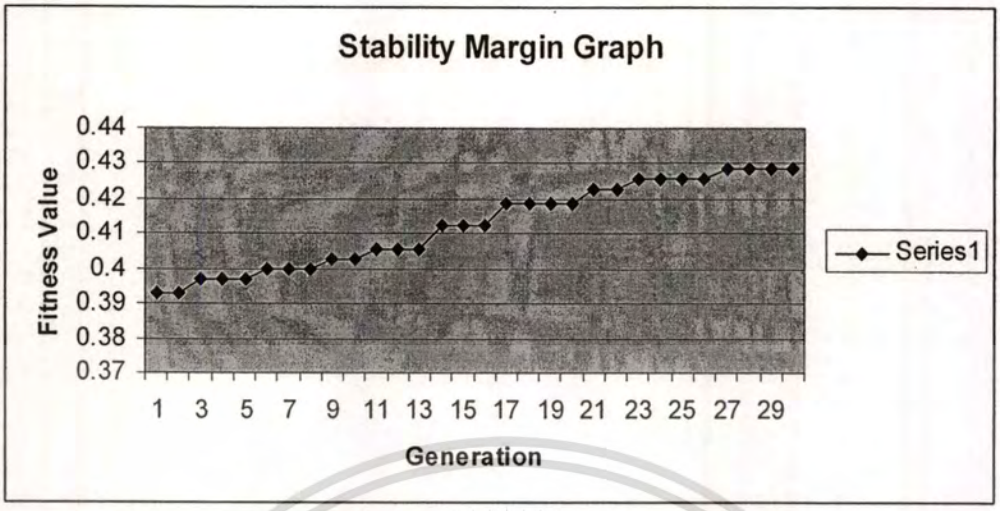

Fig. 5.3 Convergence of fitness value

5.3 Simulation results

The singular value plots of the nominal system, shaped plant, open loop with H_∞ controller, open loop with the reduced order controller, and open loop with GA based controller are given in Figure 5.4. The step responses from the H∞ loop shaping controller, the reduced order controller and GA based controller are given in Fig. 5.5. As seen in Fig. 5.4, the open loop bode plots of our reduced order controller and GA based controller are almost the same as the open loop plot of the system with classical H_∞ controller. Performance comparison for all controllers has been given in Table 5.1

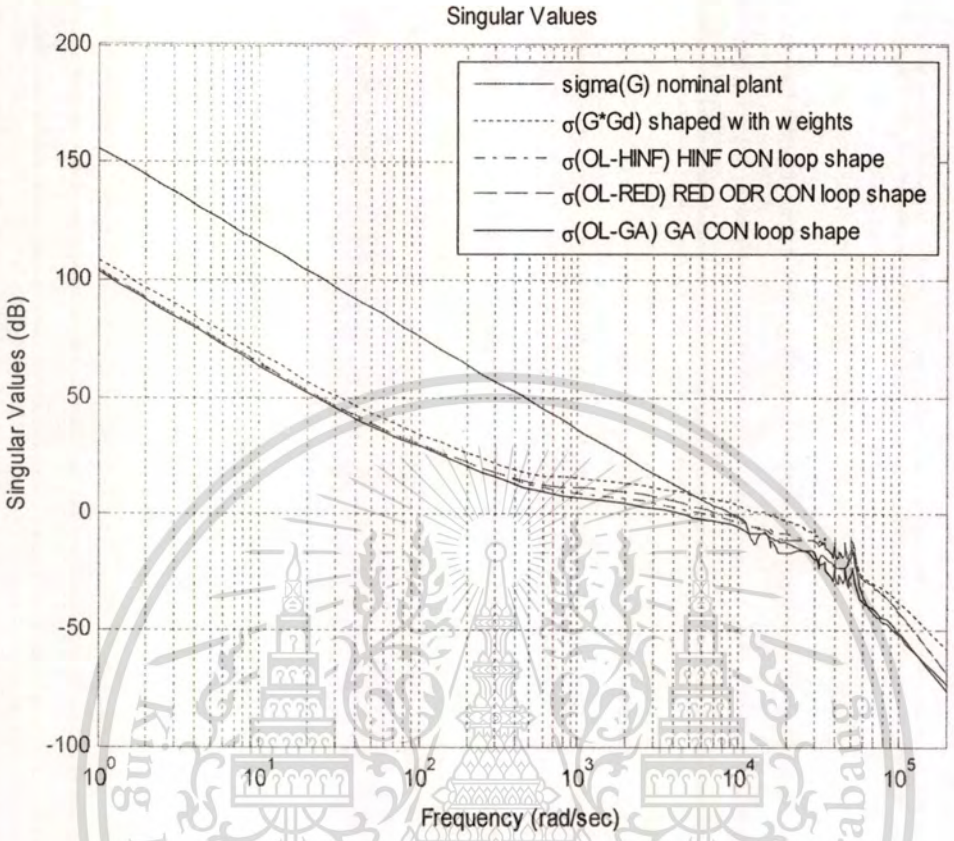

Fig 5.4: Singular value plots for nominal plant, shaped plant, plant with H-∞ controller, plant with reduced order controller and plant with GA based controller.

Table 5.1 Performance comparison table

Controller	HLS CONTROLLER	RED CONTROLLER	GA based CONTROLLER
ORDER	35	7	4
Stability Margin	0.52	0.39	0.42
Over shoot	3.7%	3.3%	4.5%
Settling time	1.85ms	1.99ms	2.00ms
Rise time	1.14ms	1.27ms	1.33ms

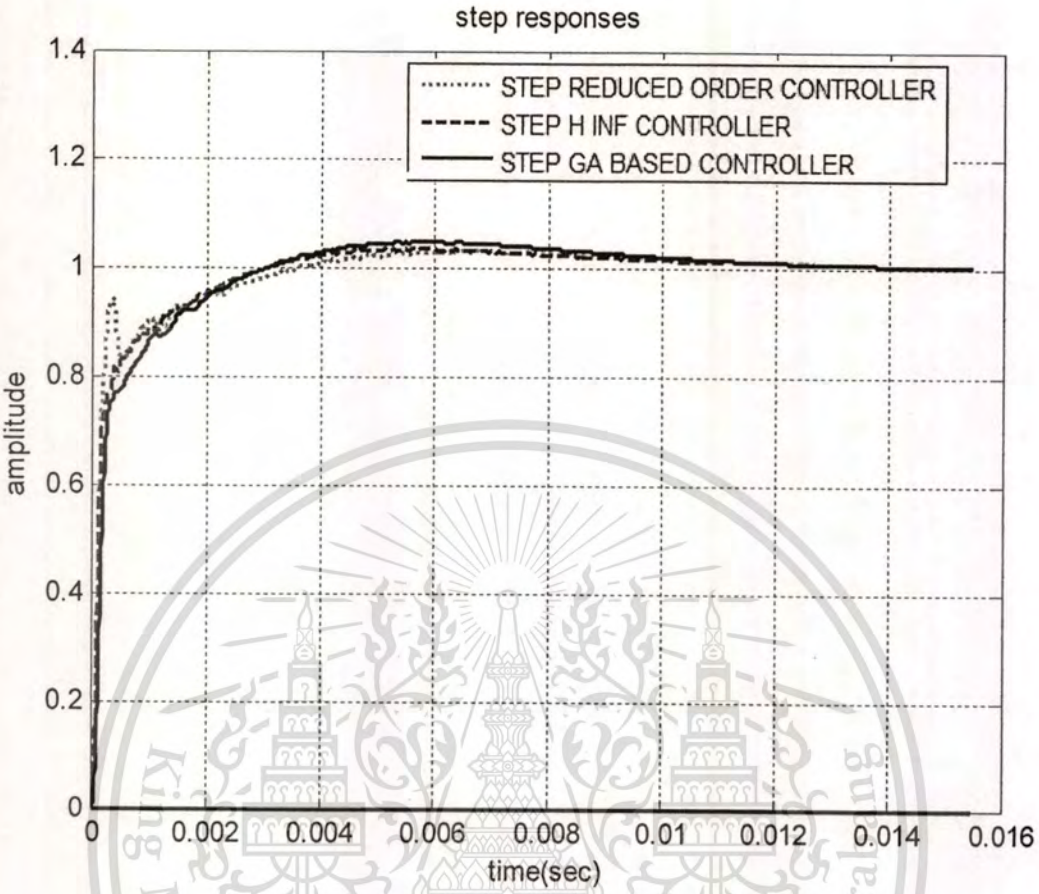

Fig 5.5: Step response of the system with MISO H-∞ controller, reduced order controller and the proposed controller.

From Table 5.1, we can see that even the order of GA based controller is lower than the reduced order controller; it has a better stability margin than the reduced order controller which indicates that GA based controller is more robust than reduce order controller. The over shoot of GA based controller is comparable to reduce order controller. Figure 5.5 shows that it provides smoother step response than the reduced order controller. In addition, its step response is almost the same as the H_∞ loop shaping control. Though the stability margin of H_∞ controller is better than GA based controller, but its order is 35 which is difficult to be implemented in actual practice as on HDD the interrupt service routine has hard deadlines and every task must be finished within that.

5.4 Robustness test

To verify the robustness of the proposed controller, the step responses at perturbed conditions which are worse than the nominal condition, are given in Figure 5.6

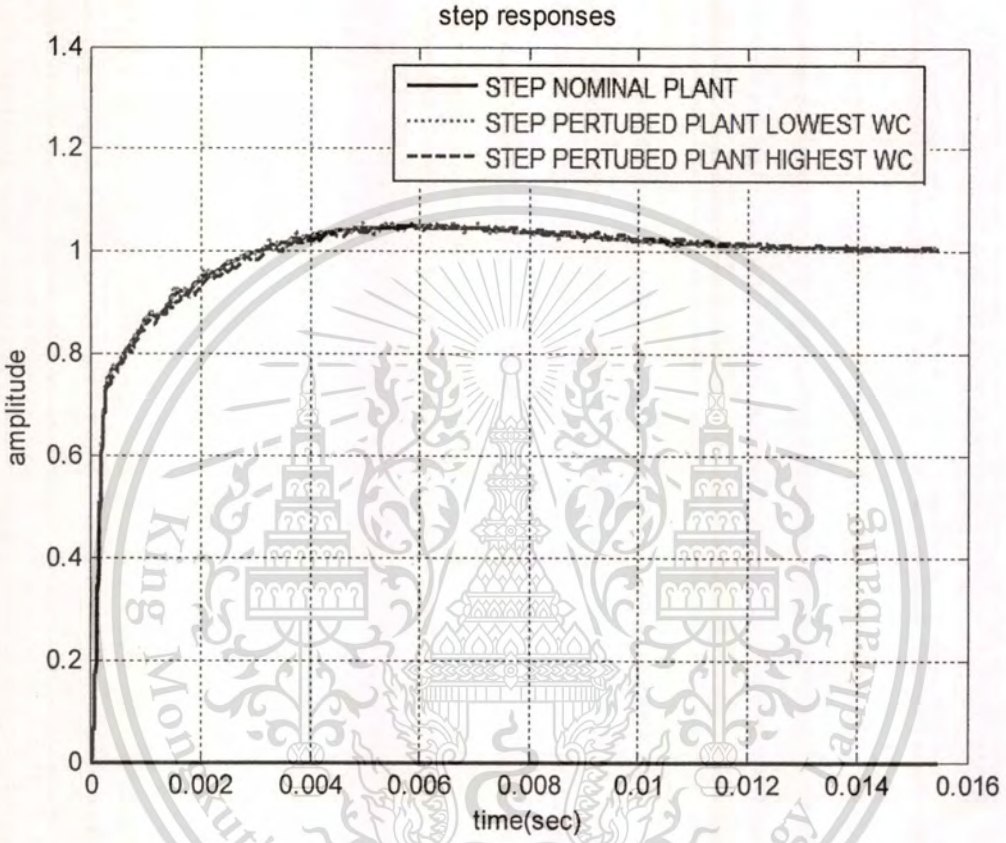

Fig 5.6: Step response of the proposed controller at nominal and perturbed plant.

In this perturbed condition, resonance mode frequencies ($\omega_{1V}, \omega_{2V}, \omega_{3V}, \omega_{4V}, \omega_{1M}, \omega_{2M}, \omega_{3M}, \omega_{4M}, \omega_{5M}$) and damping coefficients ($\xi_{1V}, \xi_{2V}, \xi_{3V}, \xi_{4V}, \xi_{1M}, \xi_{2M}, \xi_{3M}, \xi_{4M}, \xi_{5M}$) of the system have been changed to the values specified in Table 5.2. In this table the parameters has been changed to maximum and minimum tolerance limit as specified by component provider. The green line indicates the response of lower bound perturbed condition, blue line for nominal plant condition while red line for extreme upper bound perturbed conditions

Table 5.2 DSA Plant parameters at perturbed conditions

Parameter	*Nominal Value*	*Extreme Perturbed Lowest Values*	*Extreme Perturbed Highest Values*
ω_{1V}	6880.1	6779.9	6983.3
ω_{2V}	15777	15383	16172
ω_{3V}	31845	30698	32272
ω_{4V}	52257	50951	53564
ξ_{1V}	0.015	0.0142	0.0158
$\xi_{2V}, \xi_{3V}, \xi_{4V}$	0.025	0.0238	0.0263
ω_{1M}	34482	32758	36206
ω_{2M}	40062	38059	42066
ω_{3M}	42930	45077	40784
ω_{4M}	46551	48879	44223
ω_{5M}	48744	51181	46307
$\xi_{1M}, \xi_{2M}, \xi_{4M}, \xi_{5M}$	0.05	.0047	.0052
ξ_{3M}	0.0125	0.0119	0.0131

The responses of the proposed controller at the perturbed conditions are almost the same as the response at the nominal plant. The open loop singular values for the nominal plant, lowest extreme perturbed plant and highest extreme perturbed plant are shown in Figure 5.7. The stability margins for all three cases are calculated as shown in Table 5.3.

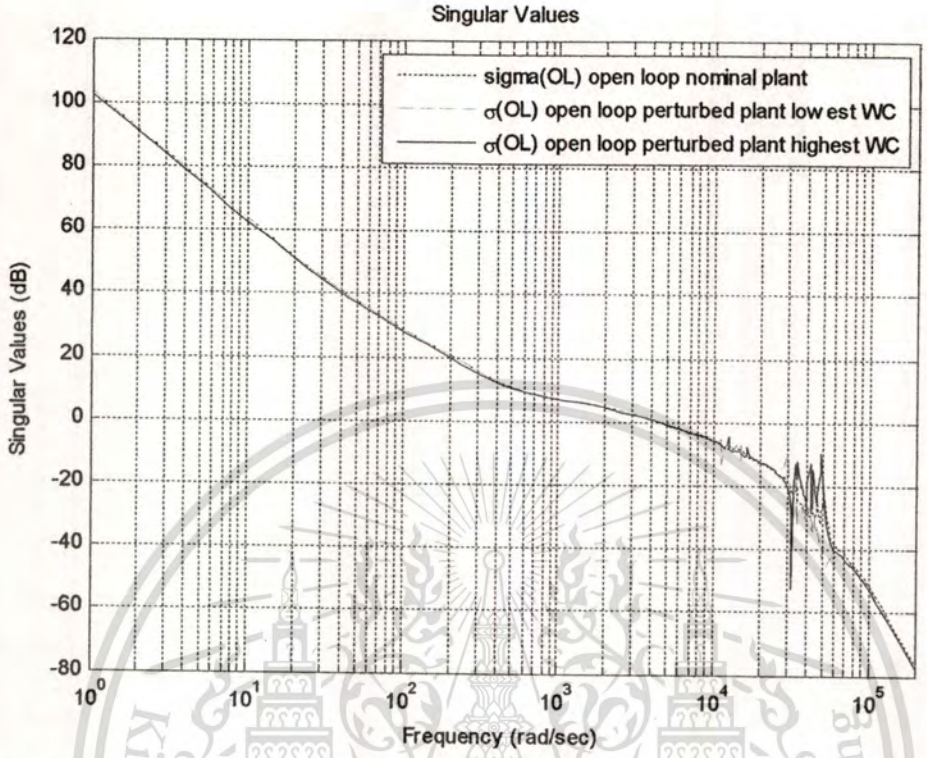

Fig 5.7: Open loop Bode Plot of the proposed controller at nominal and perturbed plants.

Table 5.3 Stability Margin for DSA plant parameters at perturbed conditions

Parameter	*Nominal Value*	*Extreme Perturbed Lowest Values*	*Extreme Perturbed Highest Values*
STABILIYTY MARGIN	0.4283	0.2918	0.3205

5.5 Conclusions

In this chapter, the designs of high-performance and robust controller for HDD MEMS DSA actuators using the conventional H_∞ loop shaping technique, the reduced Order Controller and the GA based controller have been proposed. Among those three techniques, the GA based controller has significant advantages as lower order and well performance compared to the other reduced order technique. Although the stability margin obtained from the classical H_∞ controller is slightly better

than the proposed controller; however, the order of the proposed controller is much lower than that of the full order controller. Considering this aspect, the proposed controller is easy to be implemented. The robustness test on the proposed controller has been done. Although there are some resonance issues at 5000 Hz, but those is far away from the actual interest and the gain at that point is much below than 0dB.

Chapter 6

Conclusions

In this thesis, the design of high performance and robust controller for HDD servo system using Genetic Algorithm has been proposed. We started with the session "Introduction" and the detailed description of HDD servo system e.g. servo sector mechanism for track seeking and track following. Some important researches in the area of HDD servo system have been discussed in the next issues. All the important issues in servo system for HDD and how to overcome the problem in servo system e.g. resonance compensation, RRO compensation and disturbance rejection have been discussed in Chapter 2. In the following section of the same chapter, models of the VCM actuator and micro-actuator have been discussed. Several basic methods of controller design and integration structure of the VCM and micro-actuator have been illustrated.

In the research method, we first discussed about the classical H_∞ loop shaping technique and then followed by the concept of GA and controller designed by our proposed method. A method to improve the tracking performance has been discussed. In the VCM actuator system, the results show that the response from our proposed technique has significantly lower overshoot compared to that of the conventional PID and HLS. Moreover, the order of controller is much lower than those of the HLS, but the robust performance from the proposed controller is almost the same as HLS. We verified the robustness of our proposed controller using uncertainty of the component tolerances. In order to verify our technique, we implemented a track following controller using the proposed technique; our controller was able to work well within 14.8% of the track three sigma PES value and can perform well within +/- 20nm.

We further apply our proposed technique in the controller design of dual stage MEMS actuator using direct MISO multi input single output technique. The controller designed by this technique has lower order and high performance compared to the reduced order controller. The performance from the proposed controller is similar to that of the classical HLS technique. Robustness of the proposed MISO controller has been verified and it was found that the proposed controller is robust enough within the specified parameter specification tolerance. Authors already published and presented two

papers at two international conferences (IEEE ROBIO 2009 and DST-CON 2010) and submitted the paper to an international Journal. Since the work uses the controller from the Western Digital Inc., some works have been started in association with servo group Western Digital. Though the actual implementation, its integration with other components and finally bring up to the line is very challenging and will be the next research work.

References

[1] Xinghui Huang ,Ryozo Nagamune and Roberto Horowitz July 2006 "A Comparison of Multi rate Robust Track-Following Control Synthesis Techniques for Dual-Stage and Multi sensing Servo Systems in Hard Disk Drives," *IEEE Transactions on Magnatics*, Vol.42, No.7: 1896-1904.

[2] Western Digital Technologies Inc, "Disk Drive servo control technology to preserve Position Error Signal continuity during track following operations," *United States Patent US7616399-B1*, NOV 2009.

[3] Amar Nath and Somyot Kaitwanidvilai December 2009, "High Performance HDD servo system using GA based Fixed Structure Robust Loop Shaping Control," *IEEE International Conference on Robotics and Biomimetics* ROBIO.2009 China : 1854-59

[4] Petras, Haojian Xu and Baris Fadin November 2007, "Identification and High Bandwidth Control of Hard Disk drive Servo Systems based on Sampled Data Measurements," *IEEE transactions on Control Systems Technology*, Vol.15, No.6: 1089-95

[5] Chunling Du, Lihua Xie, Jul Nee Teoh, and Guoxiao Guo September 2005, "An Improved Mixed H2/ H_∞ Control Design for Hard Disk Drives," *IEEE transactions on Control Systems Technology*, Vol.13, No.5: 832-39.

[6] Ying Li, Venkataramanan, Guoxiao Guo and Youyi Wang April 2007, "Dynamic Nonlinear Control for Fast Seek-Settling Performance in Hard Disk Drives," *IEEE Transactions On Industrial Electronics*, Vol. 54, No. 2: 951-62.

[7] Hao, Ruifeng Chen, Guoxiao Guo and Shixin Chen Feb 2003, "A Gradient-Based Track-Following Controller Optimization for Hard Disk Drive," *IEEE Transactions On Industrial Electronics*. Vol. 50, No. 1: 108-15

[8] Western Digital Technologies Inc, "A method of RRO learning before and after shipping to cancel RRO in a disk drive," *United States Patent US6545835 -B1,* APR 2003.

[9] Somyot Kaitwanidvilai and Manukid Parnichkun, July 2004, "Genetic Algorithm based Fixed-Structure Robust H_∞ Loop Shaping Control of a Pneumatic Servo System," *International Journal of Robotics and Mechatronics*, Vol.16:4 : 362-73.

[10] Sigurd Skogestad and Ian Postlethwaite, *Multivariable Feedback Control Nd Analysis and Design*, 2 ed. New York: John Wiley & Son, August 2001.

[11] Western Digital Technologies Inc, "A method of RRO learning before and after shipping to cancel RRO in a disk drive," *United States Patent* 7027256-B1, APR 2006.

[12] Massimiliano Rotunno, Raymond A. De Callafon, and Frank E.Talke September 2003 "Comparison and Design of Servo Controllers for Dual-Stage Actuators in Hard Disk Drives," *IEEE Transactions On Magnetics*, Vol. 39, No.5 : 2595-99.

[13] Xinghui Huang ,Ryozo Nagamune and RobertoHorowitz June2007, "A Comparison of Multirate Robust Track-Following Control Synthesis Techniques for Dual-Stage and Multisensing Servo Systems in Hard Disk Drives," *IEEE Transactions On Industrial Electronics*, Vol. 54, No.3: 1896-1904.

[14] Richard Conway, Sarah Felix, and Roberto Horowitz September 2007 "Model Reduction and Parametric Uncertainty Identification for Robust H2 Control Synthesis for Dual-Stage Hard Disk Drives," *IEEE Transactions on Magnetics*, Vol.43, No.9: 3763- 68.

[15] Kay-Soon Low, Tze Shyan Wong, June 2007, "A Multi objective Genetic Algorithm for Optimizing the Performance of Hard Disk Drive Motion Control System," *IEEE Transactions On Industrial Electronics*, Vol. 54, No.3: 1716-25.

[16] Hamid D Taghirad, Ehsan Jamei, January 2008 "Robust Performance Verification of Adaptive Robust Controller for Hard Disk Drives," *IEEE Transactions On Industrial Electronics*, Vol. 55, No. 1: 448-56.

[17] Venkataramanan, Kemao Peng, Chen, January 2003, "Discrete-Time Composite Nonlinear Feedback Control with an Application in Design of a Hard Disk Drive Servo System," *IEEE Trans on Control Systems Technology*, Vol. 11, No. 1:16 -23.

[18] Yang Quan Chen, Kevin L. Moore, Jie Yu and Tao Zhang, "Iterative learning control and repetitive control in hard disk drive industry—A tutorial," *International Journal of Adaptive Control and Signal Processing,* 2007.

[19] Chen, Lee, Kemao Peng and Venkatakrishnan, *Hard Disk Drive Servo System*, 2nd Ed, Springer, 2006.

[20] Chou April 1997, "Patterned magnetic nanostructures and quantized magnetic disks," *Proceedings of the IEE*, Vol. 85, No. 4: 652-71.

[21] Roberto Horowitz, Yunfeng Li, Kenn Oldham, Stanley Kon and Xinghui Huang 2007 "Dual Stage Servo Systems and Vibration Compensation in Computer Hard Disk Drives," *Science Direct Control Engineering Practice,* Vol. 15: 291-305.

[22] Franklin, Powell, and Emami-Naeini, *Feedback Control of Dynamic Systems*, 3rd ed. Reading, MA: Addison- Wesley, 1994.

[23] Mamun, Guo and Bi, *Hard Disk Drive Mechatronics and Control*, CRC press.

[24] Mohtadi March 1990, "Bode's integral theorem for discrete-time systems," *IEEE Proceedings-Control Theory and Applications*, Vol. 137, No. 2: 57-66.

[25] Goh, Li and Chen March 2001, "Design and Implementation of a Hard Disk Drive Servo System Using Robust and Perfect Tracking Approach," *IEEE Transactions On Control System Technology*, Vol.9, No.2: 221-33.

[26] Amar Nath and Somyot Kaitwanidvilai, July 2010, "Design of GA based Fixed-Structure Robust 2DOF Controller for HDD Servo System," *International Conference of Data Storage Technology DSTCON-10*, Bangkok, Thailand.

Appendix A

List of publications

[1] Amar Nath and Somyot Kaitwanidvilai December 2009, "High Performance HDD servo system using GA based Fixed Structure Robust Loop Shaping Control," *IEEE International Conference on Robotics and Biomimetics* ROBIO.2009 China.

[2] Amar Nath and Somyot Kaitwanidvilai, July 2010, "Design of GA based Fixed-Structure Robust 2DOF Controller for HDD Servo System," *International Conference of Data Storage Technology DSTCON-10*, Bangkok, Thailand.

IEEE 2009 IEEE International Conference on

Robotics and Biomimetics (ROBIO 2009)

December 19-23, 2009, Guilin, Guangxi, China

SPONSORED BY:

IEEE

Proceedings of the 2009 IEEE
International Conference on Robotics and Biomimetics
December 19 -23, 2009, Guilin, China

High Performance HDD servo system using GA based Fixed Structure Robust Loop Shaping Control

Amar Nath and Somyot Kaitwanidvilai

Abstract—High aerial density is needed for improving the capacity in Hard Disk Drive (HDD). In order to achieve this task, tracking performance and robustness of HDD servo system need to be improved. H_∞ robust controller is one of the most popular techniques for the mentioned problem; however, order of this controller is usually higher than that of the plant, making it difficult to implement practically. To overcome this problem, this paper proposes a new technique for designing a robust controller for HDD with Voice Coil motor (VCM) actuator. The control design problem, H_∞ loop shaping with structured controller, is solved by GA. Infinity norm of the transfer function from disturbances to states is used as the cost function in our optimization problem. The proposed technique does not only solve the problem of complicated and high order controller but also still retains the robust performance of conventional H_∞ control technique. In addition, structured pre-filter is also designed by GA to enhance the performance in terms of time-domain tracking. Simulation results in a HDD control system show the effectiveness of the proposed technique.

I. INTRODUCTION

The prevalent trend in hard disk design is towards smaller hard disk with increasingly larger capacities. The recording density is increasing at an impressive annual rate of 100% while the access time is decreasing; very soon the storage density is going to cross 1 Terra bit per square inch. It is expected that the necessary track density for 1 Terra-bit per square inch recording will be 500,000 tracks-per-inch (TPI), which requires a track mis-registration (TMR) budget of less than 5nm (3-sigma value) [1]. The controller for track seeking and track following has to achieve tighter regulation in the control of the servo mechanism. Currently HDD uses combination of control techniques such as lead lag compensators, PI compensators, robust control and notch filters. However, some classical methods for controlling HDD servo mechanism can no longer meet the demand of higher performance of HDD. Thus, many control approaches, e.g. adaptive robust controller in [2], Multi Objective Genetic Algorithm (MOGA) based controller in [3], Dynamic Nonlinear Control for fast seeking controller in [4], gradient based track following controller in [5], Multi-rate robust track following control synthesis techniques for Dual Stage and Multi-sensing servo system for HDD [6] etc have been proposed to solve the above mentioned problem. The most important aspect in HDD servo control system is to ensure both the stability and the performance of the system under the perturbed conditions. One of the most popular techniques is H_∞ optimal loop shaping control in which the uncertainty and performance are incorporated into the controller design [7-8]. Unfortunately, the order of the resulting controller from this technique is usually high. In this paper, we illustrate the design of a HDD controller which can guarantee stability under the perturbed conditions and which also has a simple structure. This paper uses a more recent evolutionary technique, GA, to solve a specified structure of H_∞ loop shaping optimization problem. Infinity norm of transfer function from disturbances to states is subjected to be minimized via searching and evolutionary computation. The resulting optimal parameters make the system stable and also guarantee robust performance. In addition, GA is adopted to find a structured pre-filter for increasing performance of the time domain tracking.

The remainder of this paper is organized as follows. Section II describes HDD servo system and its dynamic. Section III illustrates the conventional and proposed design. Genetic Algorithm (GA) for designing a fixed structure robust controller is also described in this section. Section IV shows the simulation results. Finally, Section V concludes the paper.

II. HDD SERVO SYSTEM AND ACTUATOR MODELING

Magnetic HDD servo system consists of VCM actuator, Read/Write (R/W) head and rotating disk coated with magnetic layer or recording medium. Data are arranged in concentric circles or tracks and are written or read by R/W head. Fig. 1 shows a simple illustration of HDD servo system. There are two main tasks of HDD servo system, i.e.,

1. To move the R/W head to the desired track location, and after that
2. Keep the R/W head on the track, i.e., position the head on the center of the track as precisely as possible so that data can be read/written quickly and reliably.

The first task is commonly referred to as track seeking, while the second is track following. The deviation between the center of the read/write head and the center of the track in turn is referred to as the head position error. The implementation of track-following servo system relies on measuring the head Position Error Seek (PES)

Manuscript received Oct 25th, 2009. This work was funded by DSTAR, KMITL, NECTEC and NSTDA (Project No. DSTAR R&D 02-03-52)

Amar Nath is with DSTAR, KMITL and Western Digital Thailand Co Ltd. Thailand (phone: 66-85-1293852; e-mail: Amar.Nath@ wdc.com).

S. Kaitwanidvilai is with Faculty of Engineering, KMITL, Bangkok 10520, Thailand. (Phone: 66-86-3327108; e-mail: drsomyotk@gmail.com).

978-1-4244-4775-6/09/$25.00 © 2009 IEEE.

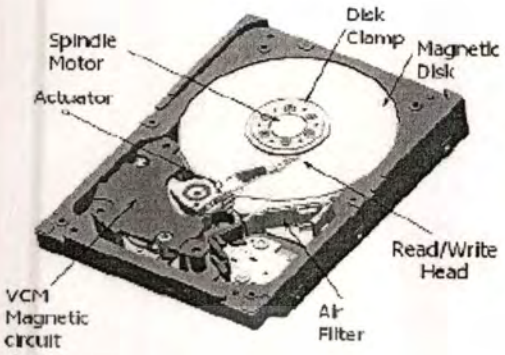

Fig. 1 HDD and VCM actuator servo system

PES can be obtained from the information encoded on the magnetic disk, in angular servo sectors that radiate out from the center of the disk. Since the servo sectors are located at discrete locations, the PES is a sampled digital signal and the disk drive control system is naturally a digital control system. Sampling frequency can be determined by the disk rotation speed and the number of servo sectors on a track. Generally, HDD servo system can be characterized as a double integrator cascaded with some high frequency resonance modes. The dynamic model of an ideal VCM actuator can be formulated as a second order state space model as follows [9].

$$\begin{pmatrix} \dot{y} \\ \dot{v} \end{pmatrix} = \begin{bmatrix} 0 & k_y \\ 0 & 0 \end{bmatrix} \begin{pmatrix} y \\ v \end{pmatrix} + \begin{pmatrix} 0 \\ k_v \end{pmatrix} u \qquad (1)$$

Where u is the actuator input (in volts), y and v are the position (in tracks) and the velocity of the Read/Write head, K_y is the position measurement gain, $K_v = \frac{K_t}{m}$, K_t is the current/force conversion coefficient and m is the mass of the VCM actuator. Consequently, the transfer function of an ideal VCM actuator model can be written as a double integrator. However, if the high-frequency resonance modes are considered, a more realistic model of the VCM actuator will be [9]:

$$G_v(s) = \frac{k_v k_y}{s^2} \prod_{i=1}^{N} G_{ri}(s) \qquad (2)$$

Where N is the number of resonance modes, $G_{ri}(s)$ is the i^{th} resonance mode term which can be modeled as:

$$G_{ri}(s) = \frac{a_i s^2 + b_i s + \omega_i^2}{s^2 + 2\xi_i \omega_i s + \omega_i^2} \qquad (3)$$

Where a_i, b_i, ξ_i and ω_i are coefficients of i^{th} resonance mode dynamic. In this paper, a HDD servo system with the model shown in Table I is studied. Table I describes the parameters and the uncertainty considered for this VCM model [9], [10].

TABLE I
VCM parameters with tolerances

Parameter	Value	Tolerance
M	.002Kg	-
k_t	20	-
k_v	64.013	-
ω_1	$2.\pi.1095$	3%
ω_2	$2.\pi.2511$	5%
ω_3	$2.\pi.5011$	5%
ω_4	$2.\pi.8317$	5%
ξ_{51}	0.015	10%
$\xi_{52}, \xi_{53}, \xi_{54}$	0.025	10%
a_1	0.912	-
a_2	0.7286	-
b_1	457.4	-
b_2	962.2	-
a_3, b_3, a_4, b_4	0	...

In order to reduce the effect of high frequency resonance mode, the notch filter is added to the plant to cancel out the unwanted responses [9]. Three notch filters [9] in (4) are adopted in this paper for achieving the above mentioned task.

$$N_r(s) = \prod_{i=1}^{N} N_{ni}(s) \qquad (4)$$

Where

$$N_{ri}(s) = \frac{s^2 + 2\xi_{ni} \omega_{ni} s + \omega_{ni}^2}{s^2 + 2\xi_{ni+1} \omega_{ni} s + \omega_{ni}^2} \qquad (5)$$

TABLE 2
VCM NOTCH PARAMETERS

Notch	ξ_{ni}	ξ_{ni+1}	ω_{ni}
1	0.01	0.10	$2.\pi.1900$
2	0.01	0.10	$2.\pi.2500$
3	0.009	0.0198	$2.\pi.5000$

Fig. 2 shows the plant with the notch filter and the proposed control structure. As seen in this figure, a pre-filter $Kr(s)$ is added to shape the command and increase the tracking performance.

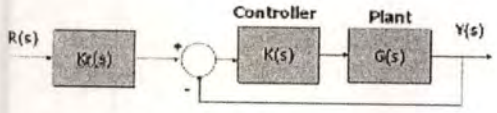

Fig.2 Controller structure in our proposed system.

By (2) and (3), the plant can be derived as:

$$Plant = \left\{ \frac{\begin{array}{l} 1.197\times10^{38}s^{4}+2.12\times10^{35}s^{3}+5.826\times10^{34}s^{2} \\ +4.366\times10^{31}s+6.189\times10^{42} \end{array}}{\begin{array}{l} s^{10}+5336s^{9}+4.124\times10^{8}s^{8}+1.302\times10^{13}s^{7} \\ +4.216\times10^{16}s^{6}+6.72\times10^{21}s^{5}+1.198\times10^{21}s^{4} \\ +7.946\times10^{24}s^{3}+9.668\times10^{34}s^{2} \end{array}} \right\} \quad (6)$$

And, by (4) and (5) we can obtain the notch filter model as [9]:

$$Notch = \left\{ \frac{\begin{array}{l} s^{6}+1181s^{5}+1.377\times10^{6}s^{4}+8.94\times10^{11}s^{3} \\ +4.194\times10^{11}s^{2}+1.244\times10^{16}s+3.47\times10^{23} \end{array}}{\begin{array}{l} s^{6}+18100s^{5}+1.453\times10^{8}s^{4}+1.148\times10^{13}s^{3} \\ +4.397\times10^{17}s^{2}+1.465\times10^{21}s+3.47\times10^{23} \end{array}} \right\} \quad (7)$$

Bode plots of the plant with notch and its perturbed plant are shown in Fig.3

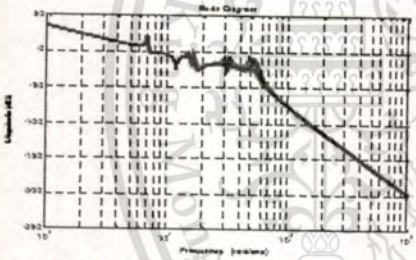

Fig 3. VCM Actuator model (nominal plant with notch filter) (Red line) and perturbed plants (Blue line)

III. H∞ Loop Shaping Control and Proposed Technique

This section illustrates the concepts of the conventional H∞ loop shaping control and the proposed technique.

A. Conventional H_∞ Loop Shaping

This approach requires only two weighting functions, W_1 (pre-compensator) and W_2 (post-compensator), for shaping the nominal plant G_0 so that the desired open loop shape is achieved. In this approach, the shaped plant is formulated as normalized co-prime factor, which separates the shaped plant G_s into normalized nominator N_s and denominator M_s factors [8]. Note that,

$$G_s = W_1 G_0 W_2 = M_s N_s^{-1} \quad (8)$$

Step 1 Shape the singular values of the nominal plant G_0 by using a pre-compensator W_1 and/or a post-compensator W_2 to get the desired loop shape. In SISO system, the weighting functions W_1 and W_2 can be chosen as:

$$W_1 = K_W \frac{s+a}{s+b} \quad (9)$$

Where a, b, K_W are positive numbers, and $b << 1$ in order to provide the integrating action. The weight W_2 can be chosen as:

$$W_2 = \frac{s+c}{s+d} \quad (10)$$

The perturbed plant of the shaped plant can be written as

$$G_\Delta = (N_s + \Delta_{Ns})(M_s + \Delta_{Ms})^{-1}$$

Where Δ_{Ns} and Δ_{Ms} are uncertainty transfer functions and $\left\| \Delta_{Ns}, \Delta_{Ms} \right\| \le \varepsilon$. Where ε is uncertainty boundary called stability margin. There are some guidelines for selecting the weights available in [8].

Step2: Calculate ε_{opt} by solving the following inequality.

$$\gamma_{opt} = \varepsilon_{opt}^{-1} = \inf_{K \text{ stab}} \left\| \begin{bmatrix} I \\ K \end{bmatrix} (I + GK)^{-1} M_s^{-1} \right\| \quad (11)$$

To calculate ε_{opt} a unique method is explained in [8]. To ensure the robust stability of the nominal plant, the weighting function is selected so that $\varepsilon_{opt} \ge 0.25$ [8]. If ε_{opt} is not satisfied, then go to step 1 to adjust the weighting functions.

Step 3 Select $\varepsilon < \varepsilon_{opt}$ and then synthesize a controller K_∞ that satisfies

$$\left\| \begin{bmatrix} I \\ K_\infty \end{bmatrix} (I + G_s K_\infty)^{-1} M_s^{-1} \right\| \le \varepsilon^{-1} \quad (12)$$

Controller K_∞ is obtained by solving the sub-optimal control problem in (12). The details of this solving are available in [8].

Step 4 Final controller (K_∞) is determined by.

$$K = W_1 K_\infty W_2 \quad (13)$$

B. Genetic Algorithm based Fixed-Structure H∞ Loop Shaping Optimization

In the proposed technique, GA is adopted in the design. This algorithm applies the concept of chromosomes and the genetic operations of crossover, mutation and reproduction. At each step, called generation, fitness value of each chromosome in population is evaluated by using fitness function. Chromosome, which has the maximum fitness value, is kept as a solution in the current generation and copied to the next generation. The new population of the next generation is obtained by performing the genetic operators such as crossover, mutation and reproduction. In this paper, a roulette wheel method is used for chromosome selection. In this method, chromosome with high fitness value has high chance to be selected. Operation type selection, mutation, reproduction or crossover depends on the pre-specified operation's probability. Normally, chromosome in genetic population is coded as binary number. However, for the real number problem, decoding binary number to floating number can be applied. The proposed technique is described in followings.

In this paper, GA is adopted to solve the fixed-structure H_∞ Loop Shaping Optimization problem. Although the proposed controller is structured, it still retains the entire robustness and performance as long as a satisfactory uncertainty boundary ε is achieved. Assume that the predefined structure of controller $K(p)$ has specified parameter p. Based on the concept of H∞ loop shaping, optimization goal is to find parameter p in the controller $K(p)$ that minimizes the infinity norm from disturbances w to states z, $\|T_{zw}\|_\infty$. From (13), assuming that W_1 and W_2 are invertible, then $K_\infty = W_1^{-1}K(p)W_2^{-1}$. Substituting this equation into (12), the ∞-norm of the transfer function matrix $\|T_{ZW}\|_\infty$ which is subjected to be minimized can be written as:

$$J_{con} = \gamma = \|T_{zw}\|_\infty = \left\| \begin{bmatrix} I \\ W_1^{-1}W_2^{-1}K(p) \end{bmatrix} (I + G_s W_1^{-1}W_2^{-1}K(p))^{-1} M_s^{-1} \right\|_\infty \quad (14)$$

The optimization problem can be written as:

$$\text{Minimize} \left\| \begin{bmatrix} I \\ W_1^{-1}W_2^{-1}K(p) \end{bmatrix} (I + G_s W_1^{-1}W_2^{-1}K(p))^{-1} M_s^{-1} \right\|_\infty$$

subject to $p_{i,\min} < p_i < p_{i,\max}$ where $p_{i,\min}$ is $p_{i,\max}$ are lower and upper bounds of the parameter p_i in controller $K(p)$ respectively. The fitness function in the controller synthesis can be written as:

$$Fitness = \begin{cases} \left(\left\| \begin{bmatrix} I \\ W_1^{-1}W_2^{-1}K(p) \end{bmatrix} (I + G_s W_1^{-1}W_2^{-1}K(p))^{-1} M_s^{-1} \right\|_\infty \right)^{-1} & \text{If } K(p) \text{ stabilizes the plant} \\ 0.00001 & \text{Otherwise} \end{cases} \quad (15)$$

The fitness is set to a small value (in this case is 0.00001) if $K(p)$ does not stabilize the plant. Our proposed algorithm can be summarized as follows.

Step 1 Follow steps 1 and 2 in conventional H_∞ Loop Shaping technique to select the weights. Specify the genetic parameters such as initial population size, crossover and mutation probability, maximum generation, etc.

Step 2 Select a controller structure $K(p)$ and randomly initialize several sets of parameters p as population in the 1st generation.

Step 3 Evaluate the fitness value of each chromosome using (16). Select the chromosome with maximum fitness value as a solution in the current generation. Increment generation for a step.

Step 4 While the current generation is less than the maximum generation, create a new population using genetic operators and go to step 3. If the current generation is the maximum generation, then stop.

Step 5 Check the performances in both frequency and time domains. If the performances are not satisfied such as too low ε (too low fitness function), go to step 2 to change the structure of controller.

IV. Simulation and Experiential Result

This section explains the design of a controller for HDD VCM actuator. Our design goal is to fulfill the stability criterion [11-12] and the following specifications [13].

1) Over shoot and undershoot of the step response should be kept less than 5% as the R/W head can start to read or write within 5% of the target.

2) The 5% settling time in the step response should be less than 2ms.

Based on (9) and (10) and guidelines in [8], the weight W_1 and W_2 can be selected as:

$$W_1 = \frac{4.99(s+617.41)}{s+1.09}, \quad W_2 = \frac{(s+81.23)}{(s+130470)}$$

By these weights, a slope of -20 dB/decade at the cross over point can be achieved, and it provides gain margin of 12dB and phase margin of 67.5^0. First, we applied the conventional H_∞ loop shaping (HLS) technique to design a robust controller. The resulting controller by this approach is 18^{th} order robust controller as shown in following:

$$HLS\_con = \frac{\begin{bmatrix} 2.238\times10^{6}s^{17} + 3.453\times10^{8}s^{16} + 1.968\times10^{9}s^{15} \\ + 1.903\times10^{10}s^{14} + 5.649\times10^{10}s^{13} + 3.56\times10^{11}s^{12} \\ + 6.737\times10^{12}s^{11} + 2.992\times10^{13}s^{10} + 3.718\times10^{13}s^{9} \\ + 1.224\times10^{14}s^{8} + 1.008\times10^{15}s^{7} + 2.542\times10^{15}s^{6} \\ + 1.314\times10^{15}s^{5} + 2.569\times10^{15}s^{4} + 6.883\times10^{14}s^{3} \\ + 9.995\times10^{14}s^{2} + 4.703\times10^{13}s + 3.194\times10^{12} \end{bmatrix}}{\begin{bmatrix} s^{18} + 1.34\times10^{2}s^{17} + 1.19\times10^{3}s^{16} + 1.03\times10^{4}s^{15} \\ + 4.27\times10^{4}s^{14} + 2.162\times10^{5}s^{13} + 6.332\times10^{5}s^{12} \\ + 2.046\times10^{6}s^{11} + 4.513\times10^{7}s^{10} + 9.5\times10^{6}s^{9} \\ + 1.646\times10^{7}s^{8} + 2.261\times10^{7}s^{7} + 3.14\times10^{7}s^{6} \\ + 2.659\times10^{7}s^{5} + 2.966\times10^{6}s^{4} + 1.272\times10^{6}s^{3} \\ + 1.089\times10^{6}s^{2} + 7.071\times10^{4}s + 5.031\times10^{4} \end{bmatrix}} \quad (16)$$

HLS controller is able to satisfy all the uncertain modes with the infinity norm, $\gamma = 1.7723$. As shown in (16), the order of HLS controller is 18. It is not easy to implement practically.

Next, a fixed-structure robust controller using the proposed algorithm is designed. The structure of controller is selected as the second order lead-lag controller. The controller structure can be expressed in (17)

$$Cont = \left\{ K_3 \frac{(s+k1)(s+k2)}{(s+k4)(s+k5)} \right\} \quad (17)$$

In the optimization, the ranges of search parameters and GA parameters are set as follows. By considering W_1 and W_2, range of controller parameters can be selected in order to maintain the integrity of the stability criteria [11-12]. $k_1 \in$ [10 100]; $k_2 \in$ [500 1500]; $k_3 \in$ [1 10]; $k_4 \in$[0.01 10]; $k_5 \in$

[10000 150000]. Population size=100; crossover probability =0.6; mutation probability=0.1; maximum generation = 30. When running GA for 14 generations, an optimal controller was found as.

$$Cont(PPD) = \left\{ 4.7787 \frac{(s+689.89)(s+51.87)}{(s+134600)(s+0.4879)} \right\} \quad (18)$$

Fig 7 shows the comparison of the shaped plant by proposed controller and HLS. In this figure, the HLS controller is able to provide gain margin of 13.4dB with phase margin of 65.3^0, while our GA based controller without pre-filter is able to provide gain margin of 12.6dB and phase margin of 66.1^0. Cleary, the bode diagrams of both controllers are almost the same.

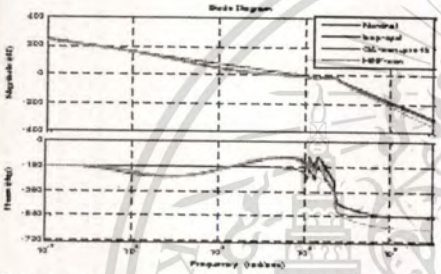

Fig.7 Bode diagrams of the open loop transfer function for: the shaped plant, nominal plant, plant with HLS, and proposed controller.

Fig.8 shows a plot of convergence of fitness function (stability margin) versus generations by genetic algorithm. As shown in the figure, the optimal robust PID controller provides a satisfied stability margin at 0.5156.

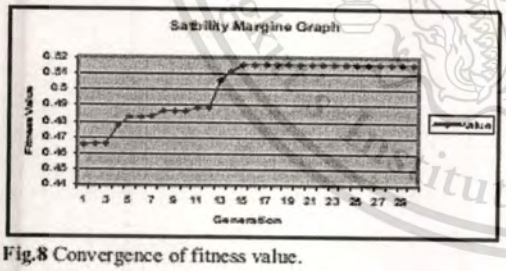

Fig.8 Convergence of fitness value.

In addition, we designed a fixed-structure pre-filter to achieve the tracking performance specification. In this filter, we selected a 1st order lead-lag controller, *Kr(s)* as [9].

$$K_r(s) = \frac{\tau_{lead}.s + 1}{\tau_{lag}.s + 1} \quad (19)$$

The pre-filter was also designed by GA by setting the constraints as follows: over shoot <=5%, and 5% settling time <= 1.5ms. Fitness function in this case is sum square error of the actual response when step command input is applied. By running GA, we found that optimal value of $K_r(s)$ is

$$K_r(s) = \frac{.001671s + 1}{.002122s + 1} \quad (20)$$

This pre-filter can improve the gain margin a bit up to 14.6 dB while we were able to achieve phase margin 60.2^0. Responses from the unit step command by HLS and the proposed robust controllers at the nominal plant are shown in Fig. 9. Table 3 shows the performance obtained by all controllers. As seen in this figure and Table 3, maximum overshoot obtained by the HLS controller and the conventional PID [9] is much higher than that of the proposed PID. 5% settling time of our proposed controller is much faster than that of the other controllers. Clearly, time domain specifications can be achieved by our proposed technique. The proposed technique has superior performance because of its pre-filter structure.

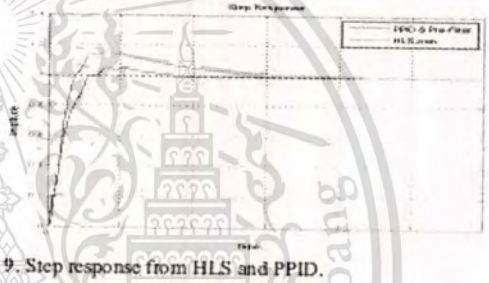

Fig 9. Step response from HLS and PPID.

TABLE 3
PERFORMANCE COMPARISON

Controller	*PID*	*HLS*	*Proposed Controller*
Over Shoot	31%	18%	<5%
Settling Time	3.1ms	3.8ms	1.00ms

To verify the robustness of the proposed controller, the step responses at perturbed conditions which are worse than the nominal condition, are given in Fig.10. In this perturbed condition, resonance mode frequencies ($\omega_1, \omega_2, \omega_3, \omega_4$) and damping coefficients ($\xi_1, \xi_2, \xi_3, \xi_4$) of the system have been changed to the values specified in Table 4. The green line indicates the response of lower bound perturbed condition, blue line for nominal plant condition while red line for extreme upper bound perturbed conditions.

Fig 10. Step Responses of the proposed controller at nominal and perturbed plants.

TABLE 4
PARAMETERS AT PERTURBED CONDITIONS.

Parameter	*Nominal Value*	*Extreme Perturbed Lowest Values*	*Extreme Perturbed Highest Values*
ω_1	6880.1	6779.9	6983.3
ω_2	15777	15383	16172
ω_3	31845	30698	32272
ω_4	52257	50951	53564
$\xi_{\omega 1}$	0.015	0.0142	0.0158
$\xi_{\omega 2}, \xi_{\omega 3}, \xi_{\omega 4}$	0.025	0.0238	0.0263

The responses of the proposed controller at the perturbed conditions are almost the same as the response at the nominal plant. We further compared our results with other controllers in [13-14] as shown in Table 5. Clearly our controller has a simple structure, gains high robust performance and can be applicable to a HDD servo system.

TABLE 5
PERFORMANCE COMPARISON AT PERTURBED PLANT.

Controller	*RPT*	*Evolved 2DOF*	*Proposed Controller*
Over Shoot	4.7%	3.98%	5.00%
Settling Time	1.75ms	1.75ms	1.00ms

V. CONCLUSIONS

In this paper, the design of high-performance and robust controller for HDD servo system using Genetic Algorithm has been proposed. Results show that the response from our proposed technique has significantly lower overshoot compared to that of the conventional PID and HLS. In addition, the order of controller is much lower than that of the HLS, but the robust performance from the proposed controller is almost the same as HLS. The tracking performance specifications can be achieved by the proposed controller. When compared to the most recent techniques, RPT and evolved 2-DOF, our proposed controller has almost the same tracking performance and the settling time of the proposed controller is better than that of the others.

ACKNOWLEDGEMENT

This work was funded by DSTAR, KMITL, NECTEC and NSTDA (Project No. DSTAR R&D 02-03-52)

REFERENCES

[1] Xinghai Huang ,Ryozo Nagamune and Roberto Horowitz "A Comparison of Multi rate Robust Track-Following Control Synthesis Techniques for Dual-Stage and Multi sensing Servo Systems in Hard Disk Drives." IEEE Transactions on Magnetics, Vol.42, No.7, July 2006, pp. 1896-1904.

[2] Hamid D. Taghirad and Ehsan Jamei, "Robust Performance Verification of Adaptive Robust Controller for Hard Disk Drives" IEEE Transactions On Industrial Electronics Vol. 55, No.1, January 2008, pp. 448-456.

[3] Kay-Soon Low, Tze-Shyan Wong, "A Multiobjective Genetic Algorithm for Optimizing the Performance of Hard Disk Drive Motion Control System" IEEE Transactions On Industrial Electronics Vol. 54, No.3, June 2007, pp 1716-1725.

[4] Ying Li, V. Venkataramanan, Guoxiao Guo and Youyi Wang "Dynamic Nonlinear Control for Fast Seek-Settling Performance in Hard Disk Drives" IEEE Transactions On Industrial Electronics, Vol. 54, No. 2, April 2007, pp. 951-962.

[5] Qi Hao, Ruifeng Chen, Guoxiao Guo, Shixin Chen "A Gradient-Based Track-Following Controller Optimization for Hard Disk Drive." IEEE Transactions On Industrial Electronics. Vol. 50, No. 1, Feb 2003, pp. 108-115.

[6] Xinghai Huang, Ryozo Nagamune, and Roberto Horowitz "A Comparison of Multirate Robust Track-Following Control Synthesis Techniques for Dual-Stage and Multisensing Servo Systems in Hard Disk Drives.", IEEE Transactions on Magnetics, Vol.42 No 7, July 2006, pp. 1896-1904.

[7] S. Kaitwanidvilai, M. Parnichkun, "Genetic Algorithm based Fixed-Structure Robust H-oo Loop Shaping Control of a Pneumatic Servo System", International Journal of Robotics and Mechatronics, Vol.16:4, 2004, pp. 1716-1725.

[8] S. Skogestad & I. Postlethwaite, "Multivariable Feedback Control Nd Analysis and Design". 2 ed. New York: John Wiley & Son, 1996, pp. 293-351.

[9] Ben M. Chen, Tong H. Lee, Kemao Peng and Venkatakrishnan "Hard Disk Drive Servo System 2nd Edition" Springer 2006, pp. 179-200.

[10] G.F.Franklin, J.D.Powell, and A.Emami-Naeini, Feedback Control of Dynamic Systems, 3rd ed. Reading, MA: Addison- Wesley, 1994. pp. 666-669.

[11] Al Mamun, Guo and Bi "Hard Disk Drive Mechatronics and Control" by CRC press, pp. 88-92.

[12] Mohtadi, C. Bode's integral theorem for discrete-time systems, IEEE Proceedings-Control Theory and Applications, Vol. 137, No. 2, March 1990, pp. 57-66.

[13] Teck B. Goh, Zhongming Li, Ben M. Chen "Design and Implementation of a Hard Disk Drive Servo System Using Robust and Perfect Tracking Approach" IEEE Transactions On Control System Technology, Vol.9, No.2, March 2001, pp. 221-233.

[14] K.C.Tan, E.F.Khor, T.H.Lee "Multiobjective Evolutionary Algorithms and Applications" Springer Verlag London Limited 2005, pp. 212-214.

Design and Implementation of GA based Fixed-Structure Robust 2DOF Controller for HDD Servo System

Amar Nath *, Somyot Kaitwanidvilai **
*DSTAR, King Mongkut's Institute of Technology Ladkrabang, Bangkok 10520, Thailand
** Electrical Engineering Department, Faculty of Engineering,
King Mongkut's Institute of Technology Ladkrabang, Bangkok 10520, Thailand
drsomyotk@gmail.com

Abstract— Since the aerial density of Hard Disk Drive (HDD) is increasing at very impressive rate, conventional technique for controlling HDD servo system can no longer meet the necessary tracking performance and robustness; a new class of servo controller will be required to address this issue. H_∞ robust controller is one of the most popular techniques for designing a robust controller and it provides necessary robustness and performance even under perturbed plant conditions. However, the order of controller designed by this technique is usually higher than that of the plant, making it difficult to implement practically. To overcome this problem, this paper proposes a new technique for designing a robust controller for HDD with Voice Coil motor (VCM) actuator. The control design problem, H_∞ loop shaping with structured controller, is solved by Genetic Algorithm (GA). Infinity norm of transfer function from disturbances to states is formulated as the cost function in our optimization problem. The proposed technique does not only solve the problem of complicated and high order controller but also still retains the robust performance of conventional H_∞ control technique. In addition, structured pre-filter is also designed by GA to enhance the performance in terms of time-domain tracking. Simulation and experimental results show the effectiveness of our proposed technique.

Keywords- HDD servo systems; Robust Controler Design; H infinity loop shaping.

I. INTRODUCTION

The prevalent trend in hard disk design is towards smaller hard disk with increasingly larger capacities. The recording density is increasing at an impressive annual rate of 100% while the access time is decreasing. The controller for track seeking and track following has to achieve tighter regulation in the control of the HDD servo mechanism. Currently, HDD uses combination of control techniques such as lead lag compensators, PI compensators, robust control and notch filters.

To design a high performance controller for HDD servo system, many advanced control approaches have been proposed, e.g. adaptive robust controller in [1-2], Multi Objective Genetic Algorithm (MOGA) based controller in [3]. One of the most important aspects in HDD servo control system is to ensure both the stability and the performance of the system under perturbed conditions. One of the most popular techniques is H_∞ optimal loop shaping control in which the uncertainty and performance are incorporated into the controller design [4-5]. Unfortunately, the order of controller from this technique is usually high and it is difficult to implement in practice. In this paper, we illustrate the design of HDD servo controller which can guarantee the stability under perturbed conditions and which also has a simple structure. This paper uses Genetic Algorithms (GA) to solve a specified structure H_∞ loop shaping optimization problem. Infinity norm of transfer function from disturbances to states is subjected to be minimized via searching and evolutionary computation. The resulting optimal parameters make the system stable and also guarantee the robust performance of entire system. In addition, GA is adopted to find a structured pre-filter for increasing the performance in terms of time domain tracking.

The remainder of this paper is organized as follows. Section II describes HDD servo system and dynamic model. Section III illustrates the conventional and proposed design. GA for designing a fixed-structure robust controller is also described in this section. Section IV shows the simulation and experimental results. Finally, Section V concludes the paper.

II. HDD SERVO SYSTEM AND ACTUATOR MODELING

HDD servo system consists of VCM actuator, Read/Write (R/W) head and rotating disk coated with magnetic layer or recording medium. Data are arranged in concentric circles or tracks and are written or read by R/W head. Fig.1 shows a typical HDD with its servo components. There are two main tasks of HDD servo system, to move the R/W head to the desired track location, and after that keep the R/W head on the track, i.e. position the head on the center of track as precisely as possible so that data can be read/written quickly and reliably. The deviation between the center of the read/write head and the center of the track is referred to as the head position error. The implementation of track-following servo system relies on measuring the head Position Error Signal (PES). The actuator and Head Stack Assembly (HAS) structure is not perfectly rigid; it contains many resonance modes.

THIS WORK WAS FUNDED BY DSTAR, KMITL, NECTEC AND NASTDA.

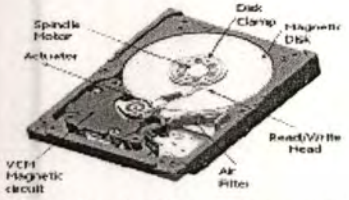

Figure 1. HDD and VCM actuator servo system

Table I shows the typical VCM parameters used in our simulation study [6].

TABLE I. VCM PARAMETERS WITH TOLERANCES

Parameter	Value	Tolerance
M	.002Kg	-
K_f	20	-
K_y	64.013	-
ω_1	$2\pi 70$	5%
ω_2	$2\pi 2200$	10%
ω_3	$2\pi 4000$	5%
ω_4	$2\pi 9000$	5%
ξ_1, ξ_3	0.05	10%
ξ_2, ξ_4	0.005	10%
K_{fric}	2.51	-

Where $\omega_1, \omega_2, \omega_3$ and ω_4 are VCM, Head Suspension, Actuator arm carrier and coil resonance modes, b1 to b8 are the resonance coupling constants for our simulation. In our simulation study, we choose the same values given in [6]. ξ_1 to ξ_4 are damping constants; k_t is the force constant; k_y is position measurement gain and K_{fric} is viscous friction coefficient. A linear state–space model for HDD servo system can be written as (1) [6].

$$\dot{x}(t) = F.x(t) - G.u(t)$$
$$y(t) = H.x(t) \quad (1)$$

The matrices F, G and H can be given by (2), (3) and (4).

$$F = \begin{bmatrix} 0 & k_y & 0 & 0 & 0 & 0 & 0 & 0 & 0 & 0 \\ 0 & \frac{k_{fric}}{m} & k_t b_1 & k_t b_2 & k_t b_3 & k_t b_4 & k_t b_5 & k_t b_6 & k_t b_7 & k_t b_8 \\ 0 & 0 & 0 & \omega_1 & 0 & 0 & 0 & 0 & 0 & 0 \\ 0 & 0 & -\omega_1 & -2\zeta\omega_1 & 0 & 0 & 0 & 0 & 0 & 0 \\ 0 & 0 & 0 & 0 & 0 & \omega_2 & 0 & 0 & 0 & 0 \\ 0 & 0 & 0 & 0 & -\omega_2 & -2\zeta\omega_2 & 0 & 0 & 0 & 0 \\ 0 & 0 & 0 & 0 & 0 & 0 & 0 & \omega_3 & 0 & 0 \\ 0 & 0 & 0 & 0 & 0 & 0 & -\omega_3 & -2\zeta\omega_3 & 0 & 0 \\ 0 & 0 & 0 & 0 & 0 & 0 & 0 & 0 & 0 & \omega_4 \\ 0 & 0 & 0 & 0 & 0 & 0 & 0 & 0 & -\omega_4 & -2\zeta\omega_4 \end{bmatrix} \quad (2)$$

$$G = [0 \ \frac{1}{m} \ 0 \ \ldots \ \omega_2 \ \ 0 \ \omega_3 \ 0]^T \quad (3)$$

$$H = [1 \ 0 \ 0 \ 1 \ 0 \ 1 \ 0 \ 1 \ 0 \ 1] \quad (4)$$

By substituting the VCM parameters into (2), (3) and (4), the linear state space model can be derived.

The effect of high frequency resonance mode can be reduced by adding notch filter [6]. In this research work, four notch filters are adopted (TABLE II) to achieving the above mentioned task.

TABLE II. VCM NOTCH PARAMETERS

Notch	ξ_{ni}	ξ_{ni+1}	ω_{ni}
1	0.3	0.33	$2\pi 2200$
2	0.07	0.001	$2\pi 3900$
3	0.030	0.0250	$2\pi 6000$
4	0.01	0.200	$2\pi 8900$

Fig. 2 shows the plant with notch filter and the proposed control structure. As seen in this figure, a pre-filter $K_r(s)$ is added to shape the command and increase the tracking performance.

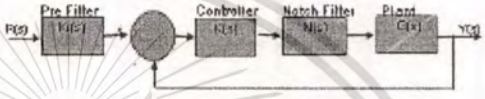

Figure 2. Controller structure in our proposed system.

III. H∞ LOOP SHAPING CONTROL AND THE PROPOSED TECHNIQUE

This section illustrates the concepts of conventional H_∞ loop shaping control and the proposed technique.

A. Conventional H_∞ Loop Shaping

This approach requires only two weighting functions, W_1 (pre-compensator) and W_2 (post-compensator), for shaping the nominal plant G_0 so that the desired open loop shape is achieved. The shaped plant G_s can be given by

$$G_s = W_1 G_0 W_2 = M_s N_s^{-1} \quad (5)$$

N_s and M_s are the normalized nominator and denominator, respectively. The steps for this technique are as follows.

Step 1 For shaping the nominal plants in HDD servo system, two weights can be chosen as

$$W_1 = K_w \frac{s+a}{s+b} \quad (6) \qquad W_2 = \frac{(s+c)(s+e)}{(s+d)(s+f)} \quad (7)$$

Where a, b, c, d, e, f and K_w are positive numbers, and $b \ll 1$ in order to provide the integrating action. The perturbed plant of the shaped plant can be written as:

$$G_\Delta = (N_s + \Delta_{Ns})(M_s + \Delta_{Ms})^{-1} \quad (8)$$

Where Δ_{Ns} and Δ_{Ms} are uncertainty transfer functions. $\left\| \Delta_{Ns}, \Delta_{Ms} \right\| \leq \varepsilon$. Where ε is uncertainty boundary called stability margin. There are some guidelines for selecting the weights available in [5].

Step2: Calculate ε_{opt} by solving the following equation.

$$\gamma_{opt} = \varepsilon_{opt}^{-1} = \inf_{stab\ K} \left\| \begin{bmatrix} I \\ K \end{bmatrix} (I + GK)^{-1} M_s^{-1} \right\| \quad (9)$$

To calculate ε_{opt}, a unique method is explained in [5]. To ensure the robust stability of the nominal plant, the weighting functions are selected so that $\varepsilon_{opt} \geq 0.25$ [5].

If ε_{opt} is not satisfied, then go to step 1 to adjust the weighting functions.

Step 3 Select $\varepsilon < \varepsilon_{max}$ and then synthesize the controller K_∞ that satisfies

$$\left\| \begin{bmatrix} I \\ K_\infty \end{bmatrix} (I + G_s K_\infty)^{-1} M_s^{-1} \right\|_\infty \le \varepsilon^{-1} \quad (10)$$

The controller K_∞ is obtained by solving the sub-optimal control problem in (10). The details of calculating ε by solving (10) are available in [5].

Step 4 Final controller (K) is determined by:

$$K = W_1 K_\infty W_2 \quad (11)$$

B. *Genetic Algorithm based Fixed-Structure H_∞ Loop Shaping Optimization*

In this paper, GA is adopted to solve the fixed-structure H_∞ Loop Shaping Optimization problem. Although the proposed controller is structured, it still retains the entire robustness and performance as long as a satisfactory uncertainty boundary ε is achieved. Assume that the predefined structure of controller $K(p)$ has specified parameter p, based on the concept of H_∞ loop shaping, optimization goal is to find parameter p in the controller $K(p)$ that minimizes the infinity norm from disturbances w to states z, $\|T_{zw}\|_\infty$. From (11), assuming that W_1 and W_2 are invertible, then $K_\infty = W_1^{-1} K(p) W_2^{-1}$. Substituting this equation into (10), the ∞-norm of the transfer function matrix $\|T_{zw}\|_\infty$ which is subjected to be minimized can be written as:

$$\gamma = \|T_{zw}\|_\infty = \left\| \begin{bmatrix} I \\ W_1^{-1} K(p) W_2^{-1} \end{bmatrix} (I + G_s W_1^{-1} K(p) W_2^{-1})^{-1} M_s^{-1} \right\|_\infty \quad (12)$$

Consequently, the optimization problem can be written as:

$$\text{minimize} \left\{ \left\| \begin{bmatrix} I \\ W_1^{-1} K(p) W_2^{-1} \end{bmatrix} (I + G_s W_1^{-1} K(p) W_2^{-1})^{-1} M_s^{-1} \right\|_\infty \right\}$$

subject to $p_{i,\min} < p_i < p_{i,\max}$ where $p_{i,\min}$, $p_{i,\max}$ are lower and upper bounds of the parameter p_i in controller $K(p)$, respectively. The fitness function in the controller synthesis can be written as:

$$Fitness = \begin{cases} \left\| \begin{bmatrix} I \\ W_1^{-1} K(p) W_2^{-1} \end{bmatrix} (I + G_s W_1^{-1} K(p) W_2^{-1})^{-1} M_s^{-1} \right\|_\infty^{-1} \\ \text{If } K(p) \text{ stabilizes the plant.} \\ 0.00001 \quad \text{Otherwise} \end{cases} \quad (13)$$

The fitness is set to a small value (in this case is 0.00001) if $K(p)$ does not stabilize the plant.

IV. Simulation and Experimental Results

This section explains the design of robust controller for HDD servo system with VCM actuator. Our design is based on the output feedback control, not state feedback control. Based on (6) and (7) and guidelines in [5], the weight W_1 and W_2 can be selected as:

$$W_1 = 9.77 \times 10^{-4} \frac{s + 116.67}{s + 0.628}, \quad W_2 = \frac{(s + 58.34)(s + 175)}{(s + 0.628)(s + 11199)}$$

By these weights, a slope of -20 dB/decade at the cross-over frequency point can be achieved, and it provides gain margin of 13.5dB and phase margin of 66.6°. First, we applied the conventional H_∞ loop shaping (HLS) technique to design a robust controller. The resulting controller by this approach is 21st order robust controller as shown in the following equation:

$$HLS\_con = \frac{\begin{bmatrix} 1.756\times10^{4}s^{20} + 1.151\times10^{8}s^{19} + 1.412\times10^{12}s^{18} \\ + 6.363\times10^{15}s^{17} + 3.903\times10^{19}s^{16} + 1.277\times10^{23}s^{15} \\ + 5.035\times10^{26}s^{14} + 1.236\times10^{30}s^{13} + 3.376\times10^{33}s^{12} \\ + 6.266\times10^{36}s^{11} + 1.193\times10^{40}s^{10} + 1.639\times10^{43}s^{9} \\ + 2.063\times10^{46}s^{8} + 1.984\times10^{49}s^{7} + 1.377\times10^{52}s^{6} \\ + 8.247\times10^{54}s^{5} + 2.915\times10^{57}s^{4} + 1.9\times10^{59}s^{3} \\ + 4.598\times1077s^{2} + 4.425\times10^{63}s + 1.353\times10^{65} \end{bmatrix}}{\begin{bmatrix} s^{21} + 8.076\times10^{3}s^{20} + 9.092\times10^{7}s^{19} + 4.885\times10^{11}s^{18} \\ + 2.82\times10^{15}s^{17} + 1.085\times10^{19}s^{16} + 4.097\times10^{22}s^{15} \\ + 1.179\times10^{26}s^{14} + 3.140\times10^{29}s^{13} + 6.836\times10^{32}s^{12} \\ + 1.321\times10^{36}s^{11} + 2.12\times10^{39}s^{10} + 2.916\times10^{42}s^{9} \\ + 3.243\times10^{45}s^{8} + 2.998\times10^{48}s^{7} + 1.928\times10^{51}s^{6} \\ + 1.011\times10^{54}s^{5} + 4.136\times10^{56}s^{4} + 2.419\times10^{59}s^{3} \\ + 6.682\times10^{61}s^{2} + 6.802\times10^{63}s + 2.137\times10^{65} \end{bmatrix}} \quad (14)$$

HLS controller is able to satisfy all specifications with the infinity norm, $\gamma = 1.7169$. As shown in (14), the order of HLS controller is 21. It is not easy to implement practically.

Next, a fixed-structure robust controller using the proposed algorithm is designed. The structure of controller is selected as the 3rd order lead-lag controller (15) [7].

$$Cont = \left\{ K_3 \frac{(s + K_1)(s + K_4)(s + K_6)}{(s + K_2)(s + K_5)(s + K_7)} \right\} \quad (15)$$

The optimization, the ranges of search parameters and GA parameters are set as follows. $k_1 \in [50, 150]$; $k_2 \in [.001, 1]$; $k_3 \in [.00001, .01]$; $k_4 \in [10, 100]$; $k_5 \in [0.1, 1]$; $k_6 \in [100, 200]$; $k_7 \in [10000, 15000]$; Population size=100; crossover probability =0.6; mutation probability=0.1; maximum generation = 30. When running GA for 27 generations, an optimal controller was found as.

$$Cont(PPD) = \left\{ 1\times10^{-3} \frac{(s + 116.32)(s + 58.87)(s + 159.89)}{(s + .5379)(s + 0.5815)(s + 12548)} \right\} \quad (16)$$

Fig 3. shows the comparison of the shaped plant by the proposed controller and HLS. Cleary, the open loop shapes of both controllers are almost the same.

In addition, we designed a fixed-structure pre-filter to achieve the tracking performance specification.

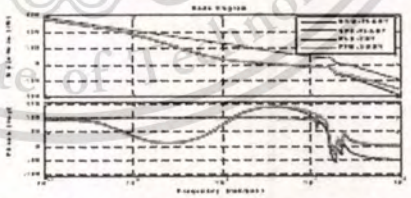

Figure 3. Bode plot of the open loop TF for: the nominal, shaped, HLS and the proposed controller.

To design the pre-filter, we selected a 1st order lead-lag controller, $Kr(s)$ as [5].

$$K_r(s) = \frac{\tau_{lead} s + 1}{\tau_{lag} s + 1} \quad (17)$$

The pre-filter was also designed by GA by setting the constraints as follows: over shoot <=5%, and settling time <= 1.5ms. In our study, first order filter with unity DC gain and time constant of ... ms is selected as the model reference. By running GA, we found that optimal value of $K_r(s)$ is

$$K_r(s)=\frac{0.001750s+1}{0.002122s+1} \qquad (18)$$

Responses from the unit step command by HLS and the proposed robust controllers at the nominal plant are shown in Fig. 4. Table III shows the performance obtained by all controllers. As seen in this figure and Table III, maximum overshoot obtained by the HLS controller and the 3rd lead-lag (1 DOF) is much higher than that of the proposed controller. Settling time of our proposed controller is much faster than that of the other controllers. Clearly, time domain specifications can be achieved by our proposed technique.

Figure 4. Step response from HLS, 3rd lead-lag (PPID) and 3rd lead-lag (PPID) with pre-filter.

TABLE III. PERFORMANCE COMPARISON

Controller	Proposed controller 3rd lead-lag (1 DOF)	HLS	Proposed Controller (2 DOF)
Over Shoot	17%	18%	<3%
5%Settling Time	3.6ms	3.8ms	1.20ms

To verify the robustness of the proposed controller, the step responses at perturbed conditions which are worse than the nominal condition, are given in Fig.5. In this perturbed condition, resonance mode frequencies ($\omega_1, \omega_2, \omega_3, \omega_4$) and damping coefficients ξ_1 to ξ_4 of the system have been changed to the values as mentioned in the tolerance column of Table I. Fig.5 shows the step response of the proposed control system. Fig.5 indicates the responses of the proposed system at the lower, upper bound and nominal conditions

Figure 5. Step Responses of the proposed controller at nominal and perturbed plants.

Clearly, the responses of the proposed controller at the perturbed conditions are almost the same as the response at the nominal plant.

In order to verify the proposed technique, we implemented our technique to design a controller in real HDD servo system with single stage VCM actuator. The real plant is adopted in our design. In addition Adaptive Feed Forward compensator is used in the system. The experimental results in Fig. 6 show that our proposed controller along with Adaptive Feed Forward compensator (AFC) is able to work well within 14.8% of the track width.

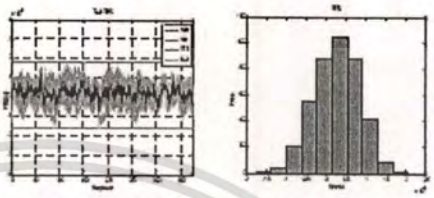

Figure 6. PES on track & Histogram of the of the PES error

From Fig.6 we can see that our proposed system can perform well within +/- 20nm which can be further enhanced by using Dual Stage Actuator (DSA).

V. CONCLUSIONS

In this paper, the design of high-performance and robust controller for HDD servo system using Genetic Algorithm has been proposed. Simulation results show that the response from our proposed technique has significantly lower overshoot compared to that of the conventional PID and HLS. In addition, the order of controller is much lower than that of the HLS, but the robust performance from the proposed controller is almost the same as HLS. Experiment verifies that our proposed technique can be implemented on the real HDD servo system.

ACKNOWLEDGMENT

This work was funded by DSTAR, KMITL and NECTEC, NSTDA.

REFERENCES

[1] Xinglun Huang ,Ryozo Nagamune and Roberto Horowitz, "A Comparison of Multi rate Robust Track-Following Control Synthesis Techniques for Dual-Stage and Multi sensing Servo Systems in Hard Disk Drives", *IEEE Transactions on Magnetics*, Vol.42, No.7, July 2006, pp. 1896–1904.

[2] Hamid D. Taghirad and Ehsan Jamei, "Robust Performance Verification of Adaptive Robust Controller for Hard Disk Drives", *IEEE Transactions on Industrial Electronics*, Vol. 55, No.1, January 2008, pp. 448–456.

[3] Kay-Soon Low, Tze-Shyan Wong, "A Multiobjective Genetic Algorithm for Optimizing the Performance of Hard Disk Drive Motion Control System", *IEEE Transactions on Industrial Electronics*, Vol. 54, No.3, June 2007, pp 1716–1725.

[4] S. Kaitwanidvilai, M. Parnichkun, "Genetic Algorithm based Fixed-Structure Robust H-∞ Loop Shaping Control of a Pneumatic Servo System", *International Journal of Robotics and Mechatronics*, Vol.16:4, 2004, pp. 1716–1725.

[5] S. Skogestad & I. Postlethwaite, *Multivariable Feedback Control Nd Analysis and Design*, 2nd. New York: John Wiley & Son, 1996, pp. 293–351.

[6] G.F.Franklin, J.D.Powell and Michel Workman, *Digital Control of Dynamic Systems*, 3rd Edition" Addison- Wesley, 1994, pp. 654–661.

[7] Al Mamun, Guo and Bi, *Hard Disk Drive Mechatronics and Control*, CRC press, pp. 88–102.